



UNIVERSIDAD NACIONAL AUTÓNOMA DE MÉXICO
POSGRADO EN CIENCIAS (FÍSICA)

Statistical properties of sparse non-Hermitian random matrices

TESIS

QUE PARA OPTAR POR EL GRADO DE:
DOCTOR EN CIENCIAS (FÍSICA)

PRESENTA

M. EN C. ANTONIO TONATIÚH RAMOS SÁNCHEZ

TUTOR PRINCIPAL

DR. ISAAC PÉREZ CASTILLO
DEPARTAMENTO DE FÍSICA, UAM-IZTAPALAPA

MIEMBROS DEL COMITÉ TUTOR

DR. JORGE GUSTAVO HIRSCH GANIEVICH
INSTITUTO DE CIENCIAS NUCLEARES, UNAM

DR. WOLFGANG PETER BIETENHOLZ
INSTITUTO DE CIENCIAS NUCLEARES, UNAM

CIUDAD DE MÉXICO, SEPTIEMBRE 2023



Universidad Nacional
Autónoma de México



UNAM – Dirección General de Bibliotecas
Tesis Digitales
Restricciones de uso

DERECHOS RESERVADOS ©
PROHIBIDA SU REPRODUCCIÓN TOTAL O PARCIAL

Todo el material contenido en esta tesis esta protegido por la Ley Federal del Derecho de Autor (LFDA) de los Estados Unidos Mexicanos (México).

El uso de imágenes, fragmentos de videos, y demás material que sea objeto de protección de los derechos de autor, será exclusivamente para fines educativos e informativos y deberá citar la fuente donde la obtuvo mencionando el autor o autores. Cualquier uso distinto como el lucro, reproducción, edición o modificación, será perseguido y sancionado por el respectivo titular de los Derechos de Autor.



In loving memory of

Maureen Vanessa Reyes Corea

who saw the beauty in me and my work, even when I could not see them, and helped me to realize the true meaning of a beautiful mind.

I know one day we will see each other again; after all, we promised it. Until then, thank you for loving me so much. Thank you for wanting a future with me. Thank you for lighting up my life. There will always be a song for you within my heart.

Querida, querida, vida mía; reflejo de luna que reía.

Si amar es cerrado, culpa mía.

Te amé, en el fondo, ¿qué es la vida? No lo sé.

El gato que está triste y azul nunca se olvida que fuiste mía.

Mas siempre serás en mi mirar lágrima clara de primavera.

El gato que está en la oscuridad sabe que en mi alma, una lágrima hay.

Un gato en la oscuridad - Roberto Carlos



Resumen

A lo largo de esta tesis se desarrollan modelos teóricos exactos para estudiar (i) la estadística completa, fluctuaciones típicas y atípicas, del número de eigenvalores \mathcal{N}_D dentro de una curva suave de Jordan en un dominio D del plano complejo y (ii) las propiedades universales de la llamada densidad espectral condicionada $\rho(z|\mathcal{R})$, i.e., la densidad espectral cuando un parámetro externo \mathcal{R} fija el número de eigenvalores dentro de la curva, para un ensamble de matrices aleatorias diluidas (matrices con varias entradas igual a cero) no-Hermitianas infinitamente grandes. Dada la complejidad de los ensambles diluidos, únicamente se tienen métodos aproximados, los cuales fallan en reproducir los aspectos clave de estos sistemas. Esta tesis desarrolla un formalismo exacto para ambos casos y obtiene teorías efectivas en términos de ecuaciones no lineales de autoconsistencia, mostrando excelentes resultados. Particularmente, los hallazgos de la densidad condicionada fortalecen conjeturas previas encontradas para ensambles diluidos Hermitianos, llevando a conjeturar los presentes resultados como propiedades universales de los ensambles diluidos tanto Hermitianos como no-Hermitianos.

Esta tesis se divide de la siguiente manera. En el Capítulo 1 se introducen las bases necesarias para el desarrollo de la investigación, las cuales contemplan el concepto de universalidad y las teorías de grandes desviaciones, de grafos, y de matrices aleatorias. Específicamente, se presentan conceptos clave como son la función generadora de cumulantes \mathcal{F} , el teorema de Gärtner-Ellis, los grafos aleatorios de Erdős-Rényi, el método de replicas, entre otros. A lo largo de este primer capítulo, se busca proporcionar, en todo momento, los aspectos más importantes de las teorías, haciendo siempre hincapié en su conexión con la física.

Posteriormente, en el Capítulo 2, se presenta el desarrollo de la investigación; esta última, es a su vez dividida en tres secciones. La primera de ellas, la Sección 2.1, introduce los ensambles de matrices aleatorias diluidas, señalando los trabajos previos más importantes del área y de los cuales se desprende la presente tesis. A continuación, en las Secciones 2.2 y 2.3, se estudia la estadística completa, fluctuaciones típicas y atípicas, del número \mathcal{N}_D y las propiedades universales de la densidad condicionada $\rho(z|\mathcal{R})$, respectivamente. Se define la variable aleatoria \mathcal{N}_D junto con las funciones \mathcal{F} (de esta se obtienen las fluctuaciones típicas y atípicas de \mathcal{N}_D) y $\rho(z|\mathcal{R})$, y se obtiene, para cada caso, una expresión general válida-en principio-para cualquier ensamble de matrices aleatorias no-Hermitianas del tipo *campo medio* (ensambles donde las fuerzas de acoplamiento no dependen de la distancia entre componentes), particularmente para matrices diluidas no-Hermitianas. Para mostrar la exactitud de ambas teorías, estas son aplicadas a la matriz de adyacencia de grafos aleatorios pesados con acoplamientos asimétricos, en los cuales herramientas estándar de la teoría de matrices aleatorias no son aplicables, y se obtienen resultados exactos para el ensamble real diluido de Ginibre. En ambos estudios, el resultado principal es una teoría efectiva que determina la estadística completa del número \mathcal{N}_D y las propiedades universales de la densidad condicionada $\rho(z|\mathcal{R})$ en términos de ecuaciones no lineales de autoconsistencia. Dada la naturaleza de dichas ecuaciones, estas son resueltas a través de métodos numéricos. Ambas teorías son comparadas con diagonalización numérica exacta para matrices de tamaño finito, mostrando excelentes resultados.

Finalmente, en el Capítulo 3 se presentan las conclusiones generales de la investigación y se señalan trabajo a futuro. Para cerrar la presente sección, se hace del conocimiento del lector que el primer proyecto concerniente a la estadística completa del número \mathcal{N}_D ya ha sido publicado [1], mientras que el segundo referido a la densidad espectral condicionada $\rho(z|\mathcal{R})$ se encuentra en su fase final.

Abstract

Throughout this thesis, we develop exact theoretical models to study (i) the complete statistics, typical and atypical fluctuations, of the number \mathcal{N}_D of eigenvalues within a smooth Jordan curve in a domain D on the complex plane \mathbb{C} and (ii) the universal properties of the so-called conditional spectral density $\rho(z|\mathcal{R})$, i.e., the spectral density when an external parameter \mathcal{R} fixes the number of eigenvalues inside the curve, for an ensemble of infinitely large sparse non-Hermitian random matrices (matrices with several entries equal to zero). Owing to the complexity of the diluted ensembles, we only count with approximate methods that fail to reproduce the key aspects of these systems. This thesis develops an exact formalism for both points (i) and (ii), and obtains effective theories in terms of self-consistency nonlinear equations, showing excellent results. In particular, our findings for the constrained density strengthen previous conjectures found for Hermitian diluted ensembles, leading us to conjecture the present results as universal properties for both Hermitian and non-Hermitian sparse ensembles.

We divide this thesis as follows. In Chapter 1, we introduce the research foundations, covering the concepts of universality, large deviation theory, graph theory, and random matrix theory. Specifically, we present key concepts such as the cumulant generating function \mathcal{F} , the Gärtner-Ellis theorem, the Erdős-Rényi random graphs, and the replica method. Throughout this first chapter, we seek to provide, at all times, the most important aspects of the theories, always emphasizing their connections with physics.

Subsequently, in Chapter 2, we present our research; the latter is further divided into three sections. We begin in Section 2.1 by introducing the diluted ensembles, emphasizing the previous works from which our research follows. Next, in Sections 2.2 and 2.3, we study the complete statistics, typical and atypical fluctuations, of the number \mathcal{N}_D and the universal properties of $\rho(z|\mathcal{R})$, respectively. We define the random variable \mathcal{N}_D , together with the cumulant generating function \mathcal{F} (from this, we deduce the typical and atypical fluctuations of \mathcal{N}_D) and $\rho(z|\mathcal{R})$, and obtain, for both, a general expression valid-in principle-for any non-Hermitian random matrix ensemble of the mean-field type (ensembles where the coupling strengths do not depend on the distance between components), particularly for sparse non-Hermitian ensembles. To demonstrate the accuracy of both theories, we apply them to the adjacency matrix of weighted random graphs with asymmetric couplings, where standard tools from random matrix theory are no longer applicable, and obtain exact results for the diluted version of the real Ginibre ensemble. In both studies, the principal outcome is an effective theory in terms of nonlinear self-consistency equations that determines the complete statistics of the number \mathcal{N}_D and the universal properties of $\rho(z|\mathcal{R})$. Due to the nature of these equations, they are solved only through numerical methods. Both theories are compared with exact numerical diagonalization for finite-size matrices, showing excellent results.

Finally, in Chapter 3, we display the general conclusions of the research and indicate future work. To close this section, we inform the reader that the first project concerning the complete statistics of the number \mathcal{N}_D of eigenvalues within a smooth Jordan curve has already been published [1], while the second one referring to the conditional spectral density $\rho(z|\mathcal{R})$ is in its final phase.

Contents

Contents	iv
Acknowledgments	v
Preface	vii
1 Introduction and preliminaries	1
1.1 Universality	1
1.2 Large deviation theory	3
1.3 Graph theory	5
1.4 Random matrix theory	9
1.4.1 Basic concepts and universality	9
1.4.2 Classical and Ginibre ensembles	11
1.4.3 Replica method	13
2 Statistical properties of sparse non-Hermitian random matrices	17
2.1 Background	17
2.2 Analytic approach for the number statistics of non-Hermitian random matrices	21
2.2.1 The analytical method	22
2.2.2 The numerical method	28
2.3 Conditioned spectral density for the diluted real Ginibre ensemble	30
2.3.1 The analytical development	33
2.3.2 Numerical analysis and results	38
3 Concluding remarks	43
A Mathematical procedure for the full counting statistics of \mathcal{N}_D	45
A.1 Constructing the path integral	45
A.2 The replica-symmetric ansatz and the path probability function	47
A.3 The continuous limit throughout the γ contour	48
A.4 Computing the rate function	49
B Mathematical handlings of the CSD for the diluted real Ginibre ensemble	50
B.1 Building the path integral	50
B.2 The replica-symmetric ansatz and the joint probability distribution	51
B.3 Computing ∂_{z^*} and ∂_z for the conditioned spectral density	52
C Population dynamics algorithm	55
D Monte Carlo methods	57
D.1 Bases	57
D.2 Simple and importance sampling	58
D.3 Markov processes	59
D.4 Ergodicity and detailed balance	59
D.5 Acceptance ratios	60

D.6 The Metropolis algorithm	61
Bibliography	73

Acknowledgments

Reflect upon your present blessings, of which every man has plenty; not on your past misfortunes, of which all men have some.

Charles Dickens (1812-1870)

It has been some years since I last expressed my most sincere gratitude to the people who, with love and friendship, have accompanied me throughout my academic journey. Despite the years, it still amazes me that a smile, as simple as it may seem, can encapsulate all the love and gratitude towards those we love and admire when words feel insufficient. Sadly, it is also true that there are times when tears are not enough to express all the sadness we feel when the loss of a loved one knocks on our door. I would like to say that all the people I love are still here, and we are still laughing; unfortunately, it is not the case. Years have taught me to value every moment we spend with those who love us. To appreciate every smile, hug, and advice we receive. To understand that no matter how different we are, there is always a place for reconciliation. As the Byrds said, *there is a time to dance, a time to mourn*.

In the following paragraphs, I wish to extend my gratitude to those who, with talks, laughs, and advice, lived by my side the challenges and rewards of a doctorate.

First of all, I would like to thank my supervisor, Dr. Isaac Pérez Castillo, for having introduced me to the fascinating world of *Random Matrix Theory*, from where I have learned and expanded my knowledge in areas as varied as *statistical physics, condensed matter, quantum field theory, probability and statistics*, among many others. Thank you for your patience and for always opening spaces where students have the opportunity to interact, discuss, and present their research.

I am also very grateful to the members of my doctoral committee, Dr. Jorge Gustavo Hirsch Ganievich and Dr. Wolfgang Peter Bietenholz, for all their support and advice. Specifically, I want to thank Dr. Hirsch for welcoming me to the ICN and permitting me to use the *Tochtli* cluster, and Dr. Bietenholz for inviting me to participate in the Department of Gravitation and Field Theory seminar and providing me with a meticulous review of my thesis.

I wish to thank Dr. Mario Alberto Diaz Torres, Dr. Thomas Gorin, Dr. Manan Vyas, and Dr. Pablo Barberis Blostein, who, through their comments and suggestions, have enriched this thesis work.

I want to express my deepest gratitude to Dr. Edgar Guzmán González, who, more than a colleague and collaborator, became a dear friend. I thank him for all the encouragement and support he had with me from my doctoral admission process to its conclusion. Thank you for always being open to talking with me about physics and mathematics.

I want to thank the National Autonomous University of Mexico (UNAM), which has been my home and guide for the last seventeen years and from which I have learned so much that it would be impossible to write it down. Thanks, because throughout my training, I have had the pleasure of learning and living through the walls and classrooms of this beautiful institution. Had I to commence from scratch, I would choose my University again.

I thank the Autonomous Metropolitan University (UAM) for allowing me to use the *Yoltla* cluster to conduct my research.

I thank the National Council for Science and Technology (CONACyT) for granting me the scholarship **No. CVU: 743998** to perform my doctoral studies.

Undoubtedly, this list would be incomplete without those who have always been here for me prior to this doctorate. Therefore, I would like to dedicate the following paragraphs to those who behind the "scenes", have supported my journey and helped me to get to this point in my life.

First, I want to extend my deepest gratitude to my mother, Anastasia Victoria Sánchez Peralta, who, with love and wisdom, has guided me through the different scenarios of this play called *Life*. None of this would have been possible without your constant encouragement to give always my best. Thank you for everything; there will never be sufficient words, neither in Spanish nor English, to express how deeply grateful I am to have you. From the bottom of my heart, thank you very much.

Next, I want to thank my brother Victor Axáyacatl Ramos Sánchez, whose laughs and support have shed light on the darkest moments of recent years. I know that you have been very brave, braver than many of us, and I know it is not fair; I wish I had the power to change things, but I do not, and it pains me that it is so. Yet, it is up to us to get up and keep going. Do not be afraid of committing mistakes; errors do not define us. It is the strength we possess to overcome difficulties that shows who we are. I have faith in you, so do not hesitate and keep moving forward.

Finally, I want to thank my brother Damián Alexander Contreras Cadena, whom I have had the pleasure to know since we were teenagers. Thank you for all the time we have spent together laughing and reminiscing about how we were when we were younger: when time seemed irrelevant and, daily, we would play the guitar. I feel very pleased to share this path with you.

Thanks to each and every one of you. All of these achievements are as much yours as they are mine.

Antonio Tonatiúh Ramos Sánchez
Mexico city, Mexico
September 2023

Preface

Physics is becoming so unbelievably complex that it is taking longer and longer to train a physicist. It is taking so long, in fact, to train a physicist to the place where he understands the nature of physical problems that he is already too old to solve them.

Eugene Wigner (1902-1995)

Undoubtedly, one of the most astonishing features in nature is the presence of a universal behaviour, i.e., a behaviour displayed by several classes of physical systems. The basis of universality ought to be understood as a collective behaviour coming from diverse microscopic effects regardless of the details that involve them. The notion of universality enters formally in the study of phase transitions, where critical exponents for many physical systems depend only on the system dimensionality and the Hamiltonian symmetries [2–4]. We need to express this extraordinary behaviour in a universal language; this is the language of mathematics. Universality and far-reaching mathematical expressions correspond to each other. For instance, we can describe the statistical behaviour near critical points for thermodynamic systems and lasers by one exponential distribution function. For such distributions, the time-space evolution is given by special differential equations such as the Fokker-Plank and Schrödinger equations. Such evolution equations can be formulated in a far-reaching way, i.e., we can use one basic evolution equation to describe many classes of physical systems. In other words, a compressed formulation of universal behaviour can be found on the level of differential evolution equations [5]. This pillar of theoretical physics appears in random matrix theory (RMT) as a fundamental result which indicates that in the large matrix size limit, various statistical properties of eigenvalues and eigenvectors are universal in the sense that they are independent of the details concerning the matrix elements. Therefore, understanding how these universal properties arise and to what extent they are valid, are essential technical elements in RMT.

Since its informal inception by Wishart in 1928 into the context of multivariate statistics [6] and later popularized by Wigner in 1955 for the problem of heavy nuclei [7, 8], RMT has transformed into an area of extensive research finding applications in areas such as physics [9, 10], mathematics [11, 12], biology [13, 14], statistics [15], and finance [16]. Its faculty for modelling systems with large degrees of freedom and its enormous predictive capacity make it an area where, in principle, all sorts of systems can be modelled. Early research in RMT focused on matrices with Hermitian symmetry and all-to-all interactions, where the degrees of freedom interacted similarly to the mean-field models in statistical physics; nowadays, we bifurcate RMT into Hermitian and non-Hermitian random matrices. One of the successes for Hermitian random matrices was obtaining the joint probability distribution of eigenvalues (JPDE) function, from where applications in quantum mechanics [17, 18], quantum chaos [19, 20], quantum cosmology [21], string theory [22, 23], among others, emerged. Another fascinating result for large Hermitian ensembles, proof of the universality, was the discovery of a limiting spectral distribution, a result known as the Wigner semicircle law [24]. For non-Hermitian ensembles, the situation is far more complicated. Thanks to the endeavours of Ginibre [25] and Girko [26–28], and recently to the work of Tao [29], we currently have a JPDE function and a limiting spectral distribution for the so-called Ginibre ensembles known as Girko’s or the circular law (the analogue to Wigner’s law). Unfortunately, in general, there is no analogous description for non-Hermitian ensembles. Consequently, little do we know about the spectral properties of non-Hermitian random matrices. This may be mainly due to the mathematical limitations: the lack of symmetries and large spectral instabilities of the spectrum under small perturbations present in non-Hermitian matrices hamper us in applying the most common mathematical methods and in establishing both a JPDE function and a limiting spectral density [30]. Clear examples are the ensembles of sparse random matrices, where their unique features make them complicated cases to explore.

Sparse ensembles consist of matrices with only a finite number of nonzero elements, where the theory and meth-

ods established for Hermitian random matrices no longer apply. In contrast with ensembles of all-to-all interactions, sparse matrices model complex systems where a given degree of freedom interacts with a small number of others. These systems can be represented in terms of random graphs, where the nodes denote the individual entities composing the system and the links connecting them their interactions [31]. Sparse ensembles find applications in studies of percolation limits [10], Anderson localization of electronic states [32], Griffiths singularities in disordered systems [33], and in general real-world complex systems, where interactions between components are often directed and depend on functional locality [34, 35]. Since Rodgers and Bray aimed to reproduce the spectral density for sparse Hermitian ensembles [36], numerous publications sought to provide an analytical method capable of unravelling the eigenvalues and eigenvectors statistical properties of these ensembles [37–40]; unfortunately, all of them were hindered by the technical difficulties arising from the combined effects of sparseness and asymmetry. Some of the authors, to overcome the obstacles, simplified their procedures leading to a series of approximate methods [41–43]; sadly, such methods ended up with an incomplete description of the spectra. During the last fourteen years, the spectral properties of sparse ensembles have become a topic of continuous research since the study of complex networks, geometrical and topological properties, has moved to the study of the spectral properties of their adjacency matrices. Nonetheless, and despite the still-growing interest, rigorous results for sparse ensembles, particularly for sparse non-Hermitian random matrices, are mainly non-existent owing to the technical difficulties their analyzes imply. Hence, convergence proofs for eigenvalues and eigenvectors to a deterministic limit at large matrix dimensions hardly exists [31].

The present doctoral thesis develops within a research group whose ultimate goal is to establish under what conditions universal features emerge in strongly correlated systems together with their range of validity, having as main objective the study of the statistical properties of an ensemble of sparse non-Hermitian random matrices. Owing to the limited knowledge we have about the spectral properties of sparse random matrices, this thesis seeks to complement the research conducted in Refs. [44, 45] and by means of diverse mathematical tools from statistical physics, RMT, and complex systems, provides accurate theoretical models to study the full statistics of the number of eigenvalues \mathcal{N}_D within a smooth Jordan curve on a domain $D \subseteq \mathbb{C}$ and the universal properties of the conditioned spectral density in the limit of infinitely large matrix dimensions for an ensemble of sparse non-Hermitian random matrices. It is my hope that future students find this work interesting and challenging enough to venture into the fascinating world of RMT and complex systems, where areas as diverse as measure, probability, quantum field theory, and condensed matter, among many others, combine to form a beautiful explosion of complexity.

Chapter 1

Introduction and preliminars

We are merely explorers of infinity in the pursuit of absolute perfection.

The man who knew infinity (film)

This first chapter provides the basic concepts and mathematical theories required for the correct development of the research conducted in this thesis; to cover them all, we have divided the chapter into four sections. We commence in Section 1.1 by introducing the concept of universality, a key term in physics and mathematics, and one of the cornerstones in random matrix theory from which a great deal of research detach. Immediately after in Section 1.2, we present large deviation theory as the mathematical modelling in charge of studying the atypical fluctuations of a random variable X , i.e., the behaviour of X far from its average. In this section, we also introduce the rate and cumulant generating functions along with the Gärtner-Ellis theorem, responsible of relating both functions through a Legendre transform. For Section 1.3 we display the essential concepts of graph theory and present the famous Erdős-Rényi random graphs. Finally, we close with Section 1.4 by formally introducing the bases of random matrix theory, such as the basic definitions, the concept of universality, Hermitian and non-Hermitian ensembles, and the replica method within the formalism of random matrices. This last section seeks to provide the reader with a clear image of the marked difference between Hermitian and non-Hermitian random matrices and point out the enormous necessity of more research for the latter case.

1.1 Universality

It is well-known that all thermodynamics systems at the macroscopic level, as time moves, will eventually reach their equilibrium state and obey the laws of thermodynamics, whichever the nature of the interactions between the atoms and molecules at the microscopic level is. In other words, *at the macroscopic level, the essential behaviour of physical systems is governed by the same laws of thermodynamics* [5,46]:

1. **First law:** in a thermodynamic process involving a closed system, the increment in the internal energy is equal to the difference between the heat accumulated by the system and the work done by it.
2. **Second law:** every process occurring in nature proceeds in the sense in which the sum of the entropies of all bodies taking part in the process increases.
3. **Third law:** the entropy of a system tends to a constant value as its temperature approaches absolute zero.

Then, the juxtaposition between the microscopic and macroscopic frameworks concentrates on the question, *how does one derive the macroscopic laws of thermodynamics from the microscopic laws of atoms?* The answer is given precisely by the fact that the same laws of thermodynamics ought to emerge despite the atomic interaction details. This notion of a collective behaviour independent of its components gives rise to the universality concept. Indeed, in statistical mechanics, *universality* is a widespread feature consisting of the observation that there are properties for a large class of systems independent of the system's dynamical details. These systems display universality in a scaling limit when a large number of interacting parts come together [5].

Universality originates in the study of *phase transitions*, where critical exponents are considered universal, i.e., independent of the details of the system's Hamiltonian. Nonetheless, they continue to depend on the dimensionality of the system and any symmetry of the Hamiltonian [2, 3]. In the vicinity of critical points, the topology concerning phase diagrams for diverse systems, such as the gas-liquid mixture and ferromagnetic materials, are astonishingly similar [4, 46]. Moreover, experiments and computer simulations have pointed out that the critical exponents of the corresponding phase transitions for broad classes of physical systems are the same and depend only on the number of components and the symmetry of the order parameter, the spatial dimension, and the character of the interactions (short-ranged or long-ranged). I.e., in the critical region, those systems behave collectively, and only global features such as their spacial dimension and symmetry play a role [46, 47]. There are cases in which the universality hypothesis is violated; nevertheless, this is generally believed to only occur in cases of very particular Hamiltonians [3].

In recent years, the concept of universality has expanded its usage to a wide variety of mathematical problems. An area called by some authors *macroscopic mathematics*. The idea is that several problems, apparently not connected, behave at the appropriate scale in the same way [48]. We find two examples of this in probability theory via the *central limit theorem* (CLT) and *extreme value theory* (EVT). Formally speaking, the CLT states that for $\{X_1, \dots, X_n\}$, a collection of random variables with finite mean μ and variance σ^2 , the probability distribution of the sum for large n will tend to a normal distribution with mean $n\mu$ and variance $n\sigma^2$ for every $a \in \mathbb{R}$ [49, 50], i.e.,

$$\lim_{n \rightarrow \infty} P \left(\frac{\sum_{i=1}^n X_i - n\mu}{\sqrt{n}\sigma} \right) = \frac{1}{\sqrt{2\pi}} \int_{-\infty}^a e^{-x^2/2} dx. \quad (1.1)$$

On the other hand, EVT focuses on the extreme samples $X_{\max} \equiv \max(X_1, \dots, X_n)$ and $X_{\min} \equiv \min(X_1, \dots, X_n)$ of the set $\{X_1, \dots, X_n\}$ and states that if $\{X_i\}_{i=1}^n$ are all independent identically distributed (i.i.d.) random variables with probability p , the cumulative probability

$$Q_n(x) \equiv \text{Prob}[X_{\max} \leq x] = \text{Prob}[X_1 \leq x, \dots, X_n \leq x] = \left(1 - \int_x^{\infty} p(x') dx' \right)^n \quad (1.2)$$

under the rescaled variable $z = (x - a_n)/b_n$ with $a_n, b_n \in \mathbb{R}$ non-universal constants, will tend to a limit distribution $F(z)$ (*extreme value distribution*) in the large n limit [51, 52]; in other words,

$$\lim_{n \rightarrow \infty} Q_n(a_n + b_n z) = F(z). \quad (1.3)$$

The universality for $Q(z)$ is provided by the *Fisher-Tippett-Gnedenko theorem*, which establishes that $F(z)$ can only be equal to the limiting distributions *Gumbel*, *Fréchet*, and *Weibull*, depending on the decaying speed of the right tail and upper endpoint of its support (analogous for X_{\min}) [53–55]. Further details can be consulted in Refs. [56–59].

Both results, CLT and EVT, illustrate a key feature within the notion of universality, the *limiting distribution* concept. Formally speaking, we say a sequence of distributions f_n converges to a limiting distribution f if

$$\lim_{n \rightarrow \infty} f_n(x) = f(x). \quad (1.4)$$

What we are indicating with Eq. (1.4) is that the sequence $\{f_n(x)\}$ converges to a universal limit regardless of the specific details of the sequence distributions [30].

This notion of universality is also present in random matrix theory (RMT) as a fundamental result in the limit of large matrix size, where various statistical properties of eigenvalues and eigenvectors are universal in the sense that they do not depend on the matrix elements details [9, 10, 31]. Hence, universality corresponds to a statement about certain limiting behaviours happening as the size of matrices tends to infinity. For instance, the spacing between eigenvalues is described by universal laws and corresponds to one of the basic features of RMT. It was the motivation behind Wigner's idea to introduce random matrices to model energy levels in quantum systems [10]; universality was the starting point for RMT. After early success in reproducing the universal features in the spectra of highly excited nuclei, RMT was used to model various physical and mathematical systems. An example is found in quantum mechanics, where a wealth of empirical and numerical evidence suggested universality for local fluctuations in quantum energy or quasi-energy spectra of systems that display global chaos in their classical phase spaces [18, 60]. In the end, universality is one of the fundamental principles of RMT.

1.2 Large deviation theory

Within nature, there are certain types of events such as earthquakes, floods, hurricanes, and financial crises (among others), which do not happen on a daily basis. Nonetheless, when such events tend to occur, the consequences are often disastrous [61]. Hence, it is desirable to possess models or theories that adequately provide information and predict the times in which those situations might occur; specifically, we require a mathematical theory to model the occurrence probabilities for those events. *Large deviation theory* (LDT) is the mathematical tool responsible for providing accurate information about the occurrence probabilities of such *atypical events*. Interestingly, the *Poisson probability distribution* is also commonly used to refer to "rare events" occurrence.

Given a discrete random variable Y , the Poisson distribution $\mathfrak{P}(y) \equiv \text{Prob}[Y = y] = e^{-\mu} \mu^y / y!$ ($\mu > 0$, the *rate parameter*) measures the probability that a certain number of random events, with the mean of occurrence constant over time, happen in a specific period [62–64]. The *law of rare events* or *Poisson limit theorem*, states that in the limit of the Binomial distribution $B(n, p)$ when the number n of independent Bernoulli trials is very large ($n \rightarrow \infty$) and the success probability p for each trial is small ($p \rightarrow 0$), $np = \mu$, the total number of events will follow, approximately, the Poisson distribution $\mathfrak{P}(\mu)$ [64]; in practice, $\mathfrak{P}(\mu)$ is an adequate approximation when $n \geq 100$ and $p \leq 0.05$ [65]. In other words, $\mathfrak{P}(\mu)$ appears when the number of opportunities for an event to occur is large, but the probability of occurrence on any trial is small. Some events modelled by \mathfrak{P} include the number of earthquakes occurring during some fixed time, wars per year [49], deaths in a given period [66, 67], and the probability of mutation for a particular cell within a large group of cells [68].

LDT sees the light for the first time in Crámer's works concerning insurance and actuarial mathematics, looking for corrections to the results provided by the central limit theorem [69]; nevertheless, it would not be until approximately thirty years later that this newborn theory would be formalized firstly by the works of Donsker and Varadhan within the context of Markov processes in the 1970s [70–73] and later, in the 1980s, by Freidlin and Wentzell [74]. Although LDT is widely known in the mathematical literature [75–77], it is not a subject commonly studied in the physics curriculum; the first informal encounter physicists have with LDT is through the use of mathematical techniques such as the *Laplace* or *saddle point* method [78]. However, LDT appears naturally in physics and has been extensively used by physicists for more than one hundred years via a different language than the one utilized by mathematicians; in fact, physicists are responsible for the first result obtained by appealing to such a theory [75–80].

LDT is a probabilistic approach centred on studying the atypical fluctuations of a random variable, i.e., the probability that a random variable y_N takes values far from its expected value $\langle y_N \rangle$. LDT assumes that the probabilities decay exponentially as the value of variable N (an extensive parameter) increases [75–81]. Formally speaking [81],

$$P_{y_N}(x) \equiv \text{Prob}[y_N \leq x] \asymp \begin{cases} e^{-\omega_N^{(-)} \psi^{(-)}(x)}, & \text{if } x < \langle y_N \rangle \\ 1 - e^{-\omega_N^{(+)} \psi^{(+)}(x)}, & \text{if } x > \langle y_N \rangle \end{cases}, \quad (1.5)$$

where $\psi^{(+)}(x)$ and $\psi^{(-)}(x)$ are the so-called right and left *rate functions* (or Crámer functions [79]) in charge of controlling the probability that y_N takes larger and smaller values than $\langle y_N \rangle$. The parameters $\omega_N^{(+)}$ and $\omega_N^{(-)}$ control the decaying speed of the probabilities, both depending on N ; to obtain non-trivial results for $\psi^{(\pm)}(x)$, we must select appropriate values for $\omega_N^{(\pm)}$ [81].

It is essential to understand the meaning of the notation in Eq. (1.5) since the large deviation principle (the basis of LDT) follows from it. The symbol \asymp indicates *asymptotic convergence* in the limit $N \rightarrow \infty$; then, we say that $P_{y_N}(x)$ fulfills the *large deviation principle* (LDP) if the following limits exist and both are different from zero [78, 79, 81],

$$\begin{aligned} - \lim_{N \rightarrow \infty} \frac{\ln P_{y_N}(x)}{\omega_N^{(-)}} &= \psi^{(-)}(x), \\ - \lim_{N \rightarrow \infty} \frac{\ln(1 - P_{y_N}(x))}{\omega_N^{(+)}} &= \psi^{(+)}(x). \end{aligned} \quad (1.6)$$

Should it happen that any of the limits in Eq. (1.6) is equal to infinity or zero for a given value of x , we say that the function $P_{y_N}(x)$ falls off either super-exponential or sub-exponential, respectively, in N . In other words, $P_{y_N}(x)$ decays faster or slower than e^{-Na} , with $a > 0$ [78]; the cases of interest for LDT are those whose limits exist and are different from zero or infinity.

Alternatively, we can state the previous definition of Eq. (1.5) via the probability density function as [78, 79]

$$\mathcal{P}_{y_N}(x) = \text{Prob}[y_N = x] \asymp e^{-W_N \psi(x)}, \text{ such that } W_N \psi(x) = \begin{cases} \omega_N^{(-)} \psi^{(-)}(x) & \text{if } x < \langle y_N \rangle \\ \omega_N^{(+)} \psi^{(+)}(x) & \text{if } x > \langle y_N \rangle \end{cases}. \quad (1.7)$$

Thus, we can display the LDP in terms of the rate function $\psi(x)$ and parameter W_N as [78, 79]

$$-\lim_{N \rightarrow \infty} \frac{\ln \mathcal{P}_{y_N}(x)}{W_N} = \psi(x). \quad (1.8)$$

The previous limit in Eq. (1.8) may not exist, yet we can still find upper and lower limits both exponential in N such that $e^{-N\psi^-(x)} \leq \mathcal{P}_{y_N}(x) \leq e^{-N\psi^+(x)}$. These two bounds establish the precise meaning of the statement that \mathcal{P}_{y_N} decays exponentially with N , giving rise to two large deviations principles defined in terms of an *inferior* and *superior limit* yielding $\psi^{(-)}(x)$ and $\psi^{(+)}(x)$, respectively [75–78]. In this thesis, we utilize Eq. (1.7) to introduce LDT assuming, at all times, that $\psi^{(-)}(x) = \psi^{(+)}(x)$ for all values of x .

When random variables are completely independent or weakly correlated, the rate function must fulfill [78, 79, 81]

- i. $\psi(x)$ is convex, i.e. $\psi''(x) > 0$;
- ii. $\psi(x) > 0$ for $x \neq \langle y_N \rangle$;
- iii. $\psi(x) = 0$ for $x = \langle y_N \rangle$;
- iv. if x is near $\langle y_N \rangle$, $\psi(x) \approx (x - \langle y_N \rangle)^2 / (2\sigma^2)$ where $\sigma^2 = 1/\psi''(x)|_{x=\langle y_N \rangle}$,

being the last point none other than the CLT. This last fact enables us to identify LDT as a generalization of the CLT.

From a practical point of view, we can think of LDT as a collection of methods gathered together to solve two principal problems [78]:

1. *Establish a large deviation principle for a given random variable,*
2. *Derive the expression for the associated rate function.*

It is possible to address both problems simultaneously; nonetheless, solving them does not always turn out to be a trivial task. In general, it may be extremely difficult or even impossible to derive large deviation principles through direct calculations; for instance, combinatorial methods based on Stirling approximations cannot be used for continuous random variables [78]. For those highly complicated cases, a general calculation path is provided by a significant LDT result known as the *Gärtner-Ellis theorem* [82, 83]. For this research, the Gärtner-Ellis theorem we use corresponds to a simplified version of the original theorem, yet, such a form is sufficient for the applications covered in this work. Before proclaiming the theorem, let us define a mathematical object within LDT, and an essential piece of our research, known as the *cumulant generating function* (CGF) from which the Gärtner-Ellis theorem emerges naturally [78, 79].

Definition 1.1 (Cumulant generating function). Let y_N be a random variable parametrized by a positive $N \in \mathbb{N}$, we define the *scaled cumulant generating function* of y_N as

$$\mathcal{F}(\mu) = \lim_{N \rightarrow \infty} \frac{1}{N} \ln \langle e^{N\mu y_N} \rangle, \quad (1.9)$$

with $\mu \in \mathbb{R}$.

Theorem 1.1 (Gärtner-Ellis). *If $\mathcal{F}(\mu)$ exists and is differentiable for all values of $\mu \in \mathbb{R}$, then y_N satisfies the large deviation principle with rate function $\psi(x)$ given by the Legendre transform of the scaled cumulant generating function,*

$$\psi(x) = \sup_{\mu \in \mathbb{R}} [\mu x - \mathcal{F}(\mu)]. \quad (1.10)$$

Proof. Let us assume that $\mathcal{F}(\mu)$ exists and is differentiable for all values of μ ; then, y_N obeys the large deviation principle, $\mathcal{P}_{y_N}(x) \asymp e^{-N\psi(x)}$. Consequently,

$$\int e^{-N[\psi(x) - \mu x]} dx \asymp \exp \left[-N \inf_{x \in \mathbb{R}} (\psi(x) - \mu x) \right],$$

and so

$$\mathcal{F}(\mu) = \sup_{x \in \mathbb{R}} [\mu x - \psi(x)].$$

Since we have assumed $\mathcal{F}(\mu)$ to be differentiable everywhere, the Legendre transform can be inverted, verifying the validity of Eq. (1.10) \square

This simple and heuristic proof seeks to illustrate two fundamental facts: firstly, to point out how the Legendre transform rises as a natural consequence of the Laplace approximation and, secondly, to demonstrate that the Gärtner-Ellis theorem is "born" as a direct implication of the LDP combined with Laplace's approximation [78, 84]. Unfortunately, even with all the excitement this theorem could carry, *not all rate functions can be calculated from it* [78, 79]. Prior to proceeding in more detail with this last statement, let us mention two important properties concerning the CGF:

1. $\mathcal{F}(\mu)$ is always convex. This comes as a general consequence of Hölder's inequality [78] and it was rigorously demonstrated in the works *inequalities* by Hardy, Littlewood, and Pólya (theorems 197 and 213) [85].
2. The convexity of $\mathcal{F}(\mu)$ directly implies continuity in the interior of its domain and differentiability everywhere except, maybe, in a denumerable number of points [86, 87].

So far, the rate functions obtained from the Gärtner-Ellis theorem are strictly convex, i.e., they do not possess linear parts. On the one hand, this last fact is verified easily from the formal definition of the Legendre transform; on the other hand, to demonstrate that such a transform yields strictly convex functions when $\mathcal{F}(\mu)$ is differentiable requires further work [78]. The details covering such proof are in Ref. [87] section 26, "*The Legendre transformation*".

Thus, if the Legendre transform yields necessarily convex functions, the immediate limitation concerning the Gärtner-Ellis theorem are non-convex rate functions and, in particular, rate functions with two or more local or global minima. The breakdown of this theorem for these functions is directly related to the differentiability condition of the CGF [78]. To correctly illustrate the last statement, let us take the example of a multi-atomic distribution whose probability density function is given by [88]

$$\mathcal{P}_{y_N}(x) = \frac{1}{2} \delta(x \pm 1). \quad (1.11)$$

Owing to the form of Eq. (1.11), the corresponding rate function for this case possesses the form,

$$\psi(x) = \begin{cases} 0, & \text{if } x = \pm 1 \\ \infty, & \text{otherwise} \end{cases}. \quad (1.12)$$

It is clear that the rate function of Eq. (1.12) has two minima; consequently, it cannot be, by any circumstance, a convex function. Thus, we cannot express it as the Legendre transform of its CGF.

Naturally, this creates more questions concerning the Gärtner-Ellis theorem and how to calculate rate functions. Interrogations as [78]: *is there a general connection between the differentiability of $\mathcal{F}(\mu)$ and the convexity of rate functions? Why is the differentiability condition for $\mathcal{F}(\mu)$ in the Gärtner-Ellis theorem so important? And, probably the most fundamental of all, what is the result of the Legendre-Fenchel transform of $\mathcal{F}(\mu)$ in general?* For the research developed in this thesis, we assume that the CGF is such that the Gärtner-Ellis theorem is valid. Should the reader wish to find answers to the previous questions, we strongly recommend Refs. [78, 86, 87].

1.3 Graph theory

If we could describe the world we live in, would we depict it as a *simple* or *complex* system where all its components interact variously? Certainly, guided by our daily experiences, many of us would agree to portray the world as a highly complex system. Interacting molecules in living cells, nerve cells in the brain, computers in a telecommunication network, and the social network of interacting people are just a few examples of complex systems that are linked together somehow [34, 35]. While it is true that we can study the behaviour of individual components, it is worthwhile performing research within the nature of their interactions in order to extract relevant information about the system. Following this line of thought, there is a crucial aspect to have in mind when we are dealing with these systems: *the pattern of connections between the components*; this pattern, for any given system, can be represented as a

network [35]. Then, it should not surprise us that, depending on particular patterns of interaction, the behaviour of the system changes [34, 35, 89]. Over the years, a large number of mathematical tools for analyzing, modelling, and understanding networks have been developed, providing useful information such as *what network is useful* for certain problems and making predictions about processes like city traffic, the internet, diseases, etc. [34, 35]. In the end, a network corresponds to simplified versions of interacting systems that capture only the basic connection patterns. Nevertheless, networks are formidable means of representing such patterns between the parts of a system [35, 89].

Being these systems modelled as networks, *Graph Theory* (GT) is the mathematical modelling investigating these complex systems. Next, we define the necessary notions of graph theory [34, 35, 89–92].

Definition 1.2 (Graph). We define a *graph* $G = (\mathcal{V}, \mathcal{E})$ as a family of two sets \mathcal{V} and \mathcal{E} , such that $\mathcal{V} = \{1, \dots, N\}$ are the so-called *vertices* and $\mathcal{E} \subseteq \mathcal{V} \times \mathcal{V}$ the *edges*.

Definition 1.3 (Neighbours). Given two vertices i and $j \in \mathcal{V}$, we say they are *neighbours* if $(i, j) \in \mathcal{E}$.

Definition 1.4 (Neighbourhood). We define the *neighbourhood* ∂i of a given vertex $i \in \mathcal{V}$ as the set of adjacent vertices to it.

Definition 1.5 (Degree). We define the degree $\deg(i) \equiv |\partial i|$ for any vertex $i \in \mathcal{V}$ as the number of edges that are incident to the vertex

Definition 1.6 (Path). We define a *path* as the set of edges that connects any sequence of different vertices

Definition 1.7 (Tree). We say a graph is a *tree* if for any two vertices there is exactly one path connecting them.

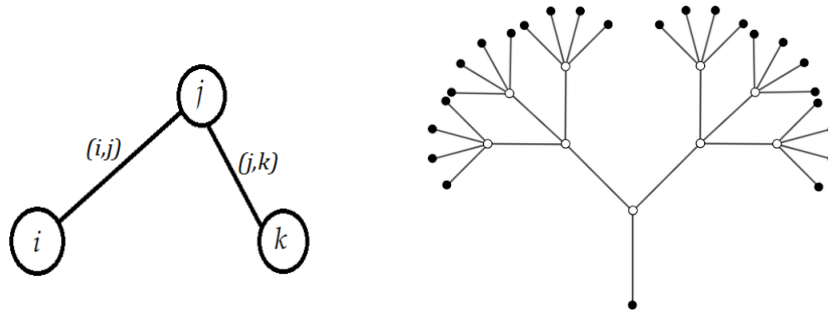


Figure 1.1: Graphic representation of a graph and a tree graph. **Left panel:** sketch of a graph picturing three vertices i , j , and k with edges (i, j) and (j, k) ; as the figure illustrates, vertices i and j , as well as j and k , are neighbours, but vertices i and k are not. **Right panel:** diagram of a tree graph picturing the fact that for any pair of vertices involved there is exactly one unique path connecting them.

Fig. 1.1 is called a *graph diagram* and acts as an intuitive representation of an actual graph [90–92]. In general, networks do not possess the regularity of a crystal lattice or any predictable architecture; they look as if they were spun randomly [34, 35, 89]. From a modelling point of view, a network is a simple object formed of only nodes and links. However, the crucial aspect when building networks is to decide where to place the links between the nodes to reproduce the complexity of real systems. One of the simplest procedures, and the one we use in this thesis, is to *place the links between the nodes randomly* [89]. This idea of *random nets* was first introduced within the context of mathematical biology for different branches [93] and popularized a decade later by Erdős and Rényi [94, 95]. Nowadays, random networks find applications not only in fields of physics and mathematics as complex networks, problems optimization, and information theory [35, 96] but also in areas such as linguistics [97], biology [98], and social sciences [99]. These prominent advances are mainly due to the research’s modern perspective in contrast with the *traditional graph theory* viewpoint. Instead of answering questions on specific graphs, current research focuses on studying the statistical properties of large graphs that appear in various scientific and social contexts [100].

Then, how do we build a network? The answer consists of only three steps [89]:

1. Start with N isolated nodes.
2. For each node pair, generate a random number between 0 and 1. If such a number is less than or equal to p (a certain probability measure), connect the node pair with a link; otherwise, leave them disconnected.

3. Repeat the previous step for the rest of the node pairs.

The resulting structure is commonly denoted as *random graph*, *random network*, or *Erdős-Rényi networks*, owing to the works of Erdős and Rényi [94, 95]. It is also called the $G(n, p)$ model, referring to all random graphs with n vertices connected via a probability p , where the presence of each edge is statistically independent of all others. There is also a second model called the $G(n, M)$ model, denoting all those graphs with n vertices connected by M edges randomly; these models are perhaps the simplest ones we can consider [35]. Also, there are two types of graphs whose characteristics depend entirely on the behaviour of their edges. If the direction of their edges matters, we say the graph is a *directed graph* or *digraph*; if not, we call it an *undirected graph*. Formally speaking, a directed graph is defined by a set of nodes and links where each link is an ordered pair of nodes [34, 90, 101]. We find this latter type of graph in areas such as biology [102, 103], where the directions of biological processes, cellular processes, and molecular functions (to mention a few) are essential [104].

From a mathematical perspective, it is convenient to define a graph by means of its *adjacency matrix* C .

Definition 1.8 (Adjacency matrix). We define $C \in M_{N \times N}(\{0, 1\})$ the *adjacency matrix* of a graph as

$$C_{ij} = \begin{cases} 1, & \text{if } (i, j) \in \mathcal{E} \\ 0, & \text{otherwise} \end{cases}. \quad (1.13)$$

The adjacency matrix encompasses all the essential information of a graph [34] and is helpful if we wish to store a large graph on a computer [90]. Furthermore, the previous concepts of directed and undirected graphs are easily translated into the matrix language. If the graph is directed (undirected), the adjacency matrix C is *non symmetric* (*symmetric*) [34, 35, 90–92, 101, 105, 106].

Since real-world-networks are characterized frequently by a finite average degree in their connections, $k = \deg(i)$ for $i \in \mathcal{V}$, a natural choice, and appealing to the $G(n, p)$ model, is to consider models with a connection probability decreasing with N , i.e. $p = \langle k \rangle / N$. To obtain the degree distribution $P(k)$, we need to use that the probabilities of creating a vertex with degree k and that vertex is connected to other k vertices, but not connected to the remaining $N - 1 - k$ vertices are the same; in other words, we deal with a *Bernoulli process* [101],

$$P(k) = \binom{N-1}{k} p^k (1-p)^{N-1-k}. \quad (1.14)$$

In the limit $N \rightarrow \infty$ for p constant, by the law of rare events [64], the binomial distribution approximates the *Poisson distribution* [107, 108]

$$P(k) = e^{-\langle k \rangle} \frac{\langle k \rangle^k}{k!}. \quad (1.15)$$

These graphs are known as *Poisson random graphs*. They have the property that the probability function for each entry in their adjacency matrix is

$$P(C_{ij}) = p\delta_{C_{ij},1} + (1-p)\delta_{C_{ij},0}. \quad (1.16)$$

Throughout this thesis, we employ the Poisson random graphs via the $G(n, p)$ model since, in real-world-networks, the number of links is rarely fixed. Also, we stipulate that the network must be a simple graph, i.e., it should not have multi-edges or self-edges, in which case the position of each edge is chosen among only those pairs that are distinct and not already connected. Consequently, the *joint probability density function* for the adjacency matrix C is given by

$$P\left(\{C_{ij}\}_{ij=1}^N\right) = \prod_{i < j} [p\delta_{C_{ij},1} + (1-p)\delta_{C_{ij},0}] \delta_{C_{ij}, C_{ji}}. \quad (1.17)$$

For these graphs, it is well-known that their spectrum contains a dense collection (an infinite number) of Dirac δ peaks [105, 109–112]. The latter can be verified in Fig. 1.2, where, for notation purposes, we have denoted $\langle k \rangle$ as c ; nomenclature that we will maintain throughout this work and will refer to as the *average connectivity* [110, 113].

The immediate observation one realizes in Fig. 1.2 is that the spectrum, depending on the c value, commences showing δ peaks all over it. These are δ peaks in the sense of *distribution theory* and correspond to exact degeneracies of the eigenvalues; nonetheless, owing to the arbitrary width of the histogram bins, their heights are not representative [110, 112]. Ref. [110] demonstrated that for any value of c and considerably large N ($N = 1000, 2000, 4000$), the highest δ peaks appear at positions $x = 0, \pm 1, \pm\sqrt{2}, \pm\sqrt{3}, \pm(\sqrt{5} \pm 1)/2, \pm\sqrt{2} \pm \sqrt{2}$, etc., and belong to small

trees eigenvalues [112]. Furthermore, the authors also proved that in the large limit $N \rightarrow \infty$ (fixed c), the spectral density displays an infinity of δ peaks at all eigenvalues of finite trees and the corresponding eigenvectors are strictly localized in the sense that the number of non-vanishing coordinates is finite [110, 112]. The δ peaks are mainly due to small trees present at all c values, and their heights are exponentially decreasing functions of c [110].

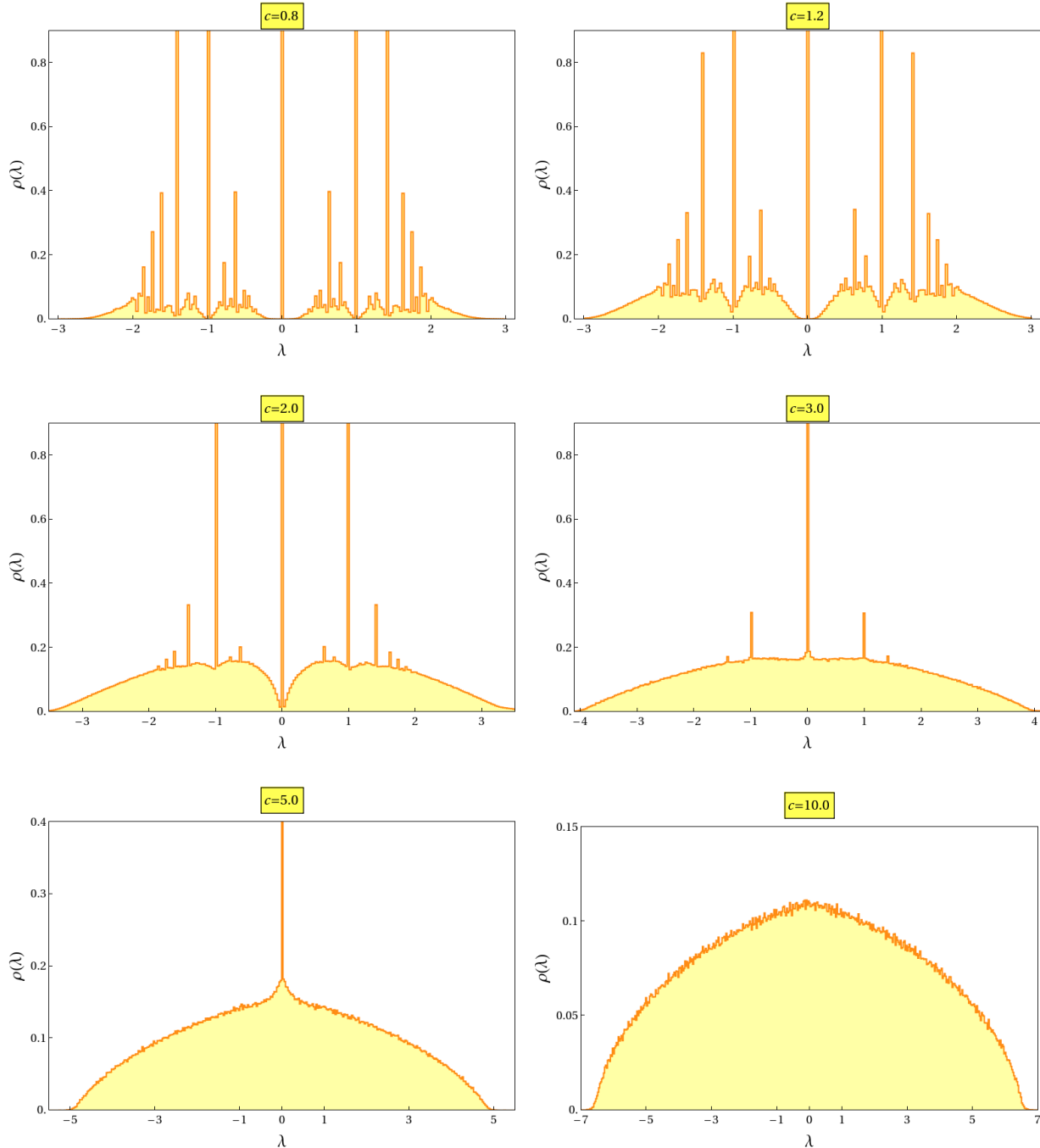


Figure 1.2: Spectral density of Poissonian random graphs for different values c of the average connectivity. Histograms of the spectrum for Poisson random graphs using fixed values of average connectivities of $c = 0.8, 1.2, 2.0, 3.0, 5.0,$ and 10.0 , for 10,000 matrices each of size 300×300

The fact that the δ peaks are more visible for small c values is related to a field known as *Percolation theory* (PT). For the research conducted on this thesis, we do not require PT; we mention it only for completeness purposes. PT provides a theoretical framework to understand the topological effects of removing nodes considering an arbitrary

network topology in which each node is occupied with probability p ; as p increases, connected components called *clusters* start emerging [101]. Recalling that the c value indicates the average number of connected nodes within a network, it is intuitive to assume that while small p forms small clusters, large p creates a *giant cluster* that fills most of the network (although there could be small clusters too), and $p = 1$ fully recovers the network [35, 101]. From a practical point of view, when we insert small values of c , we break the graph, favouring the appearance of Dirac δ peaks in the spectra. More information concerning PT can be found in Refs. [34, 35, 101], as well as in all their bibliographies.

1.4 Random matrix theory

1.4.1 Basic concepts and universality

Firstly introduced by Wishart in 1928 within the context of multivariate statistics in the analysis of large populations samples [6], and later proposed by Wigner [7, 8] in the area of nuclear physics,

the assumption is that the Hamiltonian which governs the behaviour of a complicated system is a random symmetric matrix with no particular properties except for its symmetric nature [114],

random matrix theory (RMT) has become an indispensable tool in areas besides physics and mathematics, such as biology, statistics, and finance [9–11, 13, 16]. In physics, pure and applied mathematics, a wide variety of problems are modelled by RMT in the following sense: let us say we wish to study some statistical quantities $\{a_k\}$ in a neighbourhood of some point A and we intend to compare them with the eigenvalues $\{\lambda_k\}$ of a random matrix in a vicinity of some point Λ . If the statistics of the initial $\{a_k\}$'s are described correctly by the statistics of the $\{\lambda_k\}$'s, both appropriately scaled,

$$a_k \rightarrow \tilde{a}_k = \gamma_a (a_k - A), \quad \lambda_k \rightarrow \tilde{\lambda}_k = \gamma_\lambda (\lambda_k - \Lambda)$$

with $\gamma_{a(\lambda)}$ scaling factors, we said then that the $\{a_k\}$'s are modelled by RMT [48, 115]. The crucial premise of RMT is that the large-scale behaviour of a complex system should be governed by its symmetries and the statistical properties of its many parameters and should not be sensitive to the precise details of each interacting element [31].

Mainly developed by Dyson [116], providing the foundations, and Mehta [11], describing the mathematical bases, the main objective of RMT has always been the study of the statistical properties of eigenvalues and eigenvectors of sets of matrices whose entries are completely random variables called *ensembles*. Initially, RMT was used to predict the form of the spectral correlation functions employing only certain symmetries of the systems, such as the spin value and time-reversal symmetry invariance [111]; after that, its use spread far beyond highly correlated systems. For instance, Bohigas et al. [19] introduced a conjecture, supported mainly by numeric evidence, arguing that RMT also correctly described the statistics of the spectrum of quantum systems whose classical analog is chaotic; other systems where RMT has also proved to work correctly are the so-called *disordered systems*. This last formulation was conjectured by Gor'kov and Eliashberg [117] and demonstrated in 1982 by Efetov [118]. More information concerning the general applications of RMT, as well as a review of their first implementations in physics, can be consulted in Refs. [10] and [17, 116, 119], respectively. Specifically, Ref. [116] provides an excellent introduction to RMT along with the collection of the original papers, published until 1965, of the first works realized on nuclear physics by Dyson, Mehta, Porter, and other authors.

Nowadays, the research field of RMT in physics has grown considerably, encompassing areas such as quantum mechanics [17], quantum chaos [19, 20], string theory [22, 23], quantum cosmology [21], disordered systems [120–124], quantum chromodynamics [125], among others [126]. Noteworthy is that RMT has become a branch *sui generis* of theoretical physics with its own concepts and mathematical methods [17]. We commence establishing the basic definitions of RMT:

Definition 1.9 (Random matrix). The array $\mathbf{A} \in M_{N \times M}(K)$ whose entries A_{ij} correspond to random variables taking values over $K = \mathbb{R}, \mathbb{C}, \mathbb{H}$, and \mathbb{O} is denominated as *random matrix*.

Definition 1.10 (Spectrum). Let $\mathbf{A} \in M_{N \times N}(K)$ be a random matrix; the set of the eigenvalues of \mathbf{A} , $\Lambda_{\mathbf{A}} = \{\lambda_1, \dots, \lambda_N\}$ such that $\lambda \in \mathbb{R}, \mathbb{C}, \mathbb{H}$, and \mathbb{O} , is called the *spectrum* of \mathbf{A} .

In applications, the entries A_{ij} represent the strength and sign of pairwise interactions between elements. Depending on the context, various properties of the system under study lie within the corresponding eigenvalues λ_j and eigenvectors v_j , whether the latter are *left* or *right eigenvectors* [31]. For this thesis, we focus on the case $K = \mathbb{C}$ and introduce the following definition:

Definition 1.11 (Empirical spectral density). Given $\mathbf{A} \in M_{N \times N}(\mathbb{C})$ a random matrix with spectrum Λ , we define the *empirical spectral density* (ESD) as

$$\rho_{\mathbf{A}}(z) = \frac{1}{N} \sum_{i=1}^N \delta(z - \lambda_i), \quad (1.18)$$

with $z \in \mathbb{C}$ and δ the Dirac delta distribution on the complex plane.

The ESD is one of the simplest ways to capture the spectral properties of matrices as well as operators [31]. Commonly, the interest in this quantity lies in its averaged limit distribution at large N , i.e.,

$$\rho(z) = \lim_{N \rightarrow \infty} \frac{1}{N} \left\langle \sum_{i=1}^N \delta(z - \lambda_i) \right\rangle_{\mathbf{A}}. \quad (1.19)$$

Depending on the random matrix ensemble selection, as $N \rightarrow \infty$, the spectrum and *averaged empirical spectral density* (AESD) $\rho(z)$ may converge to a deterministic distribution [31]. The AESD $\rho(z)$ results from averaging $\rho_{\mathbf{A}}(z)$ over \mathbf{A} .

Generally, research focuses on the spectral properties of operators such as the Hamiltonian or, more generally, matrix operators describing certain types of correlations. Nonetheless, providing mathematical expressions for such operators is not always possible, and even if it were, their analyses turn out to be highly complicated. RMT replaces those deterministic operators by random matrices, transforming unsolvable problems into solvable ones while keeping many of their principal features. Since several physical systems display universal characteristics, i.e. properties that do not depend on the system details, we can employ appropriate random matrix models, which may be solvable analytically, for such systems. Hence, the importance of RMT as an alternative tool to deterministic operators mainly lies in the *universality* of the spectral properties of random matrices. In other words, *establishing universality for matrix ensembles is a crucial technical element in RMT* [10].

We can assign three meanings to the concept of universality [10]:

1. Several statistical properties of eigenvalues and eigenvectors in the limit $N \rightarrow \infty$ are independent of the probability distribution choice for the matrix elements.
2. In the $N \rightarrow \infty$ limit, RMT becomes equivalent to other more physically-motivated *effective field theories* that depend on the same global symmetries. Thus, we can think of RMT as the simplest, solvable model that captures the fundamental degrees of freedom of a theory.
3. The emerging limiting distributions in the $N \rightarrow \infty$ limit also appear as the limit of other statistical ensembles, not necessarily related to random matrices.

The *conjecture of universality* for symmetric and Hermitian random matrices establishes that [10, 31]:

local eigenvalues statistics of many random matrix ensembles in the large matrix size limit are the same, i.e., they do not depend on the exact probability distribution placed on a set of matrices but only on some general characteristics of the ensemble.

There are specific features that play a role in determining the so-called *universality classes* [10]:

1. Invariance of ensembles under specific conjugation operations.
2. The distinction between real symmetric or complex Hermitian random matrix ensembles. Even without the invariance assumption, universality of local eigenvalue statistics is conjectured to hold [127–130]. Universality is also expected to exist in certain classes of non-Hermitian matrices [10, 131].
3. The nature of the point where we consider the local statistics of eigenvalues. Depending on the spectrum point, there are specific universality classes such as the *bulk*, *edge* and *hard-edge universality*; details in Refs. [9, 10].

Ref. [10] provides a formal statement of universality for symmetric and Hermitian random matrices via the k -point correlation function. Let $\{X_1, \dots, X_n\}$ be a collection of random variables with $P_n(x_1, \dots, x_n) \in \mathbb{R}^n$ a symmetric, invariant under coordinates permutations probability density, and the k -point correlation function defined as

$$R_{nk}(x_1, \dots, x_k) = \frac{n!}{(n-k)!} \int \cdots \int P_n(x_1, \dots, x_n) dx_{k+1} \cdots dx_n. \quad (1.20)$$

Next, let $x^* \in \mathbb{R}$ be a reference point and $c_n > 0$ a constant such that each point x_i , $i = 1, \dots, n$, can be centred around x^* and rescaled by c_n , i.e.,

$$(x_1, x_2, \dots, x_n) \rightarrow (c_n(x_1 - x^*), c_n(x_2 - x^*), \dots, c_n(x_n - x^*)).$$

Consequently, the centred and scaled points will have a rescaled k -th point correlation function of the form

$$\frac{1}{c_n^k} R_{n,k} \left(x^* + \frac{x_1}{c_n}, x^* + \frac{x_2}{c_n}, \dots, x^* + \frac{x_n}{c_n} \right). \quad (1.21)$$

Universality at x^ means that for a suitable sequence (c_n) , the rescaled k -point correlation function will have a finite specific limit as $n \rightarrow \infty$.* In other words, the statistics of the random variable $R_{nk}(x_1, \dots, x_n)$ remains asymptotically unchanged in the limit $n \rightarrow \infty$ as each X_i is rescaled [30]. The universality classes are determined by the form the k -point correlation function is rewritten (details in Refs. [9, 10, 48]).

1.4.2 Classical and Ginibre ensembles

Within RMT, there is a wide variety of ensembles, but perhaps, the most common explored over the years have been the *Gaussian* [9, 11] or *Wigner-Dyson* [132] ensembles, also known as *classical ensembles* [18]. Since we commonly characterize systems by their Hamiltonians, which by definition are represented by Hermitian matrices, these ensembles are introduced as $N \times N$ Hermitian matrices whose entries are drawn from a Gaussian distribution with different mean and variance depending on whether or not the entries are on the diagonal (details in Ref. [9]) and joint distribution invariant under conjugation operations by appropriate unitary matrices U [9, 11, 115].

We say $\mathbf{A} \in M_{N \times N}(K)$ belongs to the Gaussian ensembles if \mathbf{A} is drawn according to the distribution [9, 11, 115]

$$P(\mathbf{A}) d\mathbf{A} = \frac{1}{Z_N} e^{-\frac{\beta}{2} \text{Tr} \mathbf{A}^2} d\mathbf{A}, \quad (1.22)$$

with β the *Dyson index* having values $\beta = 1, 2$, and 4 whenever $K = \mathbb{R}, \mathbb{C}$, or \mathbb{H} , respectively; $d\mathbf{A}$ the *volume form* or *volume measure* implying the *wedge product* of the independent elements of $d\mathbf{A}$, and the normalization constant

$$Z_N = \int e^{-\frac{\beta}{2} \text{Tr} \mathbf{A}^2} d\mathbf{A}. \quad (1.23)$$

The classical ensembles divide into different classes depending on whether their elements are real, complex, or real quaternion and their invariance under conjugation $\mathbf{A} \rightarrow \mathbf{U} \mathbf{A} \mathbf{U}^{-1}$ by orthogonal, unitary, and unitary symplectic matrices, respectively; these invariances are deeply connected to the concept of *time-reversal symmetry* in quantum mechanics [9, 11, 18, 115, 132]. Consequently, we classify them according to their properties concerning the *time-reversal operator* T and relate them to a specific value of the Dyson index (*Dyson's threefold way* [11, 133]) as follows [9, 18, 115]:

1. **Gaussian Orthogonal Ensemble** GOE ($\beta = 1$): models the statistical properties of physical systems with time-reversal symmetry such that the time-reversal operator fulfills $T^2 = 1$;
2. **Gaussian Unitary Ensemble** GUE ($\beta = 2$): models the statistical properties of physical systems lacking time-reversal symmetry;
3. **Gaussian Symplectic Ensemble** GSE ($\beta = 4$): models the statistical properties of physical systems with time-reversal symmetry such that the time-reversal operator fulfills $T^2 = -1$.

One of the achievements of RMT has been expressing the *joint probability distribution of eigenvalues* (JPDE) of the three ensembles in a unified analytical expression of the form [9, 11]

$$P_\beta(x) = \frac{1}{Z_\beta} \exp \left(-\frac{\beta}{2} \sum_{i=1}^N x_i^2 \right) \prod_{1 \leq i < j \leq N} |x_j - x_i|^\beta, \quad (1.24)$$

with $x_i \in \mathbb{R}$ and Z_β a constant that permits to normalize $P_\beta(\mathbf{x})$ to unity, i.e.

$$\int P_\beta(\mathbf{x}) d\mathbf{x} = 1. \quad (1.25)$$

Def. 1.9 on page 9 establishes that K could also take values on \mathbb{O} ; then, the immediate question is whether or not there is a Dyson labelling for this case. Effectively, the classification exists for real octonion elements, having Eq. (1.24) as the JPDE function with the modification $N = 2$ and $\beta = 8$; further details can be consulted in Ref. [9]. Since we do not require this case for future developments in this thesis, we will omit it for the subsequent chapters.

Eq. (1.24) illustrates that the probability of two eigenvalues being close together is small and vanishes like a power of β as the distance between them increases [48]. Dyson went a step further [133–137] and, introducing the function $V : \Lambda \rightarrow \mathbb{R}$, rewrote Eq. (1.24) as a Gibbs-Boltzmann distribution

$$P_\beta(\mathbf{x}) = \frac{1}{Z_N} e^{-\frac{\beta}{2}F(\mathbf{x})}, \text{ such that } F(\mathbf{x}) = \sum_{i=1}^N V(x_i) - \sum_{i \neq j}^N \ln|x_i - x_j|; \quad (1.26)$$

clearly, for the Gaussian ensembles $V(x) = x^2$. Written in such a form, Eq. (1.26) describes the thermodynamical properties of a one-dimensional gas of N equally charged (*one-component* [9]) particles constrained to move along a one-dimensional line confined by the external potential $V(x)$ and with pairwise interaction equal to $-\ln|x_i - x_j|$. We refer to this charged gas as the *one-dimensional Coulomb gas* or *Dyson one-component log gas* [9, 132–137]. Eq. (1.26) is not restricted only to the Gaussian ensembles; by adequately writing V , we can recover, for instance, the Wishart-Laguerre ensemble JPDE [9, 10, 138].

After the classical ensembles, Ginibre moved forward and placed the natural generalization to non-Hermitian random matrices by simply dropping the used symmetries [25]. The so-called *Ginibre ensemble* consists of $N \times N$ random matrices with all their entries independent and drawn from a Gaussian distribution with variance $1/N$, modelling complex systems where all their elements interact with directed interaction. As for the classical ensembles, Ginibre deduced the JPDE function for the non-Hermitian Gaussian matrices with complex and quaternion entries [25]; it was not until approximately twenty-six years later that Lehmann and Sommers [139] derived the JPDE for the real Ginibre ensemble case. Owing to its form,

$$P(z_1, \dots, z_N) = \frac{1}{Z_N} \exp \left(-N \sum_{i=1}^N \|z_i\|^2 + 2 \sum_{i < j} \ln \|z_i - z_j\| \right) \quad (1.27)$$

with Z_N a normalization constant, the JPDE for the complex Ginibre ensemble (Eq. (1.27)) can also be mapped to a Boltzmann distribution describing a one-component two-dimensional Coulomb gas of N interacting charges confined to move in a quadratic potential with a neutral background and pairwise interaction equal to $2 \ln \|z_i - z_j\|$ [9, 25]. Both equations, (1.26) and (1.27), illustrate two competing interactions for the fluid of charged particles: a quadratic potential thrusting all particles toward the origin and a logarithmic repulsion spreading any pair of particles apart.

These two types of ensembles (Gaussian and Ginibre) offer each one a universal result for the spectral distribution convergence in the thermodynamic limit $N \rightarrow \infty$. On the one hand, for the Gaussian ensembles, and in general for Wigner matrices (symmetric and Hermitian) [30], the limiting spectral density converges almost surely to

$$\rho_W(\lambda) = \begin{cases} \frac{1}{\pi} \sqrt{2N - \lambda^2}, & \text{if } |\lambda| < \sqrt{2N} \\ 0, & \text{if } |\lambda| > \sqrt{2N} \end{cases}, \quad (1.28)$$

the so-called *Wigner semicircle law* [11, 24]. In more recent textbooks, such as Ref. [9], the author refers to Eq. (1.28) as the *particle density* for the log-potential systems (Eq. (1.26)) and the limiting value of the global density,

$$\tilde{\rho}(x) \equiv \lim_{N \rightarrow \infty} \sqrt{\frac{2}{N}} \rho_W(\sqrt{2N}x), \quad (1.29)$$

as the Wigner semicircle law

$$\tilde{\rho}_W(x) = \frac{2}{\pi} \sqrt{1 - x^2}, \quad (1.30)$$

for $|x| < 1$ and equal to zero otherwise (Fig. 1.3, left panel) [9]. On the other hand, for the complex [11] an real [140] Ginibre ensembles, and in general for non-Hermitian matrices with complex entries of zero mean and unit variance [29], as $N \rightarrow \infty$ the normalized limiting spectral density (eigenvalues rescaled as λ/\sqrt{N} , $\lambda \in \mathbb{C}$) converges both in probability and almost surely to the unit disk on the complex plane

$$\rho_G(z) = \frac{1}{\pi} \mathbf{1}_{[0,1]}(\|z\|) dz, \quad (1.31)$$

where the indicator function $\mathbf{1}_\Omega(x)$ is equal to one if $x \in \Omega$ and zero otherwise. Eq. (1.31) is known as *Girko's circular law* or simply *circular law* (Fig. 1.3, right panel) [26–28]. For small N , the density of states on the real axis is higher than the average density, whereas slightly above and below the real axis, it is smaller than the average. Ref. [141] demonstrated that this non-uniform behaviour was due to finite-size effects (Fig. 3, Ref. [141]) and originated from the fact that the level repulsion of eigenstates near the real axis is less than the average level repulsion. This effect vanishes as $N \rightarrow \infty$ roughly as $N^{-1/2}$ [141].

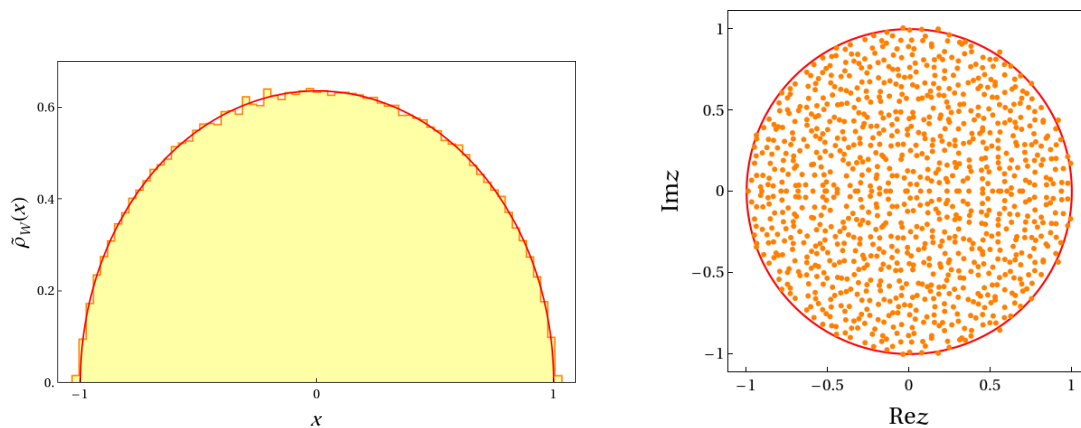


Figure 1.3: Limit distribution for the classical and Ginibre ensembles. **Left panel:** Wigner semicircle law for symmetric and Hermitian random matrices. **Right panel:** Girko's circular law for fully asymmetric and non-Hermitian random matrices.

Both limiting spectral distributions, Eq. (1.30) and (1.31), illustrate the roots of universality: the details of the distributions characterizing the all-to-all random interactions for Hermitian and non-Hermitian systems lack of importance for the spectral distribution in the limit of infinitely large random matrices [31].

Inspired by the Wigner semicircle law, it was conjectured that Girko's law should also be a universal result for non-Hermitian random matrices. This conjecture was just recently proved for non-Hermitian matrices whose entries A_{ij} are independent complex random variables with zero mean and unit variance [29]; for further background on Girko's circle law, see Refs. [30, 142]. The main problem one faces in providing a limiting spectrum in the $N \rightarrow \infty$ limit for non-Hermitian random matrices is their spectral instability. While the well-known methods employed for large Hermitian matrices ensure spectral stability, small perturbations of order $\varepsilon > 0$ for large non-Hermitian matrices can lead to large fluctuations within the spectrum, making the usual techniques highly inefficient [30]. This last argument, combined with an unknown JPDE function for many non-Hermitian ensembles, make the study of the statistical properties of non-Hermitian random matrices a still-open problem.

1.4.3 Replica method

Let us suppose we have a physical system whose Hamiltonian $H_J[\sigma]$ depends on the configuration $[\sigma]$ of the spins that form it and on some other control variables J (*quenched variables*), which are distributed according to a probability distribution P_J [143]; an example of a system with such characteristics is the *Ising model* [3, 144]. For each choice of the J s, we define the partition function

$$Z_J = \sum_{\sigma} e^{-\beta H_J[\sigma]} \quad (1.32)$$

and free energy

$$F_{\mathbf{J}} = -\frac{1}{\beta N} \ln \sum_{\boldsymbol{\sigma}} e^{-\beta H_{\mathbf{J}}[\boldsymbol{\sigma}]}, \quad (1.33)$$

with N representing the total number of the $\boldsymbol{\sigma}$ variables [143].

Statistical mechanics deals with computing the free energy at given \mathbf{J} s; at all times, we assume the latter are random variables whose probability distribution is known. Physically, computing of Eq. (1.33) at fixed values of the quenched variables comes from the fact that changes in the \mathbf{J} s tend to happen on infinitely larger time scales than the ones characterizing the $\boldsymbol{\sigma}$ shifts [143]. For instance, let us consider the Ising model with N spins with no external magnetic field ($h = 0$), whose Hamiltonian is given by

$$H_{\mathbf{J}}[\boldsymbol{\sigma}] = -\sum_{\langle i,j \rangle} J_{ij} \sigma_i \sigma_j, \quad (1.34)$$

where the symbol $\langle i,j \rangle$ means the sum over nearest neighbours. The quenched variables J_{ij} , for all $i, j \in \{1, \dots, N\}$, represent the *magnetic coupling* between the neighbouring sites i and j , whereas the σ_i variable (*spin* at site i) switches between two possible configurations: *spin up* ($\sigma_i = +1$) and *spin down* ($\sigma_i = -1$) for all sites $i = 1, \dots, N$ [3,145,146]. Before analyzing the Hamiltonian (1.34), it is necessary to determine all the couplings J_{ij} so they remain fixed all the time (details in Ref. [145]); this process leads to a particular choice, or *realization*, of the couplings [145]. If interactions within the system are not too complicated, thermodynamics arguments assure that in the limit $N \rightarrow \infty$, $F_{\mathbf{J}}$ assumes the same value for each set of the control parameters \mathbf{J} that has a non-vanishing probability, i.e., $F_{\mathbf{J}}$ is a *self-averaging quantity* [143]. For disordered systems with self-averaging quantities, their thermodynamic properties are the same regardless of the specific choice of quenched variables. Hence, these must be a kind of average over the disorder caused by the realization. In other words, an average over the *quenched disorder* [147,148].

We are commonly interested in deriving the so-called *free energy per particle*

$$f \equiv \lim_{N \rightarrow \infty} \langle F_{\mathbf{J}} \rangle_{\mathbf{J}} = -\frac{1}{\beta} \lim_{N \rightarrow \infty} \frac{1}{N} \langle \ln Z_{\mathbf{J}} \rangle_{\mathbf{J}}, \quad (1.35)$$

where the symbol $\langle \dots \rangle_{\mathbf{J}}$ denotes the quenched disorder average [143,149]. To obtain f , we must compute the disorder average after calculating the logarithm but before evaluating the thermodynamic limit $N \rightarrow \infty$ [149]. In general, direct attempts to compute Eq. (1.35) are very complicated. To overcome this difficulty, we appeal to a mathematical technique known as the *replica method*. The basis of this method lies in the computation of f by some analytic continuation procedure from the average of the partition function for n uncoupled replicas of the initial system [143,149,150]. Practically, we depart from the exact relation

$$\ln Z = \lim_{m \rightarrow 0} \frac{Z^m - 1}{m} \quad (1.36)$$

and rewrite Eq. (1.32) as

$$Z_{\mathbf{J}}^n = \sum_{\boldsymbol{\sigma}_1} \cdots \sum_{\boldsymbol{\sigma}_n} \exp \left(-\sum_{a=1}^n \beta H_{\mathbf{J}}[\boldsymbol{\sigma}_a] \right), \quad (1.37)$$

where we have assumed $n \in \mathbb{Z}^+$ and introduced n replicas of the same system [143]; then, averaging the logarithm of Eq. (1.35) is equivalent to averaging Eq. (1.37) and taking the $n \rightarrow 0$ limit [150]. Indeed, the partition function of the n replicas of the same system is the partition function of the original system powered to n . In principle, we must first calculate the $n \rightarrow 0$ limit followed by the $N \rightarrow \infty$ limit; nonetheless, in practice, we reverse the order of the limits [143,150]. Despite a non-existent formal mathematical justification for such an inversion, numerical results have demonstrated the efficiency of this approach.

Throughout this thesis, and inspired by the terminology used in Ref. [149], we refer to Eq. (1.37) as the *replica trick* and the complete procedure for computing Eq. (1.35) as the replica method. Hence, the replica method encompasses the following three steps [143]:

- (i) compute Eq. (1.37) for positive integer n ,
- (ii) extend the resulting equation to an analytic function for n , and
- (iii) calculate the free energy f .

The replica method was first translated to the language of RMT in the seminal work of Edwards and Jones [151] as an alternative proof to Mehta's derivation of the Wigner semicircle law [12] based on expressing the ESD of an $N \times N$ symmetric random matrix M as the product of n multiple Fresnel integrals [152]. Appealing to Eq. (1.36), the authors expressed the ESD (Eq. (1.18)) as

$$\rho_M(\lambda) = \lim_{\varepsilon \rightarrow 0^+} \lim_{n \rightarrow 0} \frac{-2}{Nn\pi} \text{Im} \frac{\partial}{\partial \lambda} \left\{ \left(\frac{e^{i\frac{\pi}{4}}}{\sqrt{\pi}} \right)^{Nn} \int \left(\prod_{j=1}^N \prod_{a=1}^n dx_{ja} \right) \exp \left[-i \sum_{j,k=1}^N \sum_{a=1}^n x_{ja} (\lambda_\varepsilon \mathbf{I}_N - M)_{jk} x_{ka} \right] - 1 \right\}, \quad (1.38)$$

where they defined $\lambda_\varepsilon \equiv \lambda - i\varepsilon$ ($\varepsilon > 0$), assuming at all times that integration held for all values of n and the analytic continuation was possible. Eq. (1.38) pointed out the replica method as a new and straightforward technique for calculating the spectrum of symmetric and Hermitian random matrices [151].

In general, for square symmetric and Hermitian matrices \mathbf{H} , RMT follows the same path carried out by the physics of disordered systems and determines the desired statistical properties of the eigenvalues and eigenvectors via the trace of the *resolvent* (*Stieltjes transform*) [150] or *Green matrix* [36] $G(z) = (z\mathbf{I}_N - \mathbf{H})^{-1}$ with $z \in \mathbb{C} \setminus \Lambda_{\mathbf{H}}$ commonly defined as $z = \lambda - i\varepsilon$ ($\varepsilon > 0$) [153], expressing the AESD (Eq. (1.19)) as

$$\rho(\lambda) = \lim_{N \rightarrow \infty} \lim_{\varepsilon \rightarrow 0^+} \frac{1}{N\pi} \text{Im} \langle \text{Tr} G(z) \rangle_{\mathbf{H}}. \quad (1.39)$$

The immediate advantage of Eq. (1.39) is the possibility of extracting useful information employing basic mathematical manipulations [31]; some authors [10, 153, 154] follow a similar procedure and express the AESD as $\rho(\lambda) = -\lim_{N \rightarrow \infty} \frac{1}{N\pi} \partial_{z^*} \langle \text{Tr} G(z) |_{z=\lambda} \rangle_{\mathbf{H}}$.

To facilitate the handling of Eq. (1.39), RMT uses the equality of Eq. (1.36) and reformulates the average of the resolvent trace as

$$\langle \text{Tr} G(z) \rangle_{\mathbf{H}} = -2 \lim_{n \rightarrow 0} \frac{1}{n} \partial_z \langle \mathcal{Z}^n(z) \rangle_{\mathbf{H}}, \quad (1.40)$$

with

$$\mathcal{Z}^n(z) = \int \left(\prod_{i=1}^N \prod_{a=1}^n \frac{d\psi_{ia}}{\sqrt{2\pi}} \right) \exp \left[-\frac{1}{2} \sum_{i,j=1}^N \sum_{a=1}^n \psi_{ia} (z\mathbf{I}_N - \mathbf{H})_{ij} \psi_{ja} \right] \quad (1.41)$$

the partition function of n replicas on the initial random system running over the auxiliary real vector field $\psi = (\psi_1, \dots, \psi_N)^T$ and \mathbf{H} the $N \times N$ Hermitian random matrix modelling the Hamiltonian's system [150].

Although the spectrum of Hermitian matrices has *zero Lebesgue measure* on the real axis \mathbb{R} , the spectrum of non-Hermitian matrices generally possesses a *non-zero Lebesgue measure* on the complex plane \mathbb{C} ; consequently, the usage of the resolvent is no longer possible. In order to proceed with the last argument, it is worth recalling that while the spectrum of matrices is composed of different discrete sets of eigenvalues, the spectrum of an operator also has continuous components and eigenvalues of infinite multiplicity [31]. According to *Borel's* and *Lebesgue's decomposition* theorems [155, 156], the spectral distribution ρ for operators can be divided into three mutually singular components [31]

$$\rho = \rho_{ac} + \rho_{sc} + \rho_{pp}, \quad (1.42)$$

each supported by an analogous split within the spectrum

$$\Lambda = \Lambda_{ac} \cup \Lambda_{sc} \cup \Lambda_{pp}. \quad (1.43)$$

The *absolute continuous* part ρ_{ac} stands as a function supported on $\Lambda_{ac} \subseteq \mathbb{C}$, a set of non-zero Lebesgue measure; the *singular continuous* component ρ_{sc} is a continuous distribution on $\Lambda_{sc} \subseteq \mathbb{C}$, a set with zero Lebesgue measure; and, finally, the *pure point* contribution ρ_{pp} corresponds to a countable sum of weighted Dirac δ distributions supported on a collection of points Λ_{pp} . Furthermore, the pure point part of the spectrum can be bifurcate into eigenvalues of finite and infinite multiplicity, being the former the discrete part of the spectrum. For finite dimensional matrices, the ESD ρ_A is discrete; however, as the matrix dimension tends to infinity, ρ_A can converge to a spectral distribution ρ that may have continuous components and eigenvalues of infinite multiplicity [31].

It is the fact that the spectrum for symmetric and Hermitian matrices lies on \mathbb{R} , the cornerstone for inferring the eigenvalue distribution ρ from the trace of $G(z)$, which exists in the non-real part of \mathbb{C} . Appealing to the *Sokhotski–Plemelj theorem* [157], $\delta(x) = 1/\pi \lim_{\varepsilon \rightarrow 0^+} \text{Im} (x - i\varepsilon)^{-1}$, and the *Lorentzian* representation of the δ distribu-

tion, we can prove that for $\mathbf{H} \in M_{N \times N}(\mathbb{C})$ a Hermitian matrix,

$$\frac{1}{\pi} \operatorname{Im} \left[\frac{1}{N} \operatorname{Tr} G(\lambda - i\varepsilon) \right] = \frac{1}{\pi} \int_{-\infty}^{+\infty} \frac{\varepsilon}{\varepsilon^2 + (x - \lambda)^2} \rho_{\mathbf{H}}(x) dx; \quad (1.44)$$

tending $\varepsilon \rightarrow 0^+$, we recover the ESD $\rho_{\mathbf{H}}(\lambda)$ for $\lambda \in \mathbb{R}$. Eq. (1.44) corresponds to the regularized version of the spectral density and is considered the cornerstone of Hermitian RMT since both limits $\varepsilon \rightarrow 0^+$ and $N \rightarrow \infty$ can be safely interchangeable, allowing us to work entirely with the well-behaved resolvent defined in the upper half part of \mathbb{C} [31]. Unfortunately, for non-Hermitian random matrices, the spectrum does not have zero Lebesgue measure on \mathbb{C} , setting aside the safe ground provided by the resolvent. Should we wish to appeal to the trace of the resolvent for non-Hermitian matrices, we would find ourselves with the equivalent of Eq. (1.39) under the modification [158]

$$\operatorname{Tr} G(z, z^*) = \sum_{i=1}^N \frac{1}{(x - \operatorname{Re}\lambda_i) + i(y - \operatorname{Im}\lambda_i)}. \quad (1.45)$$

Even when it is desirable to proceed with Eq. (1.45), handling it is far from an easy task. Then, one is tempted to appeal to quaternionic variables and rewrite the sum of Eq. (1.45) as

$$\sum_{i=1}^N \frac{1}{(\mathbf{q} - \lambda_i) |\mathbf{q} - \lambda_i|}, \quad (1.46)$$

with $\mathbf{q} = a + bi + cj + dk$ a quaternionic variable and $|\mathbf{q}| \equiv \sqrt{a^2 + b^2 + c^2 + d^2}$ its absolute value. The form Eq. (1.46) has taken, is far from being written as a simple trace, making any attempt to use Eq. (1.39) a dead end [158]. To use the replica method on non-Hermitian matrices, we need to introduce certain modifications to the non-Hermitian problems so we can apply the tools from Hermitian RMT (the details of this argument will be mentioned in the following chapter). In the same way, the usage of the replica method may naturally arise within the mathematical handlings of certain systems, leading to an extension of n not only to real but also to complex values. This remarkable extension has the feature that now the analytic continuation is allowed to reach further values in both \mathbb{R} and \mathbb{C} .

From a formal mathematical perspective, the usage of the replica method seems like a counterintuitive construction: we depart from a particular integration that makes no sense for n other than positive integers and attempt to analytically continue it to a close vicinity of $n = 0$ or other value. Certainly, this procedure stands as a non-trivial task. Firstly, the analytic continuation, in general, is not unique, and secondly, to retain control over the continuation, the latter must rest on an exact calculation of the average replicated partition function for $n \in \mathbb{Z}^+$ [153]. Naturally, these facts lead to more interrogations concerning the mathematical formality behind the analytical extension to real or complex values of n . Ref. [149] provides a series of answers based on the analyticity and convexity of the replicated partition function (Eq. (1.37)). Sadly, the analyticity argument ends on a dead end due to the difficulty in demonstrating that Eq. (1.37) is analytical and bounded; on the other hand, the convexity argument offers a simpler alternative to formally prove the analytic continuation of the replicated partition function (for specific details see Ref. [149]). In the end, the existing mismatch between the available partition function ($n \in \mathbb{Z}^+$) and the needed partition function ($n \in \mathbb{R}$ or \mathbb{C}) is at the heart of the trickery of the replica field theories and the center of many discussions about the applicability of the method [153]. For this thesis, we appeal to the convexity argument to base the analytic continuation of our equations as well as the existence of the thermodynamic limit and its interchange with the replica limits through our calculations.

To conclude this subsection, we highlight that the replica method is not the only available technique to explore the statistical properties of the different ensembles of random matrices. Along with it, there are several methods as the *Painlevé equations*, "*supersymmetry*", *orthogonal polynomials*, and *cavity method*, among others. If the reader wishes to know more about these methods, we recommend Refs. [10].

Chapter 2

Statistical properties of sparse non-Hermitian random matrices

Science is not a collection of truths. It is a continuing exploration of mysteries.

Freeman John Dyson (1923-2020)

This second chapter displays the achievements obtained in this doctoral research for sparse non-Hermitian random matrices. To provide a complete picture of these kinds of ensembles, we separate the chapter into three sections. In Section 2.1, we introduce sparse random matrices by mentioning the seminal work of Rodgers and Bray, the famous approximate methods EMA, SDA, DEMA, and SEMA (to be introduced in this section), and the recent research of Kühn et al., the immediate predecessors of our research. We display the crucial elements of the mentioned studies and highlight the equations responsible for the actual status of the area; the remaining two sections show the entire findings of our research for sparse non-Hermitian random matrices applied to the particular case of the diluted version of the real Ginibre ensemble. In Section 2.2, we obtain the complete statistics, typical and atypical fluctuations, of the number of eigenvalues \mathcal{N}_D inside a smooth Jordan curve in a region D contained in the complex plane for the diluted real Ginibre ensemble. Finally, for Section 2.3, we retake \mathcal{N}_D and constrain it to have a specific quantity of eigenvalues within the Jordan curve, introducing an adjustable parameter within our theory and computing the so-called constrained spectral density. For both final sections, all our findings are analyzed and compared with exact numerical diagonalization for ensembles of finite random matrices, displaying excellent agreement.

2.1 Background

Large *sparse random matrices* (SRMs) arise naturally in the adjacency matrix of large graphs, whose vertices present degrees selected from a fixed distribution [10]. Formally speaking, SRMs are matrices having a mean finite number p of non-zero elements per row with a general distribution $\rho(J)$ [36–39]. In contrast to their non-diluted counterparts, SRMs model complex systems where a given degree of freedom interacts only with a small number of others; also, it is possible to find sparsity in *disordered quantum systems*, such as the *quantum Ising chains*, where the spins in the chain interact with a small additional number of spins from a total added to the model [159]. Commonly, real-world complex systems such as neuronal networks and ecosystems interact via directed interactions; then, it is appropriate to model these systems throughout *sparse non-Hermitian* random matrices [31]. Contrary to the well-known classical and Ginibre ensembles, where the limiting distribution for the spectral density follows the Wigner semicircle and Girko’s law (Fig. 1.3), respectively, sparse matrices are the only non-trivial ensembles with i.i.d. elements whose spectral limiting behaviour differs [39]. Surprisingly, the introduction of sparsity within the ensembles greatly complicates their analysis, making our understanding of the spectral properties rudimentary [10]. For instance, sparse random ensembles are not invariant under the $O(N)$ and $U(N)$ symmetries; consequently, many of the methods applied to unitary and orthogonal ensembles with successful results are no longer valid for the sparse cases. Furthermore, standard techniques, such as the use of the resolvent (Eq. (1.40)), lack validity on sparse non-Hermitian random matrices [31]. In other words, every possible advance related to this type of ensemble seems hampered due to the lack of standard mathematical techniques to conduct proper research [10].

In general, we obtain an SRM ensemble by diluting any known classical random matrix ensemble, allowing us to consider the limits of validity of the Wigner-Dyson theories and their universal statistics when matrices strongly deviate from their classical analogue [32, 39]. The study of the spectral properties of SRMs was first motivated by *mean-field spin systems* [160–162] where the exchange interactions are significantly diluted but of infinite range and by *combinatorial optimization problems* [163–165]. Sparse models also work as representations to study the quantum-mechanical behaviour of systems that are classically chaotic [166], for *exponential relaxation in glassy systems* [40], percolation limits (see [10] and references therein), *Anderson localization* of electronic states [32], *Lifshitz tails* [167], *Griffiths' singularities* in disordered systems [33], and as a tool to study the largest eigenvalue in d -regular graphs [168, 169]. Nowadays, the interest in these systems is directed towards complex networks, where geometric and topological features are translated to the spectral properties of adjacency matrices [170, 171]. Despite the still-growing interest in SRMs, fundamental questions about eigenvalue distributions remain unanswered [31]. For instance, one of the central pieces in RMT that is still missing for the SRM ensembles is the joint probability distribution of eigenvalues (JPDE) function.

Motivated to understand the role of *Griffiths' singularities* in both the statistics and dynamics of dilute spin systems at temperatures between the critical temperatures of the dilute and non-dilute systems, Rodgers and Bray published in 1988 the *seminal paper* [36] on SRMs. In their publication, the authors considered an $N \times N$ real symmetric matrix \mathbf{J} whose elements J_{ij} , for all $i, j = 1, \dots, N$, were i.i.d. random variables following the probability distribution

$$P(J_{ij}) = \left[1 - \frac{p}{N}\right] \delta(J_{ij}) + \frac{p}{2N} [\delta(J_{ij} - 1) + \delta(J_{ij} + 1)]; \quad (2.1)$$

then, appealing to the Green's matrix trace (Eq. (1.40)) and replica method, the authors expressed the AESD as

$$\rho(\mu) = \lim_{N \rightarrow \infty} \lim_{\varepsilon \rightarrow 0^+} \lim_{n \rightarrow 0} \frac{2}{Nn\pi} \text{Im} \partial_\mu \langle Z^n(\mu + i\varepsilon) \rangle_{\mathbf{J}}, \quad (2.2)$$

with $\varepsilon > 0$ and $\langle Z^n(\mu + i\varepsilon) \rangle_{\mathbf{J}}$ the Gaussian integral

$$\langle Z^n(\mu + i\varepsilon) \rangle_{\mathbf{J}} = \int \left(\prod_{i,a=1}^{N,n} d\phi_{ia} \right) \exp \left[\frac{i}{2} (\mu + i\varepsilon) \sum_{i,a=1}^{N,n} \phi_{ia}^2 + \frac{p}{2N} \sum_{i,j=1}^N \left\{ \cos \left(\sum_{a=1}^n \phi_{ia} \phi_{ja} \right) - 1 \right\} \right]. \quad (2.3)$$

To decouple the sites of Eq. (2.3), the authors employed the famous Hubbard-Stratonovich transformation and expanded the function $f(x) = \cos(x) - 1$ to construct an equivalent *functional* self-consistency problem described by a non-linear integral equation for a function g defined via a suitable average of the function f

$$g(\phi) = \frac{\int [\cos(\phi \cdot \psi) - 1] e^{F(\psi)} d^n \psi}{\int \exp[F(\psi)] d^n \psi}, \quad (2.4)$$

with $\phi = (\phi_1, \dots, \phi_n)$ a vector in the n -dimensional replica space and

$$F(\psi) = \frac{i}{2} \mu \psi^2 + pg(\psi). \quad (2.5)$$

Since the integral expression of Eq. (2.4) could not be solved by analytical methods, the authors appealed to a perturbative expansion in powers of $1/p$ with the leading term reproducing the Wigner semicircle law to approximate a solution [36]. Subsequent analyzes based on the supersymmetric method [37–40] were conducted to determine the spectral properties of SRM such as the average spectrum [37, 38] and correlation functions [39], leading to integral expressions too complicated to be solved by means of analytical procedures.

Afterwards, a series of approximate methods [41–43] based on the replica method were published to solve the hamper caused by the integral expressions obtained in Refs. [36–40]. The first difference between these approximate methods to the previous approaches came with the decoupling of sites. Instead of employing the Hubbard-Stratonovich transformation, these series of works appealed to a very useful way to study the mean-field theory of diluted systems by introducing a function $\rho(\phi)$ called the *replicated density* [172], measuring the fraction of sites with a field ϕ_i equal to a chosen value ϕ (the vector denoting the n -dimensional replica space),

$$\rho(\phi) = \frac{1}{N} \sum_i \delta(\phi - \phi_i). \quad (2.6)$$

The implementation of Eq. (2.6) led to a path integral formulation for the AESD in terms of an effective action S_{EFF} (see Eq. (17) in Ref. [42]) solved by means of the saddle-point method, leading to a stationary condition for the S_{EFF} . Such an equation could not be solved using any known analytical procedures, resulting in the use of approximations. The first approximate method, known as *effective medium approximation* (EMA), considered the extended part of the spectrum and postulated that all matrix elements were of the same order of magnitude, i.e. all sites were equivalent and played the same role, simplifying the replicated density with a Gaussian ansatz (see Eqs. (6) and (22) of Refs. [41] and [42] respectively). Since EMA assumes uniform connectivity, it does not reflect geometry fluctuations within the spectrum, making its description for the diluted ensembles better for large c values of the average connectivity. For low and moderate values of c , it does not yield an accurate description of the central part of the spectrum, as well as the tails and the presence of weighted Dirac δ peaks throughout the spectral density [42].

To solve the inaccuracies of EMA, a second approximation known as the *single defect approximation* (SDA) was introduced. In this scheme, the original saddle-point equation from EMA was modified such that any chosen site had k neighbours following a Poisson distribution, and each one interacted with the central site through an effective Hamiltonian (Eq. (8) in Ref. [41]). Hence, in SDA, the connectivity for any site was allowed to fluctuate, but its neighbours continued to be treated as part of the effective medium [41, 42]. Although SDA emerged as an enhancement of EMA capable of reflecting the geometry fluctuations within the spectral density, its description of the full spectrum was still incomplete. For instance, in Poisson random graphs, SDA is capable of reproducing the weighted Dirac δ peak at the spectrum's centre for low and moderate values of the average connectivity c ; nevertheless, it is unable to display the remaining δ peaks at the left and right of the central peak as well as the tails of the spectrum (see Fig. 3 in Ref. [173]). Later, the approximate methods *dual effective medium approximation* (DEMA) and *symmetric medium approximation* (SEMA) were introduced to study the spectrum of *covariance matrices* of the form $\mathbf{J} = \mathbf{A}^T \mathbf{A}$, with $\mathbf{A} \in M_{M \times N}(\mathbb{R})$ a sparse random matrix, approximating the replicated densities by Gaussian ansatz, providing decent results but failing to correctly describe the tails of the spectrum, as well as the highest part of it (see Figs. 1 and 2 of Ref. [43]). For further details on the DEMA and SEMA methods, check Ref. [43].

It was the research conducted by Kühn [174] and subsequently by Rogers, Pérez Castillo, and Takeda [173] that introduced new methods capable of providing accurate results for the spectral properties of sparse Hermitian random matrices. Starting from the key principles of Refs. [36–38, 41–43], Ref. [174] took Poisson and Laplacian random graphs and successfully obtained stationary conditions for the replicated density parameter ρ and its conjugate variable $\hat{\rho}$. As with the approximate methods, the saddle-point equations proved to be too complicated to be solved by analytical methods. Instead of appealing to the Hubbard-Stratonovich transformation or a Gaussian ansatz to approximate the replicated density, Kühn used the fact that a solution preserving both the permutation symmetry among replicas and rotational symmetry in the replica space is exact for the problem at hand and proposed a *replica-symmetric ansatz* where ρ and $\hat{\rho}$ were uncountably infinite superpositions of normalized complex Gaussians of the form

$$\rho(\mathbf{u}) = \int \pi(\omega) \prod_a \frac{e^{-\frac{\omega}{2} \mathbf{u}_a^2}}{\sqrt{2\pi/\omega}} d\omega \quad (2.7)$$

and

$$i\hat{\rho}(\mathbf{u}) = \hat{c} \int \hat{\pi}(\hat{\omega}) \prod_a \frac{e^{-\frac{\hat{\omega}}{2} \mathbf{u}_a^2}}{\sqrt{2\pi/\hat{\omega}}} d\hat{\omega}, \quad (2.8)$$

with $\mathbf{u} \equiv (u_1, \dots, u_n)$ a vector in the replica space and $\pi, \hat{\pi}$ weight functions to be determined. The implementation of Eqs. (2.7) and (2.8) changed entirely the previous frameworks and permitted the authors to arrive at a self-consistent equation for AESD that can be solved utilizing iterative processes [174].

The research conducted by Rogers et al. followed the same path as Ref. [174] and using the *cavity method*, an equivalent technique to the replica method, provided an analytical expression for the AESD not only for Poisson random graphs but also for covariance matrices [173]. Moreover, the authors went a step ahead and analytically demonstrated that in the large c limit, it was possible to recover the Wigner semicircle law for the Poisson random graphs and the Marcenko-Pastur law [175] for the covariance matrices. Their results not only did accurately reproduce the spectrum of Hermitian Poisson random graphs and covariance matrices but also fulfilled the existing gaps in the approximate methods. On the one hand, for Poisson random graphs, the analytical results perfectly described the tails and weighted Dirac δ peaks of the spectrum (see Figs. 3, 4, and 5 of Ref. [173]); on the other hand, for covariance matrices, the method correctly reproduced the highest part and tails of the spectrum (Fig. 6 in Ref. [173]).

Both previous techniques carried a crucial ingredient. Since the previous methods failed to reproduce the presence of weighted Dirac δ peaks, Refs. [173] and [174] approximated the δ peaks with Lorentzian functions by introducing a

small quantity $\varepsilon > 0$ in the replica and cavity equations; we refer to this small value as *the regularizer*. The immediate step came with Rogers and Pérez Castillo [44], who, appealing anew to the cavity method, developed a powerful machinery capable of reproducing the spectrum of sparse non-Hermitian random matrices; this technique has its core at the so-called *Hermitisation method* [158, 176]. The idea behind such a method is to introduce a regularisation to non-Hermitian spectra by enlarging the dimension of the problem via a $2N \times 2N$ block matrix with the regularising parameter $\varepsilon > 0$ [158]; the method name refers to early implementations where the introduced $2N \times 2N$ block matrix was Hermitian, permitting access to the standard tools of Hermitian RMT [158, 176]. Hence, appealing to the Hermitisation method, Ref. [44] expressed the AESD as a Gaussian integral over a set of N spinors $\psi = (u, v)^T$ ($u, v \in \mathbb{C}$), displaying a straightforward connection with the language of statistical physics. The usage of the cavity method resulted in a set of equations whose solution not only reproduced the spectrum of asymmetric Poisson random graphs for low and moderate values of c (Figs. 1 and 2 of Ref. [44]) but also demonstrated the recovery of Girko's law in the fully connected limit $c \rightarrow \infty$.

Thanks to the equivalence between the cavity and replica methods, a treatment for the spectrum of sparse non-Hermitian random matrices through a replica analysis is possible by adequately handling the corresponding saddle-point equations and a suitable replica-symmetric ansatz. Both schemes, the cavity and replica methods, faithfully reproduce the spectrum of symmetric Poisson random graphs with asymmetric weights for distinct values of the average connectivity c . Fig. 2.1 illustrates the comparison of the AESD, at $\text{Re}z = 0.10$, between the exact analytical results by the replica method and numerical diagonalization for a set of finite asymmetric Poisson random graphs with average connectivities $c = 5$ and $c = 10$. The existing discrepancies in the tails of the spectra were previously reported in Ref. [44] and attributed to the discretization effects of the histogram due to the finite size of the matrices employed in the diagonalization.

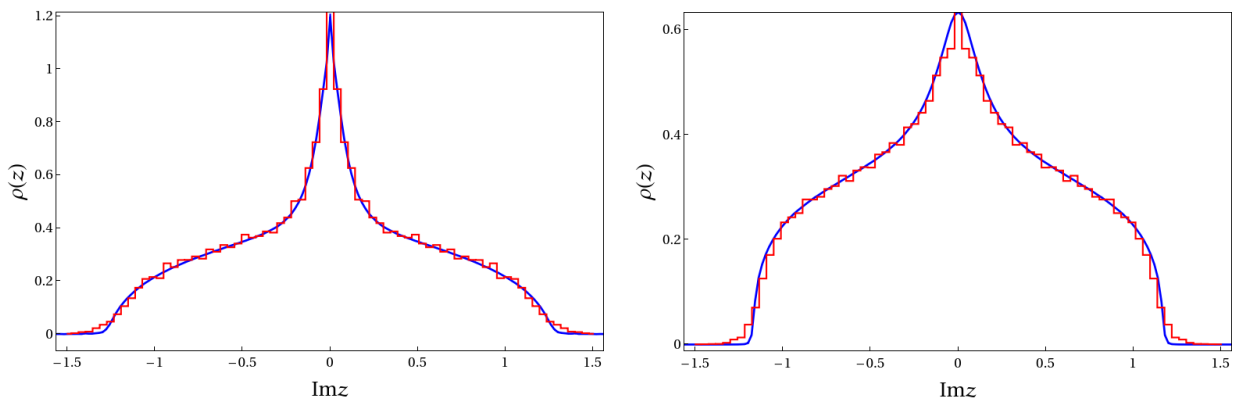


Figure 2.1: Comparison between the theoretical findings obtained by the replica method and exact diagonalization results of the AESD (Eq. (1.19)) at the cut $\text{Re}z = 0.10$ for Poisson random graphs with Gaussian edge weights. Continuous blue lines stand as the theoretical findings and red grid lines (histogram) correspond to exact diagonalization results for average connectivities of $c = 5$ (*left panel*) and $c = 10$ (*right panel*).

Thanks to the all previously mentioned research, now we have powerful methods capable of tackling the spectral properties of sparse Hermitian and non-Hermitian random matrices; nonetheless, we are far from answering all possible interrogations concerning sparse ensembles. For instance, questions about how spectral properties, such as *the distribution of interaction strengths* and *the distribution of the number of links per node*, depend on the structural details of the associated random graph [31] and a theoretical framework for *localization* in sparse ensembles, are just examples of the extensive research that must be carried out.

In the following sections, we display all the work realized throughout this doctoral research. We take as a departing point the work carried out by Rogers et al. in Refs. [44, 45, 173], and via a replica analysis, we develop analytical methods to study *i*) the full statistics (typical and atypical fluctuations) of the number of eigenvalues \mathcal{N}_D within a smooth Jordan curve contained in a domain D of the complex plane \mathbb{C} , and *ii*) the atypical fluctuations of the AESD (Eq. (1.19)), when we impose an external constraint fixing a prescribed fraction \mathcal{R} of the number of eigenvalues \mathcal{N}_D inside the curve; the so-called conditioned spectral density. To demonstrate the exactness of our research, we apply all our results to the diluted version of the real Ginibre ensemble. In order to properly display all our work, we divide our findings into two independent sections, each divided into a *theory* and *results* subsection. In Section 2.2, we show all the research conducted for the full statistics of \mathcal{N}_D , while in Section 2.3, we show our analysis for the atypical

fluctuations of the AESD. We compare our results with numerical diagonalization for ensembles of finite random matrices, displaying excellent agreement.

2.2 Analytic approach for the number statistics of non-Hermitian random matrices

One of the observables in RMT that one can study is the distribution of the number \mathcal{N}_D of eigenvalues contained in a domain $D \subseteq \mathbb{C}$ (the index) delimited by a *smooth Jordan curve*, the so-called *number statistics* or *full counting statistics*. The research concerning the fluctuations of \mathcal{N}_D stands as a rich mathematical problem by itself and finds applications in the study of the ground state of spinless "fermions" in a harmonic trap [177–181], the number of stable directions around the stationary points on disordered energy landscapes [120, 123], localized or extended nature of eigenstates in disordered quantum systems [111, 182, 183], and the stability of large interacting biological systems [184–186], where many problems turn into a task of counting the number of eigenvalues of a random matrix inside a specific domain. Due to the excellent machinery of the Coulomb fluid method [134–137], a considerable deal of results characterizing the typical and atypical fluctuations of the index have emerged, especially for Gaussian Hermitian random matrices with complex, real, and real quaternion entries [177–179, 187]. Concerning non-Hermitian random matrices, the question of how many eigenvalues lie in a certain region of \mathbb{C} was addressed for the complex and real Ginibre ensembles [188, 189], providing analytical expressions for the probability distribution and rate function [189]. On the contrary, the number statistics information has only been extracted for the complex Ginibre ensemble [180, 181] due to its analogy with the Coulomb fluid method (Eq. (1.27)), where the location of the N eigenvalues is mapped into the position of N fermions on a $2D$ rotating harmonic trap in the ground state [181]; regarding the shape of D , Refs. [180, 181, 189] have all employed circular domains. While studies such as [190], [191], and [192] focused their endeavours on the local and global relations between Gaussian analytic functions and the Ginibre ensembles considering non-circular domains, results for sparse non-Hermitian random matrices are scarce and for very complicated domains are out of reach.

Non-Hermitian matrices with real entries find crucial applications in high-dimensional non-equilibrium systems [31, 141, 184–186, 193–195], where the matrices model the pairwise interaction among the system components. A salient example lies in *neural networks*, where it is acquainted that such systems display an explosion of complexity as a function of certain disorder parameters, springing up a phase transition to chaos [193, 194, 196, 197]; the mechanism underpinning such phase transition remains unclear [196]. Although methods such as *Fredholm determinants* and *Pfaffians* [9, 10] are used to tackle the index, there is not yet a general procedure for its study. Hence, \mathcal{N}_D remains poorly characterized, especially for sparse non-Hermitian matrices. Mainly departing from Ref. [44], this first project seeks to provide a complete description of the index \mathcal{N}_D for an ensemble of sparse non-Hermitian random matrices. The strongest feature of our theory is that we can perform the analysis of \mathcal{N}_D for arbitrarily large ensembles of non-Hermitian random matrices without knowing the corresponding JPDE function. We appeal to the replica method and explicitly derive results for the diluted version of the real Ginibre ensemble where we consider symmetric adjacency matrices of Poisson random graphs with asymmetric couplings. The principal outcome of the theory is a set of effective equations valid for infinitely large sparse non-Hermitian random matrices from which the first two cumulants (mean and variance) as well as the rate function controlling the typical and atypical fluctuations of \mathcal{N}_D detach. To demonstrate the effectiveness of our theory, we support all our theoretical results with exact diagonalization carried out for finite random matrices displaying excellent agreement.

Although the method can, in principle, be applied to any non-Hermitian random matrix ensemble, its success will depend on the specific details of the ensemble at hand. Key elements such as the replica technique, as we presented it, can be applied successfully to ensembles of the mean-field type, such as the adjacency matrix of asymmetric Erdős-Rényi random graphs with arbitrary degree distributions [101], where the coupling strengths do not depend on the distance between their components. It has been known for a long time that, in general, dimensionality performs a crucial role in determining whether or not the results obtained by the mean-field theory are accurate [198]. Thanks to the *Ginzburg criterion* [199], we know that better results will come for high-dimensional systems [198]; hence, models of small and finite-dimensional lattices [200] and optical lattices with non-Hermitian disorder [201, 202] are not treatable by the replica method and consequently not solvable via our theory.

This section is organized as follows. We commence in Subsection 2.2.1, where we introduce the CGF \mathcal{F} of the number \mathcal{N}_D and explain how to get an analogy of the latter with the partition function of a system of N spinors placed over a graph. Immediately after, we introduce the ensemble of sparse random matrices with asymmetric couplings,

obtaining a path integral formulation for the CGF. Appealing to the saddle-point method and replica-symmetric ansatz formalism, we obtain an effective theory for \mathcal{F} valid for infinitely large sparse non-Hermitian random matrices. We close in Subsection 2.2.2, where resorting to the population dynamics algorithm, we numerically solve the effective equations and apply the results to the diluted version of the real Ginibre ensemble. We compare our findings with numerical diagonalization for finite-size matrices, showing excellent agreement. All the details of our derivations are properly shown in Appendices A.

2.2.1 The analytical method

The path integral formalism

Let $\mathbf{A} \in M_{N \times N}(\mathbb{C})$ be a non-Hermitian random matrix drawn from a distribution $\mathcal{P}(\mathbf{A})$ and $\Lambda = \{\lambda_1, \dots, \lambda_N\}$ its spectrum, with $\{\lambda_i\}_{i=1}^N \in \mathbb{C}$. The number of eigenvalues within a domain $D \subseteq \mathbb{C}$ enclosed by a smooth Jordan curve $\gamma \equiv \partial D$ is provided by

$$\mathcal{N}_{\mathbf{A}}(\gamma) = N \int_D \rho_{\mathbf{A}}(x, y) dx dy, \quad (2.9)$$

with $\rho_{\mathbf{A}}(x, y)$ the ESD (Eq. (1.18)) around the point $z = x + iy$. Since $\mathcal{N}_{\mathbf{A}}(\gamma)$ is a random variable, we extract all its statistics information in the $N \rightarrow \infty$ limit via the CGF, which we define as

$$\mathcal{F}_{\gamma}(\mu) = - \lim_{N \rightarrow \infty} \frac{1}{N} \ln \left\langle e^{-\mu \mathcal{N}_{\mathbf{A}}(\gamma)} \right\rangle, \quad (2.10)$$

with $\langle \dots \rangle$ the average over the probability distribution $\mathcal{P}(\mathbf{A})$. Resorting to Hölder's inequality [156], we can prove that the momentarily defined function $\mathcal{L}(\mu) \equiv N^{-1} \ln \langle \exp[-\mu \mathcal{N}_{\mathbf{A}}(\gamma)] \rangle$ is convex. However, from how we have defined $\mathcal{F}_{\gamma}(\mu)$, in contrast with $\mathcal{F}(\mu)$ (Eq. (1.9)), it is clear that the first one is concave. Fortunately, this does not modify our results since $\mathcal{F}_{\gamma}(\mu)$ can be thought of as $-\mathcal{F}(-\mu)$ [84]. Furthermore, since we have assumed the Gärtner-Ellis theorem holds (Theorem 1.1 in Section 1.2), the limit $N \rightarrow \infty$ exists and differs from zero or infinity.

In order to extract the cumulants of $\mathcal{N}_{\mathbf{A}}$ (and consequently the statistical information), we need to derivate Eq. (2.10) and evaluate it at $\mu = 0$ [78]; formally speaking, the n -th cumulant κ_n is given by $\kappa_n = \partial_{\mu}^n \mathcal{F}_{\gamma}(\mu) |_{\mu=0}$. Hence, the intensive mean $N\kappa_1 = \langle \mathcal{N}_{\mathbf{A}} \rangle$ and variance $N\kappa_2 = \langle \mathcal{N}_{\mathbf{A}}^2 \rangle - \langle \mathcal{N}_{\mathbf{A}} \rangle^2$ read

$$\kappa_1 = \partial_{\mu} \mathcal{F}_{\gamma}(\mu) |_{\mu=0} \text{ and } \kappa_2 = -\partial_{\mu}^2 \mathcal{F}_{\gamma}(\mu) |_{\mu=0}. \quad (2.11)$$

The usage of the CGF does not remain only in its capacity to deduce the cumulants via a simple relation. Its importance goes further as it provides crucial information about the atypically large fluctuations of $\mathcal{N}_{\mathbf{A}}$. Appealing to LDT (Eq. (1.7)), we know that the probability for $\mathcal{N}_{\mathbf{A}} = Nn$, with $0 \leq n \leq 1$, in the $N \rightarrow \infty$ limit, decays as [79]

$$\text{Prob}[\mathcal{N}_{\mathbf{A}} = Nn] \asymp e^{-N\phi_{\gamma}(n)}, \quad (2.12)$$

with $\phi_{\gamma}(n)$, the associated rate function. Moreover, thanks to the Gärtner-Ellis theorem, we can deduce the behaviour of the rate function via the Legendre transform of the CGF \mathcal{F}_{γ}

$$\phi_{\gamma}(n) = - \inf_{\mu \in \mathbb{R}} [n\mu - \mathcal{F}_{\gamma}(\mu)]. \quad (2.13)$$

Noteworthy is that $\phi_{\gamma}(n)$ complies with being a convex function, regardless of the CGF shape [84].

Thus, the calculation of the CGF is our principal goal throughout this first work since, as manifest in Eqs. (2.11) and (2.13), the complete statistics of $\mathcal{N}_{\mathbf{A}}$, typical and atypical fluctuations, detach from it. It is worth remembering that, in the statistical physics context, the CGF \mathcal{F}_{γ} and rate function ϕ_{γ} correspond to the *canonical free energy* and *microcanonical entropy*, respectively [78]. Thus, the first and second cumulants of \mathcal{F}_{γ} are the *average energy* and *heat capacity*. For further details, we refer the reader to Refs. [78, 79].

To commence with the calculation, we need to understand how $\mathcal{N}_{\mathbf{A}}$ depends on matrix \mathbf{A} so we can compute the average of Eq. (2.10). We depart rewriting the ESD (Appendix A.1, Eqs. (A.2) and (A.3)) as

$$\rho_{\mathbf{A}}(z, z^*) = \frac{1}{N\pi} \partial_{z^*} \partial_z \ln \det \left[(z\mathbf{I}_N - \mathbf{A})(z\mathbf{I}_N - \mathbf{A})^{\dagger} \right], \quad (2.14)$$

where we have defined $\partial_z \equiv \frac{1}{2}(\partial_x - i\partial_y)$, $\partial_{z^*} \equiv \frac{1}{2}(\partial_x + i\partial_y)$, and \mathbf{I}_N the $N \times N$ identity matrix. Inserting Eq. (2.14) into Eq. (2.9) and using Green's theorem (Appendix A.1, Eqs. (A.4) and (A.5)), we find that

$$\mathcal{N}_{\mathbf{A}}(\gamma) = -\frac{1}{2\pi i} \oint_{\gamma} \partial_z \ln Q_{\mathbf{A}}(z, z^*) dz, \quad (2.15)$$

with

$$Q_{\mathbf{A}}(z, z^*) = \frac{1}{\det \left[(z\mathbf{I}_N - \mathbf{A})(z\mathbf{I}_N - \mathbf{A})^\dagger \right]} \quad (2.16)$$

and $(\dots)^*$, $(\dots)^\dagger$ the complex and Hermitian conjugated, respectively.

The next step is to discretize the γ contour, which is traversed once counterclockwise, into a series of finite points $\{z_\ell\}_{\ell=1}^L \subseteq \mathbb{C}$ such that $z_{L+1} \equiv z_1$ and $\Delta z_\ell \equiv z_{\ell+1} - z_\ell$. Consequently, we rewrite Eqs. (2.10) and (2.15) as

$$\mathcal{N}_{\mathbf{A}}(\gamma) = -\frac{1}{2\pi i} \lim_{L \rightarrow \infty} \sum_{\ell=1}^L [\ln Q_{\mathbf{A}}(z_{\ell+1}, z_\ell^*) - \ln Q_{\mathbf{A}}(z_\ell, z_\ell^*)] \quad (2.17)$$

and

$$\mathcal{F}_\gamma(\mu) = -\lim_{N \rightarrow \infty} \lim_{L \rightarrow \infty} \frac{1}{N} \ln \left\langle \prod_{\ell=1}^L [Q_{\mathbf{A}}(z_{\ell+1}, z_\ell^*)]^{n_+} [Q_{\mathbf{A}}(z_\ell, z_\ell^*)]^{n_-} \right\rangle, \quad (2.18)$$

where n_\pm are non-integer numbers defined as $n_\pm \equiv \pm \frac{\mu}{2\pi i}$.

Even though Eqs. (2.16) and (2.17) display the exact dependence of the variable $\mathcal{N}_{\mathbf{A}}$ on the random matrix \mathbf{A} , to succeed in computing the CGF (Eq. (2.18)) we need to appeal to multidimensional Gaussian integrals rewriting $Q_{\mathbf{A}}$ in a quadratic form. Then, appealing to the Hermitization method [158, 176], we introduce the $2N \times 2N$ block matrix

$$\mathbf{F}_\eta(z, z^*) = \begin{pmatrix} \eta \mathbf{I}_N & i(z\mathbf{I}_N - \mathbf{A}) \\ i(z\mathbf{I}_N - \mathbf{A})^\dagger & \eta \mathbf{I}_N \end{pmatrix}, \quad (2.19)$$

such that we recover Eq. (2.16) via the relation $Q_{\mathbf{A}} = \lim_{\eta \rightarrow 0^+} (\det \mathbf{F}_\eta)^{-1}$. The parameter $\eta > 0$ is *the regularizer* [173, 174, 176] and ensures that \mathbf{F}_η has a positive Hermitian part, enabling us to represent $Q_{\mathbf{A}}$ as a Gaussian integral over a set of spinors $\psi_i \in \mathbb{C}^2$ ($i = 1, \dots, N$),

$$Q_{\mathbf{A}}(z, z^*) = \lim_{\eta \rightarrow 0^+} \int \left(\prod_{i=1}^N \frac{d\psi_i d\psi_i^\dagger}{\pi^2} \right) \exp \left[-\sum_{i=1}^N \psi_i^\dagger \mathbf{M}_\eta(z, z^*) \psi_i + i \sum_{i,j=1}^N \psi_i^\dagger \mathbf{B}_{ij} \psi_j \right], \quad (2.20)$$

with matrices \mathbf{M}_η and \mathbf{B}_{ij} defined as

$$\mathbf{M}_\eta(z, z^*) \equiv \eta \mathbf{I}_2 + i(z\boldsymbol{\sigma}_+ + z^*\boldsymbol{\sigma}_-), \quad \mathbf{B}_{ij} \equiv A_{ij}\boldsymbol{\sigma}_+ + A_{ij}^\dagger \boldsymbol{\sigma}_-, \quad (2.21)$$

and $\boldsymbol{\sigma}_+$, $\boldsymbol{\sigma}_-$ the usual ladder operators

$$\boldsymbol{\sigma}_+ = \begin{pmatrix} 0 & 1 \\ 0 & 0 \end{pmatrix} \quad \text{and} \quad \boldsymbol{\sigma}_- = \begin{pmatrix} 0 & 0 \\ 1 & 0 \end{pmatrix}. \quad (2.22)$$

The form of $Q_{\mathbf{A}}$ in Eq. (2.20) resembles the partition function of a system of N spinors placed over a graph and coupled through the set of 2×2 complex matrices $\{\mathbf{B}_{ij}\}_{i,j=1}^N$. In other words, \mathbf{B}_{ij} , for all $i, j = 1, \dots, N$, quantifies the existing pairwise interaction between spinors ψ_i and ψ_j ; both $\{\mathbf{B}_{ij}\}_{i,j=1}^N$ and the graph structure are determined by the specific properties of $\mathcal{P}(\mathbf{A})$.

The analogy of $Q_{\mathbf{A}}$ with a partition function permits us to use well-known tools from statistical physics. Nonetheless, there is still the problem of evaluating the complex-valued exponents n_\pm ; as long as we have not assessed the complex exponents, any direct attempt at computing Eq. (2.18) is hampered. To overcome this inconvenience, we appeal to the replica method and evaluate the average of Eq. (2.18) assuming $n_\pm \in \mathbb{N}^+$. Immediately after, we compute the $N \rightarrow \infty$ limit and, finally, we analytically continue the resulting \mathcal{F}_γ to its limiting value $n_\pm \rightarrow \pm \mu/2\pi i$. As

a consequence of assuming the Gärtner-Ellis theorem holds, the thermodynamic limit $N \rightarrow \infty$ in Eq. (2.18) exists and is different from zero or infinite (a proof of this limit for the free energy in the *Sherrington-Kirkpatrick model* can be found in Ref. [203]). The existence of the remaining limits, as well as the analytic continuation of $\mathcal{F}_\gamma(\mu)$, are not proved rigorously. However, throughout the entire calculation, we assume the expressions to be such that all limits exist and are interchangeable; assumptions that we later verify in the numerical procedure. Therefore, inserting Eq. (2.20) into Eq. (2.18), we obtain a general expression for the cumulant generating function

$$\begin{aligned} \mathcal{F}_\gamma(\mu) = & - \lim_{N \rightarrow \infty} \lim_{L \rightarrow \infty} \lim_{n_\pm \rightarrow \frac{\pm\mu}{2\pi i}} \lim_{\eta \rightarrow 0^+} \frac{1}{N} \ln \int \left(\prod_{i=1}^N \prod_{\ell=1}^L \prod_{a=1}^{n_+} d\Psi_{i\ell a} \right) \left(\prod_{i=1}^N \prod_{\ell=1}^L \prod_{b=1}^{n_-} d\Phi_{i\ell b} \right) \\ & \times \exp \left[- \sum_{i=1}^N \sum_{\ell=1}^L \left(\sum_{a=1}^{n_+} \psi_{i\ell a}^\dagger \mathbf{M}_\eta(z_{\ell+1}, z_\ell^*) \psi_{i\ell a} + \sum_{b=1}^{n_-} \phi_{i\ell b}^\dagger \mathbf{M}_\eta(z_\ell, z_\ell^*) \phi_{i\ell b} \right) \right] \\ & \times \left\langle \exp \left[i \sum_{i < j} \sum_{\ell=1}^L \left\{ \sum_{a=1}^{n_+} (\psi_{i\ell a}^\dagger \mathbf{B}_{ij} \psi_{j\ell a} + \psi_{j\ell a}^\dagger \mathbf{B}_{ij}^\dagger \psi_{i\ell a}) + \sum_{b=1}^{n_-} (\phi_{i\ell b}^\dagger \mathbf{B}_{ij} \phi_{j\ell b} + \phi_{j\ell b}^\dagger \mathbf{B}_{ij}^\dagger \phi_{i\ell b}) \right\} \right] \right\rangle, \end{aligned} \quad (2.23)$$

where, for simplicity, we have set $A_{ii} = 0$ and $d\Psi_i \equiv d\psi_i d\psi_i^\dagger / \pi^2$, $d\Phi_i \equiv d\phi_i d\phi_i^\dagger / \pi^2$ for all $i = 1, \dots, N$. We emphasize that Eq. (2.23) is fully general and valid for any contour $\gamma \in \mathbb{C}$ and arbitrary non-Hermitian random matrix ensemble. Nevertheless, the success in computing the average and obtaining a final expression for the CGF depends on the choice of $\mathcal{P}(\mathbf{A})$.

Having established a general expression for the CGF, we apply the method to an ensemble of sparse non-Hermitian random matrices; we have opted for the adjacency matrix of random graphs with asymmetric couplings [34, 35, 101]. Then, we write the matrix \mathbf{A} elements as $A_{ij} = c_{ij} J_{ij}$, where $\{c_{ij}\}_{i,j=1}^N$ correspond to the entries of the adjacency matrix \mathbf{C} (Definition 1.8) and $\{J_{ij}\}_{i,j=1}^N$ are i.i.d. random variables drawn from a distribution p_J . While $\{c_{ij}\}_{i,j=1}^N$ encode the topology of the graph, $\{J_{ij}\}_{i,j=1}^N$ represent the asymmetric interaction strengths between sites, i.e., the element J_{ij} weights the influence of site i over site j , for all $i, j \in \{1, \dots, N\}$. Therefore, the set $\{J_{ij}\}_{i,j=1}^N$ denotes the *quenched variables* of the system. On the other hand, the adjacency matrix \mathbf{C} entries $\{c_{ij}\}_{i,j=1}^N$ are drawn from Eq. (1.17), with $c \in \mathbb{R}^+$ the average connectivity independent of N . Hence, the random matrix \mathbf{A} corresponds to the adjacency matrix of a weighted random graph with directed edges, where the number of neighbours connected to each node follows a Poisson distribution with an average connectivity c [35, 95]. This type of matrix encodes what some authors denominate *asymmetric information* [34] and are found in areas such as economy [34], sociology [99], and biology [98].

After performing the average over \mathbf{C} , Eq. (2.23) takes the form

$$\begin{aligned} \mathcal{F}_\gamma(\mu) = & - \lim_{N \rightarrow \infty} \lim_{L \rightarrow \infty} \lim_{n_\pm \rightarrow \frac{\pm\mu}{2\pi i}} \lim_{\eta \rightarrow 0^+} \frac{1}{N} \ln \int \left(\prod_{i=1}^N \prod_{\ell=1}^L \prod_{a=1}^{n_+} d\Psi_{i\ell a} \right) \left(\prod_{i=1}^N \prod_{\ell=1}^L \prod_{b=1}^{n_-} d\Phi_{i\ell b} \right) \\ & \times \exp \left[- \sum_{i=1}^N \sum_{\ell=1}^L \left(\sum_{a=1}^{n_+} \psi_{i\ell a}^\dagger \mathbf{M}_\eta(z_{\ell+1}, z_\ell^*) \psi_{i\ell a} + \sum_{b=1}^{n_-} \phi_{i\ell b}^\dagger \mathbf{M}_\eta(z_\ell, z_\ell^*) \phi_{i\ell b} \right) \right] \\ & \times \exp \left[\frac{c}{2N} \sum_{i,j=1}^N \left\langle \exp \left[i \sum_{\ell=1}^L \left\{ \sum_{a=1}^{n_+} (\psi_{i\ell a}^\dagger \mathbf{J} \psi_{j\ell a} + \psi_{j\ell a}^\dagger \mathbf{J}^\dagger \psi_{i\ell a}) + \sum_{b=1}^{n_-} (\phi_{i\ell b}^\dagger \mathbf{J} \phi_{j\ell b} + \phi_{j\ell b}^\dagger \mathbf{J}^\dagger \phi_{i\ell b}) \right\} \right] - 1 \right\rangle_{\mathbf{J}} \right], \end{aligned} \quad (2.24)$$

with $\langle \dots \rangle_{\mathbf{J}}$ indicating the average over the *quenched disorder* $\mathbf{J} = \mathbf{J}\sigma_+ + \mathbf{J}'\sigma_-$ and the real-valued interaction strengths \mathbf{J} and \mathbf{J}' independently drawn from p_J .

In order to decouple the sites in Eq. (2.24), we follow the work done by Refs. [41–43] through Eq. (2.6) and introduce the following order-parameter function

$$P(\Psi, \Phi) = \frac{1}{N} \sum_{i=1}^N \prod_{\ell=1}^L \left[\prod_{a=1}^{n_+} \delta(\psi_{\ell a} - \psi_{i\ell a}) \right] \left[\prod_{b=1}^{n_-} \delta(\phi_{\ell b} - \phi_{i\ell b}) \right], \quad (2.25)$$

with the shorthand notation $P(\Psi, \Phi) \equiv P(\Psi, \Phi; \{\Psi_i, \Phi_i\}_{i=1}^N)$, $\Psi \equiv \{\psi_{\ell a}\}$, and $\Phi \equiv \{\phi_{\ell b}\}$, for $\ell = 1, \dots, L$, $a = 1, \dots, n_+$, and $b = 1, \dots, n_-$. Analogously, we denote $\{\Psi_i\} \equiv \{\psi_{i\ell a}\}$ and $\{\Phi_i\} \equiv \{\phi_{i\ell b}\}$ for $i = 1, \dots, N$.

After a sequence of algebraic manipulations (Appendix A.1, Eqs. (A.6)-(A.11)), we express Eq. (2.24) as the logarithm of a *path integral* over the order parameter P and conjugated order parameter \hat{P} ,

$$\mathcal{F}_\gamma(\mu) = - \lim_{N \rightarrow \infty} \lim_{L \rightarrow \infty} \lim_{n_\pm \rightarrow \frac{\pm \mu}{2\pi i}} \lim_{\eta \rightarrow 0^+} \frac{1}{N} \ln \int e^{-N\mathcal{S}[\{P, \hat{P}\}]} \mathcal{D}[\{P, \hat{P}\}], \quad (2.26)$$

with the corresponding action $\mathcal{S}[\{P, \hat{P}\}]$ defined as

$$\begin{aligned} \mathcal{S}[\{P, \hat{P}\}] = & - \ln \left(\int e^{-\tau(\Psi, \Phi) - i\hat{P}(\Psi, \Phi)} d\Psi d\Phi \right) - i \int P(\Psi, \Phi) \hat{P}(\Psi, \Phi) d\Psi d\Phi \\ & - \frac{c}{2} \int \left\langle e^{i\Xi(\Psi, \Phi, \Psi', \Phi')} - 1 \right\rangle_J P(\Psi, \Phi) \hat{P}(\Psi', \Phi') d\Psi d\Phi d\Psi' d\Phi'. \end{aligned} \quad (2.27)$$

Given the length of the terms involved in $\mathcal{S}[\{P, \hat{P}\}]$, we have introduced the auxiliary functions

$$\tau(\Psi, \Phi) \equiv \sum_{\ell=1}^L \left(\sum_{a=1}^{n_+} \psi_{\ell a}^\dagger M_\eta(z_{\ell+1}, z_\ell^*) \psi_{\ell a} + \sum_{b=1}^{n_-} \phi_{\ell b}^\dagger M_\eta(z_\ell, z_\ell^*) \phi_{\ell b} \right) \quad (2.28)$$

and

$$\Xi(\Psi, \Phi, \Psi', \Phi') \equiv \sum_{\ell=1}^L \left[\sum_{a=1}^{n_+} \left(\psi_{\ell a}^\dagger \mathbf{J} \psi'_{\ell a} + \psi'_{\ell a}{}^\dagger \mathbf{J}^\dagger \psi_{\ell a} \right) + \sum_{b=1}^{n_-} \left(\phi_{\ell b}^\dagger \mathbf{J} \phi'_{\ell b} + \phi'_{\ell b}{}^\dagger \mathbf{J}^\dagger \phi_{\ell b} \right) \right]. \quad (2.29)$$

The replica-symmetric ansatz

Thanks to the form of the cumulant generating function, we can solve the integral utilizing the saddle-point method [204]. Consequently, in the $N \rightarrow \infty$ limit, the path integral of Eq. (2.26) converges to

$$\int e^{-N\mathcal{S}[\{P, \hat{P}\}]} \mathcal{D}[\{P, \hat{P}\}] \asymp e^{-N\mathcal{S}[\{P_0, \hat{P}_0\}]}, \quad (2.30)$$

where P and \hat{P}_0 are the pair of functions that extremize the action functional $\mathcal{S}[\{P, \hat{P}\}]$. Thus, the stationary conditions for P and \hat{P} are given via the following saddle-point equations

$$-i\hat{P}(\Psi, \Phi) = c \int \left\langle e^{i\Xi(\Psi, \Phi, \Psi', \Phi')} - 1 \right\rangle_J P(\Psi', \Phi') d\Psi' d\Phi' \quad (2.31)$$

and

$$P(\Psi, \Phi) = \frac{e^{-\tau(\Psi, \Phi) - i\hat{P}(\Psi, \Phi)}}{\int e^{-\tau(\Psi', \Phi') - i\hat{P}(\Psi', \Phi')} d\Psi' d\Phi'}, \quad (2.32)$$

where for simplicity we have chosen to drop the subindex 0 in the functions P and \hat{P} . Contrary to the approximate methods EMA, SEMA, DEMA, and SDA [41–43], where the authors performed certain simplifications to Eq. (2.32) to study the spectral density, we follow Refs. [44, 45, 172–174] and realize that the problem at hand can be exactly solved by means of self-consistent equations.

As we had previously mentioned, the CGF, Eq. (2.26), represents the system's free energy; consequently, we can think about the existence of the *free energy landscape* (FEL). Geometrically, an energy landscape is a graph of the energy functions across the system's configuration space. Thus, the FEL is essentially a *rugged* energy landscape with a large number of local minima, with the lowest one being the global minimum; the system's dynamics depends on how the minima are connected throughout the landscape. For a system to attain equilibrium, it needs to navigate toward the global minimum [145, 146, 205–207]. The FEL is a stable object since it is uniquely determined by the equilibrium properties of the system, with no dynamics or time involved [205].

To proceed with the derivation, we need to appeal to the foundations of the saddle-point method (Eq. (2.30)) and formulate an *ansatz* on the state's structure in which the system is trapped. Therefore, we place the following *replica-symmetric* (RS) ansatz regarding the functional form of the order parameter $P(\Psi, \Phi)$ that emerges in the *effective*

replica theory,

$$P(\Psi, \Phi) = \int \left(\prod_{\ell=1}^L d\Sigma_\ell d\Gamma_\ell \right) \omega \left(\{\Sigma_\ell, \Gamma_\ell\}_{\ell=1}^L \right) \prod_{\ell=1}^L \left[\prod_{a=1}^{n_+} \frac{e^{-\psi_{\ell a}^\dagger \Sigma_\ell^{-1} \psi_{\ell a}}}{\det \Sigma_\ell} \prod_{b=1}^{n_-} \frac{e^{-\phi_{\ell b}^\dagger \Gamma_\ell^{-1} \phi_{\ell b}}}{\det \Gamma_\ell} \right], \quad (2.33)$$

where Σ_ℓ and Γ_ℓ are 2×2 complex matrices defined for each $z_\ell \in \gamma$ and $\omega \left(\{\Sigma_\ell, \Gamma_\ell\}_{\ell=1}^L \right)$ is the joint probability distribution of the pair of matrices $\{\Sigma_\ell, \Gamma_\ell\}_{\ell=1}^L$ along the L points of the contour. We take the joint distribution to be normalized to unity, i.e.,

$$\int \left(\prod_{\ell=1}^L d\Sigma_\ell d\Gamma_\ell \right) \omega \left(\{\Sigma_\ell, \Gamma_\ell\}_{\ell=1}^L \right) = 1. \quad (2.34)$$

The RS ansatz in Eq. (2.33) means that we assume that the state in the FEL on which the system is located corresponds to the global minimum without any additional internal structure [205].

The physical interpretation of Eq. (2.33) is as follows [205]: suppose we throw n replicas at the global minimum of the FEL to probe its structure. If the minimum is a plain paraboloid, there is no reason for any couple of the replicas to be exceptional; once they have equilibrated inside the state, all are equivalent and can be permuted as we please without modifying the physics of the problem. This argument is present indeed in Refs. [172] and [174], where the RS ansatz preserves both *permutation symmetry* among replicas and *rotational symmetry* in the replica space. Should it happen that the bottom contains different sub-minima, the situation would change completely. The replicas thrown at the bottom would end up in the different sub-minima, impeding the replica permutation [205]. For this scenario, we must introduce an ansatz based on grouping the replicas into distinct blocks representing the sub-minima; within the blocks, we assume replica symmetry though not between them [172].

Inserting the RS ansatz into the action and saddle-point expressions (Eqs. (2.27), (2.31), and (2.32), respectively), and after some algebraic manipulations (Appendix A.2, Eqs. (A.12)-(A.19)), we deduce the exact expression for the joint probability function ω ,

$$\begin{aligned} \omega \left(\{\Sigma_\ell, \Gamma_\ell\}_{\ell=1}^L \right) &= \frac{1}{\Lambda} \sum_{k=0}^{\infty} \frac{e^{-c} c^k}{k!} \int \left[\prod_{r=1}^k \left(\prod_{\ell=1}^L d\Sigma_{r\ell} d\Gamma_{r\ell} \right) \omega \left(\{\Sigma_{r\ell}, \Gamma_{r\ell}\}_{\ell=1}^L \right) \right] \\ &\times \left\langle \exp \left[-\frac{\mu}{2\pi i} \sum_{\ell=1}^L (\ln \det \Upsilon_\ell - \ln \det \zeta_\ell) \right] \prod_{\ell=1}^L \delta(\Sigma_\ell - \Upsilon_\ell^{-1}) \delta(\Gamma_\ell - \zeta_\ell^{-1}) \right\rangle_{\mathbf{J}_{1,\dots,k}}, \end{aligned} \quad (2.35)$$

and action \mathcal{S} ,

$$\begin{aligned} \mathcal{S} &= -\ln \left(\sum_{k=0}^{\infty} \frac{e^{-c} c^k}{k!} \int \left[\prod_{r=1}^k \left(\prod_{\ell=1}^L d\Sigma_{r\ell} d\Gamma_{r\ell} \right) \omega \left(\{\Sigma_{r\ell}, \Gamma_{r\ell}\}_{\ell=1}^L \right) \right] \left\langle e^{-\frac{\mu}{2\pi i} \sum_{\ell=1}^L (\ln \det \Upsilon_\ell - \ln \det \zeta_\ell)} \right\rangle_{\mathbf{J}_{1,\dots,k}} \right) \\ &+ \frac{c}{2} \int \left[\prod_{\ell=1}^L d\Sigma_\ell d\Gamma_\ell d\Sigma'_\ell d\Gamma'_\ell \right] \omega \left(\{\Sigma_\ell, \Gamma_\ell\}_{\ell=1}^L \right) \omega \left(\{\Sigma'_\ell, \Gamma'_\ell\}_{\ell=1}^L \right) \left\langle e^{-\frac{\mu}{2\pi i} \sum_{\ell=1}^L (\ln \det \nu_\ell - \ln \det \xi_\ell)} \right\rangle_{\mathbf{J}} - \frac{c}{2}, \end{aligned} \quad (2.36)$$

with Λ in Eq. (2.35) a normalization constant and the symbol $\langle \dots \rangle_{\mathbf{J}_{1,\dots,k}}$ in both expressions the average over the set $\mathbf{J}_1, \dots, \mathbf{J}_k$. In both equations, (2.35) and (2.36), we have computed the replica limits $n_\pm \rightarrow \pm\mu/2\pi i$ assuming they yield to correct results and have introduced the following pairs of 2×2 complex auxiliary matrices

$$\Upsilon_\ell \equiv M_\eta(z_{\ell+1}, z_\ell^*) + \sum_{r=1}^k \mathbf{J}_r \Sigma_{r\ell} \mathbf{J}_r^\dagger, \quad \zeta_\ell \equiv M_\eta(z_\ell, z_\ell^*) + \sum_{r=1}^k \mathbf{J}_r \Gamma_{r\ell} \mathbf{J}_r^\dagger, \quad (2.37)$$

and

$$\nu_\ell \equiv I_2 + \Sigma_\ell \mathbf{J} \Sigma'_\ell \mathbf{J}^\dagger, \quad \xi_\ell \equiv I_2 + \Gamma_\ell \mathbf{J} \Gamma'_\ell \mathbf{J}^\dagger. \quad (2.38)$$

The remaining step is the computation of the continuum limit $L \rightarrow \infty$ so that we obtain the final expression for the CGF. In Appendix A.3 (Eqs. (A.20)-(A.25)), we explain how to calculate such a limit. So far, we have computed

all limits assuming they yield correct results and are interchangeable; these conjectures are some of our strongest assumptions since our final results follow from them.

The main outcome of our method is an *effective theory* defined over the space of functions mapping each point $z \in \gamma$ onto a pair of 2×2 complex matrices $(\mathbf{\Gamma}(z), \mathbf{R}(z))$ with the CGF given by the expression

$$\mathcal{F}_\gamma(\mu) = -\frac{c}{2} + \lim_{\eta \rightarrow 0^+} \left[\ln \left\langle e^{-\frac{\mu}{2\pi i} \oint_\gamma \text{Tr}[\mathbf{\Gamma}^{-1}(z)\mathbf{R}(z)] dz} \right\rangle_{\{\mathbf{\Gamma}, \mathbf{R}\}} + \frac{c}{2} \left\langle \left\langle e^{-\frac{\mu}{2\pi i} \oint_\gamma \text{Tr}[\mathbf{G}(z)\mathbf{H}(z)] dz} \right\rangle_J \right\rangle_{\{\mathbf{\Gamma}, \mathbf{R}\}, \{\mathbf{\Gamma}', \mathbf{R}'\}} \right], \quad (2.39)$$

where, to keep the notation simple, we have introduced the 2×2 complex auxiliary matrices at $z \in \gamma$

$$\mathbf{G}(z) = [\mathbf{I}_2 + \mathbf{\Gamma}(z)\mathbf{J}\mathbf{\Gamma}'(z)\mathbf{J}^\dagger]^{-1} \quad \text{and} \quad \mathbf{H}(z) = \mathbf{\Gamma}(z)\mathbf{J}\mathbf{R}'(z)\mathbf{J}^\dagger + \mathbf{R}(z)\mathbf{J}\mathbf{\Gamma}'(z)\mathbf{J}^\dagger. \quad (2.40)$$

The brackets $\langle \cdots \rangle_{\{\mathbf{\Gamma}, \mathbf{R}\}}$ in the different elements of Eq. (2.39) denote the average over all possible paths $\{\mathbf{\Gamma}, \mathbf{R}\}$ throughout the γ curve. Any path $\{\mathbf{\Gamma}, \mathbf{R}\}$ can be thought of as the limit $L \rightarrow \infty$ of a sequence $\{\mathbf{\Gamma}(z_\ell), \mathbf{R}(z_\ell)\}_{\ell=1}^L$, with $z_\ell \in \gamma$; thus, the path measure takes the form $d\{\mathbf{\Gamma}, \mathbf{R}\} \equiv \lim_{L \rightarrow \infty} \prod_{\ell=1}^L d\mathbf{\Gamma}(z_\ell) d\mathbf{R}(z_\ell)$. Formally speaking, the average over $\{\mathbf{\Gamma}, \mathbf{R}\}$ for any arbitrary functional $S[\{\mathbf{\Gamma}, \mathbf{R}\}]$ reads

$$\langle S[\{\mathbf{\Gamma}, \mathbf{R}\}] \rangle_{\{\mathbf{\Gamma}, \mathbf{R}\}} = \int \omega[\{\mathbf{\Gamma}, \mathbf{R}\}] S[\{\mathbf{\Gamma}, \mathbf{R}\}] d\{\mathbf{\Gamma}, \mathbf{R}\}, \quad (2.41)$$

with $\omega[\{\mathbf{\Gamma}, \mathbf{R}\}]$ the *path probability distribution* following from the solution of the self-consistency equation

$$\omega[\{\mathbf{\Gamma}, \mathbf{R}\}] = \frac{1}{\Lambda} \sum_{k=0}^{\infty} \frac{e^{-c} c^k}{k!} \int \left(\prod_{r=1}^k d\{\mathbf{\Gamma}_r, \mathbf{R}_r\} \omega[\{\mathbf{\Gamma}_r, \mathbf{R}_r\}] \right) e^{\mu W[\{\mathbf{\Gamma}, \mathbf{R}\}]} \times \langle \delta_F[\mathbf{R}(z) - \mathbf{\Pi}_k(z)] \delta_F[\mathbf{\Gamma}(z) - \mathbf{\chi}_k(z)] \rangle_{\mathbf{J}_{1, \dots, k}}; \quad (2.42)$$

the symbol δ_F in the average $\langle \cdots \rangle_{\mathbf{J}_{1, \dots, k}}$ represents the functional Dirac δ in the path space and the normalization constant Λ finally reads

$$\Lambda = \left[\int e^{-\mu W[\{\mathbf{\Gamma}, \mathbf{R}\}]} \omega[\{\mathbf{\Gamma}, \mathbf{R}\}] d\{\mathbf{\Gamma}, \mathbf{R}\} \right]^{-1}. \quad (2.43)$$

The statistical contribution of each path in Eq. (2.42) is weighted by the function $\exp(\mu W[\{\mathbf{\Gamma}, \mathbf{R}\}])$ known as the *weighted factor*, which is controlled by the term

$$W[\{\mathbf{\Gamma}, \mathbf{R}\}] = \frac{1}{2\pi i} \oint_\gamma \text{Tr}[\mathbf{\Gamma}^{-1}(z)\mathbf{R}(z)] dz; \quad (2.44)$$

as we indicated in Eq. (2.39) for the CGF, the path probability distribution $\omega[\{\mathbf{\Gamma}, \mathbf{R}\}]$ ought to be solved in the $\eta \rightarrow 0^+$ limit. As we did with the previous equations, to keep the notation as simple as possible, we have introduced in Eq. (2.42) the auxiliary matrices

$$\mathbf{\chi}_k(z) = \left(\mathbf{M}_\eta(z, z^*) + \sum_{r=1}^k \mathbf{J}_r \mathbf{\Gamma}_r(z) \mathbf{J}_r^\dagger \right)^{-1} \quad \text{and} \quad \mathbf{\Pi}_k(z) = -\mathbf{\chi}_k(z) \left(i\sigma_+ + \sum_{r=1}^k \mathbf{J}_r \mathbf{R}_r(z) \mathbf{J}_r^\dagger \right) \mathbf{\chi}_k(z) \quad (2.45)$$

at $z \in \gamma$. Noteworthy is that the matrix $\mathbf{\chi}_k$ corresponds to the inverse of the matrix ζ_ℓ (Eq. (2.37)) once the $L \rightarrow \infty$ limit has been computed; we opted to make this change in the notation to differentiate the status of the calculation.

In order to obtain the first and second cumulants, κ_1 and κ_2 , we need to compute the first and second derivatives of $\mathcal{F}_\gamma(\mu)$ and evaluate them at $\mu = 0$. As with the CGF, we assume both expressions exist and yield correct results. Hence, appealing to Eq. (2.11), we obtain

$$\kappa_1 = - \lim_{\eta \rightarrow 0^+} \left[\langle W[\{\mathbf{\Gamma}, \mathbf{R}\}] \rangle_{\{\mathbf{\Gamma}, \mathbf{R}\}} + \frac{c}{2} \left\langle \left\langle \oint_\gamma \left\langle \text{Tr}[\mathbf{G}(z)\mathbf{H}(z)] \frac{dz}{2\pi i} \right\rangle_J \right\rangle_{\{\mathbf{\Gamma}, \mathbf{R}\}, \{\mathbf{\Gamma}', \mathbf{R}'\}} \right] \quad (2.46)$$

and

$$\kappa_2 = \lim_{\eta \rightarrow 0^+} \left[\langle (W[\{\mathbf{\Gamma}, \mathbf{R}\}])^2 \rangle_{\{\mathbf{\Gamma}, \mathbf{R}\}} - \langle W[\{\mathbf{\Gamma}, \mathbf{R}\}] \rangle_{\{\mathbf{\Gamma}, \mathbf{R}\}}^2 + \frac{c}{2} \left\langle \left\langle \left(\oint_{\gamma} \text{Tr} [\mathbf{G}(z) \mathbf{H}(z)] \frac{dz}{2\pi i} \right)^2 \right\rangle \right\rangle_{\{\mathbf{\Gamma}, \mathbf{R}\}, \{\mathbf{\Gamma}', \mathbf{R}'\}} \right], \quad (2.47)$$

for the first and second cumulants, respectively. Recalling the Gärtner-Ellis theorem, we deduce the rate function ϕ_γ from the CGF via the Legendre transform, obtaining a parametric expression for it in terms of the fraction n of eigenvalues within the γ curve (Appendix A.4, Eqs. (A.28)-(A.30)),

$$\{(n, \phi(n))\} = \{(\kappa_1(\mu), \mathcal{F}_\gamma(\mu) - \mu\kappa_1(\mu))\}. \quad (2.48)$$

Although Eqs. (2.46), (2.47), and (2.48) are the ones we compute to extract the statistical information of the number \mathcal{N}_A , all detach from the CGF $\mathcal{F}_\gamma(\mu)$ and path probability $\omega[\{\mathbf{\Gamma}, \mathbf{R}\}]$. Hence, Eq. (2.39) for the cumulant generating function and Eq. (2.42) for the path probability are the main outcomes of our work, since it is from them that we deduce the typical and atypical fluctuations of \mathcal{N}_A for an ensemble of sparse non-Hermitian random matrices.

2.2.2 The numerical method

In general, there is no analytical solution for Eq. (2.42); consequently, we need to resort to a variation of the statistical numerical *population dynamics* method [96] known as *weighted population dynamics* [208] to obtain numerical solutions for the path probability $\omega[\{\mathbf{\Gamma}, \mathbf{R}\}]$. For this numerical procedure, we discretize the γ curve into a finite collection of points $\{z_1, \dots, z_L\}$ and define the finite set of 2×2 complex random matrices $\{\mathbf{\Gamma}(z_i), \mathbf{R}(z_i)\}_{i=1}^L$ sampled consistently with Eq. (2.42) via a Monte Carlo scheme. Thus, we switch from the functional density $\omega[\{\mathbf{\Gamma}, \mathbf{R}\}]$ to the joint distribution $\omega[\{\mathbf{\Gamma}(z_\ell), \mathbf{R}(z_\ell)\}_{\ell=1}^L]$. Since the matrices $\mathbf{\Gamma}$ and \mathbf{R} are correlated for any collection of points along the γ curve, both $\omega[\{\mathbf{\Gamma}, \mathbf{R}\}]$ and $\omega[\{\mathbf{\Gamma}(z_\ell), \mathbf{R}(z_\ell)\}_{\ell=1}^L]$ do not factorize.

We introduce a population with a number of M sets of matrices $\{\mathbf{R}_\alpha(z_1), \dots, \mathbf{R}_\alpha(z_L), \mathbf{\Gamma}_\alpha(z_1), \dots, \mathbf{\Gamma}_\alpha(z_L)\}_{\alpha=1}^M$ at each point $z_\ell \in \gamma$. Hence, the joint probability distribution $\omega[\{\mathbf{\Gamma}(z_\ell), \mathbf{R}(z_\ell)\}_{\ell=1}^L]$ formally reads

$$\omega[\{\mathbf{\Gamma}(z_\ell), \mathbf{R}(z_\ell)\}_{\ell=1}^L] \sim \frac{1}{M} \sum_{\alpha=1}^M \left(\prod_{\ell=1}^L \delta[\mathbf{R}(z_\ell) - \mathbf{R}_\alpha(z_\ell)] \delta[\mathbf{\Gamma}(z_\ell) - \mathbf{\Gamma}_\alpha(z_\ell)] \right) e^{\mu W[\{\mathbf{\Gamma}(z_\ell), \mathbf{R}(z_\ell)\}_{\ell=1}^L]}, \quad (2.49)$$

with $W[\{\mathbf{\Gamma}, \mathbf{R}\}]$ given by Eq. (2.44). While for the standard population dynamics algorithm, the update only involves the actualization of one element per iteration, for the weighted population dynamics algorithm, the weighted factor $e^{\mu W[\{\mathbf{\Gamma}(z_\ell), \mathbf{R}(z_\ell)\}_{\ell=1}^L]} \equiv \Theta[\{\mathbf{\Gamma}(z_\ell), \mathbf{R}(z_\ell)\}_{\ell=1}^L]$ indicates the number of elements that change per iteration according to the rule

$$n_p = \left\lfloor \Theta[\{\mathbf{\Gamma}(z_\ell), \mathbf{R}(z_\ell)\}_{\ell=1}^L] \right\rfloor + r, \quad (2.50)$$

with $\lfloor \dots \rfloor$ the floor function and $r \in [0, 1]$ a random number equal to one with probability $\Theta[\{\mathbf{\Gamma}(z_\ell), \mathbf{R}(z_\ell)\}_{\ell=1}^L] - \lfloor \Theta[\{\mathbf{\Gamma}(z_\ell), \mathbf{R}(z_\ell)\}_{\ell=1}^L] \rfloor$ and equal to zero otherwise [208].

To demonstrate the exactness of the method, we have selected as γ curves disks with different radii centred at the origin and, as a sparse ensemble, the diluted version of the real Ginibre ensemble. Fig. 2.2 depicts the first two cumulants κ_1 and κ_2 depending on the various radii R of the disks with the matrix entries drawn from p_J a Gaussian distribution with zero mean and variance $1/c$, and average connectivities of $c = 3$ and $c = 10$; the shaded regions displayed within the figure delimit the error involved in the numerical solution of Eq. (2.42) via the *sample standard deviation*. The latter is an *estimator* (a statistic used to predict the value of a population parameter) of a *population standard deviation* σ . Suppose we have a sample $\{X_1, \dots, X_n\}$ from a population whose variance σ^2 is unknown, and we wish to estimate it via the sample data. If the population mean is unknown, we replace it with its estimator \bar{X} and estimate σ^2 through

$$s^2 = \frac{1}{n-1} \sum_{i=1}^n (X_i - \bar{X})^2. \quad (2.51)$$

Defined in such a form, Eq. (2.51) is an unbiased estimator, i.e., $\langle s^2 \rangle = \sigma^2$. Taking the square root of s^2 does not affect its unbiased estimator condition; therefore,

$$s = \sqrt{\frac{1}{n-1} \sum_{i=1}^n (X_i - \bar{X})^2} \quad (2.52)$$

corresponds to the sample standard deviation, formally known as the *corrected sample standard deviation* [209]. Fig. 2.2 compares the theoretical findings of Eqs. (2.46) and (2.47) with the results obtained by the Metropolis algorithm (Appendix D, Section D.6) for $N \times N$ adjacency matrices \mathbf{A} with directed edges and different values of N . While the first cumulant κ_1 exhibits an excellent agreement between the theoretical findings and the Metropolis algorithm, whatever the value of N , the second cumulant κ_2 shows a stronger dependence with the matrix dimension N , achieving better convergence between results as the value of N increases.

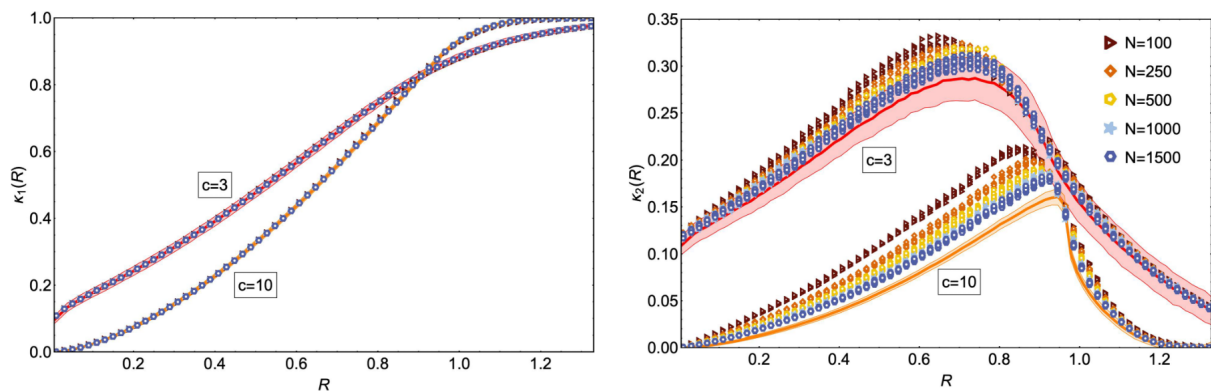


Figure 2.2: The intensive mean κ_1 (left panel) and variance κ_2 (right panel) of the number of eigenvalues $\mathcal{N}_{\mathbf{A}}$ within a disk of radius R centred at the origin of the complex plane \mathbb{C} . The matrix \mathbf{A} corresponds to the adjacency matrix of a weighted random graph of directed edges with average connectivities $c = 3$ (solid red line) and $c = 10$ (solid orange line). The asymmetric interactions are independently drawn from a Gaussian distribution p_J with zero mean and variance $1/c$. Theoretical solid lines are obtained from Eqs. (2.46) and (2.47) via the weighted population dynamics algorithm, while the markers result from the Metropolis algorithm for sets of $N \times N$ random matrices. For the theoretical results, the disk is discretized into 3000 points and a population of 10^4 is iterated 4×10^7 times. For the Metropolis algorithm, 10^4 samples are averaged and the process is repeated 10 times.

It is well-known that for small and moderate values of c , the spectral density of sparse non-Hermitian random matrices displays δ -peaks at the origin $z = 0$ [44]; consequently, for $c = 3$ both cumulants, κ_1 and κ_2 , ought to converge to a finite value at the $R \rightarrow 0^+$ limit. In contrast, for larger values of c , the sparse matrices commence to fill up and the δ -peaks start to "disappear"; consequently, we should expect that the behaviour displayed by the first cumulant resembles that of the complex Ginibre ensemble. For $c = 3$, Fig. 2.2 shows for both κ_1 and κ_2 convergence to a finite value as R goes to zero from above, pointing out the fact that the theory is capable of reproducing the mean and variance behaviour of the weighted δ peaks characterizing the spectrum in the $N \rightarrow \infty$ limit. On the other hand, for $c = 10$, the average κ_1 indeed resembles the complex Ginibre behaviour $\kappa_1 \propto R^2$ in the large N limit [180]; for values of $R \approx 0$, κ_1 is slightly bigger than R^2 and starts to approach it from above as the value of c gets bigger (Fig. 2.2, left panel). In both cases, $c = 3$ and $c = 10$, and as R increases, the limiting value of κ_1 turns out to be one (Girko's law). While this indeed happens for both values of c , the rate at which it occurs varies: for $c = 3$ the convergence of κ_1 is slower compared to $c = 10$, whose at $R \approx 1.12$ has already reached the limiting value. This behaviour clearly illustrates the distinct level of dilution in the ensemble depending on the different values of c .

The behaviour exhibited by κ_2 , in contrast to κ_1 , turns out to be interestingly far different. It has been demonstrated that sparse and asymmetric random matrices commonly possess delocalized and localized eigenvectors around the origin $z = 0$ and close to the spectrum's border, respectively, and that eigenvalue repulsion is stronger within the delocalized region [14, 32, 174, 210, 211]. The first difference in the variance of $\mathcal{N}_{\mathbf{A}}$ between the diluted real and complex Ginibre ensembles comes from the scaling behaviour: contrary to the complex case whose variance divides into three significantly different regimes [180], Fig. 2.2 makes clear that since κ_2 is finite for $R > 0$, it exhibits a linearly scaling behaviour with $N \gg 1$ due to the weak eigenvalue repulsion at the boundaries of $\rho(z)$. A feature absent in the complex Ginibre ensemble. For $c = 10$, the variance of $\mathcal{N}_{\mathbf{A}}$ displays a marked maximum at some radius

value close to $R = 1$; ahead of it, an abrupt decay of the curve. For $c = 3$, the variance shows a less-decaying continuous behaviour after its maximum (Fig. 2.2, right panel). The reason for such conduct lies within the spectrum's nature in the $N \rightarrow \infty$ limit: whereas for higher values of c , the matrix dilution decreases, resembling the real Ginibre ensemble [25–27, 180], for small and moderate values of c , such as $c = 3$, the spectrum's diamond shape extends a bit beyond the disk of $R = 1$ [44], enabling the variance of \mathcal{N}_A to take extreme values. This characteristic is also visible in the error bars of the variance: for lower values of c , the matrix is considerably diluted, leading to stronger fluctuations within the spectrum (Fig. 1.2) [112] and bigger error bars; a feature absent for larger values of c .

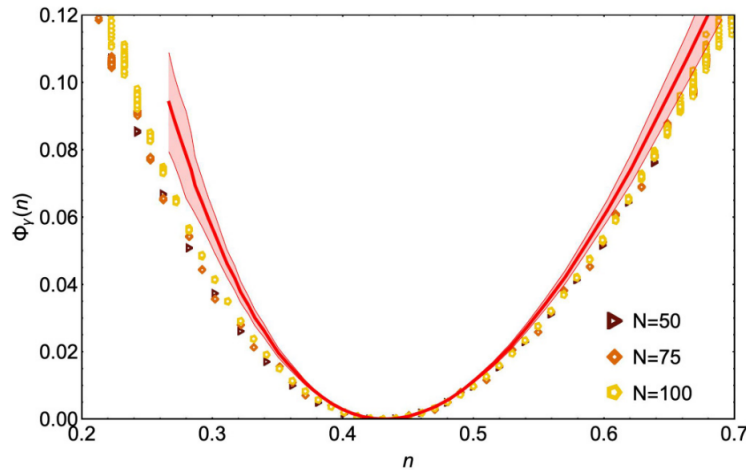


Figure 2.3: Rate function $\phi_\gamma(n)$ for the fraction $n = \mathcal{N}_A/N$ of eigenvalues inside a disk of radius $R = 0.5$ centred at the origin of the complex plane \mathbb{C} . The matrix \mathbf{A} corresponds to the adjacency matrix of a Poisson random graph with connectivity $c = 4$ and asymmetric Gaussian weights of zero mean and variance $1/c$. The continuous red line represents the theoretical findings at $N \rightarrow \infty$ and the different markers are the results of numerical diagonalization for sets of $N \times N$ random matrices. The diagonalization results are averaged over 10^7 samples and the process is repeated 10 times; for the theoretical findings, a population of 10^4 iterated 4×10^7 times is used with a discretization of 3000 points over the disk.

Fig. 2.3 presents the theoretical results for the rate function $\phi_\gamma(n)$ of the fraction $n = \mathcal{N}_A/N$ of eigenvalues inside a disk of radius $R = 0.5$ obtained by Eq. (2.48) together with direct diagonalization for three different sizes N of random matrices. The continuous red line stands as our theoretical findings, the symbols the results via direct diagonalization, and the shaded region is the error involved in the numerical solution of Eq. (2.42). Just as it happened with κ_2 , the results displayed in Fig. 2.3 demonstrate better agreement between theory and numerical diagonalization as the value of N increases, supporting the exactness of the method. The more surprising feature of $\phi_\gamma(n)$ for the diluted real Ginibre ensemble, compared to the complex case [180], lies in the asymmetry around its minimum located at $n = \kappa_1$. Owing to the strong eigenvalue repulsion around the origin $z = 0$, large fluctuations of n involving more attraction of eigenvalues within the disk are less probable; consequently, the rate function grows faster for values $n > \kappa_1$ in contrast to $n < \kappa_1$. Since this type of repulsion is absent for the complex Ginibre ensemble, its corresponding rate function stands as a symmetric function around its minimum (Fig. 3, Ref. [180])

2.3 Conditioned spectral density for the diluted real Ginibre ensemble

The study of stability conditions in several physical systems, such as food webs [212], is a current example where RMT has proved to be extremely useful. Firstly introduced in 1972, it is the seminal work of May [213], the key research that establishes the necessary criteria for studying stability conditions in the dynamics of several systems. Such a criterion indicates that *if all the real parts of the eigenvalues are negative (positive) the equilibrium is stable (unstable)* [213]. It is well-known that structures within the field of *disordered systems* as liquids and spin glasses, exhibit extremely complicated energy or free energy landscapes displaying an enormous amount of maxima, minima, and saddle points, whose effects on the dynamics and statistics of the systems are noticeable [120]. Hence, it is an area where ideas and methods from RMT are widely used, resulting in plenty of results [111, 121, 124, 183, 214, 215]. The local stability of an extreme on an N -dimensional potential energy surface $V(\mathbf{x})$ is entirely determined by the symmetric Hessian matrix \mathcal{H} of the potential $\mathcal{H}_{\ell m} = \partial_{x_\ell x_m}^2 V$, with all its N eigenvalues measuring the curvature of the potential energy. If all its eigenvalues are positive (negative), the corresponding stationary point is a *local*

minimum (local maximum); if some, but not all, are positive, the stationary point is a *saddle*. However, owing to the dependence on the systems' configurations, the entries of \mathcal{H} at a stationary point are often correlated, making the exact derivation of \mathcal{H} highly difficult. Fortunately, a fructiferous scheme substituting the Hessian matrix with an appropriate random matrix has demonstrated to be extremely helpful. In many cases, significant information about the systems' dynamics is obtained by discarding these correlations and replacing \mathcal{H} with an $N \times N$ real symmetric Gaussian matrix [123, 216, 217]. The implementation of this technique, denominated by Majumdar et al. as the *random Hessian model* (RHM) [187], has proven to be a successful tool in areas such as cosmology [218], quantum cosmology [21, 219, 220], string theory [22, 23], and neural networks [221].

The *index*, defined by some authors as the number of eigenvalues exceeding a certain threshold [187, 222] and by others as the number of eigenvalues below it [45, 223], is a random variable that has recently attracted much attention due to its connection with the study of stability conditions. For $N \times N$ symmetric and Hermitian random matrices with spectrum $\{\lambda_1, \dots, \lambda_N\}$, the number of eigenvalues exceeding a threshold $x \in \mathbb{R}$ is defined as

$$\mathfrak{n}(x) \equiv \sum_{i=1}^N \Theta(\lambda_i - x), \quad (2.53)$$

where $\Theta(x)$ is the *Heaviside step function*. The random variable $\mathfrak{n}_+ \equiv \mathfrak{n}(0)$ (the number of positive eigenvalues) arises naturally in the study of the potential landscape $V(x)$ stability, where it is a crucial indicator of the number of directions in which a stationary point is stable [187, 222]. However, one may be interested in the curvature distribution around specific saddle points with a given number of stable directions, i.e., saddle points having a prescribed fraction of positive eigenvalues. In such a context, the so-called *Conditioned Spectral Density* (CSD) arises, namely, the Hessian eigenvalue distribution constrained to have a *fixed* fraction of positive eigenvalues. The CSD provides a way to study the spectrum of constrained rare samples deviating from the typical behaviour [45].

By means of the well-known Coulomb fluid method [133–137], Satya et al. computed the CSD for ensembles of Gaussian [123, 187, 216], Wishart [224], and Cauchy [222] random matrices, where the effect of constraining the eigenvalues in different regions was modelled as having one or more confining walls; their research aimed to study the probability distribution of the ensembles having a fraction $k = \mathfrak{n}_+/N$ of positive eigenvalues. Departing from Eq. (2.53), the authors defined such probability as

$$\mathcal{P}_\beta(\mathfrak{n}_+ = kN, N) = \int P_\beta(\lambda) \delta\left(\mathfrak{n}_+ - \sum_{i=1}^N \Theta(\lambda_i)\right) d\lambda \quad (2.54)$$

and, appealing to the JPDE function for the Gaussian, Wishart, and Cauchy ensembles (Eq. (1.26)), rewrote it as a path integral in the space of normalized densities $\rho_{\mathbf{H}}(\lambda)$ (Eq. (1.18)); details at Refs [57, 123, 187, 216, 222, 224]. Utilizing the saddle-point method, the authors demonstrated that for the three ensembles in the large limit $N \rightarrow \infty$, $\mathcal{P}_\beta(\mathfrak{n}_+ = kN, N) \asymp \exp[-\beta N^2 \psi(k)]$, with ψ the rate function defined for $0 \leq k \leq 1$ and β -independent, and that the constrained density $\rho^*(\lambda)$ (using the authors' notation), i.e. the AESD having a prescribed fraction of k positive eigenvalues, displayed three universal features resulting from the repulsive Coulomb interaction between eigenvalues:

1. $\rho^*(\lambda)$ was an asymmetric function with a noncompact support.
2. The eigenvalues accumulated at the walls.
3. There was an abrupt transition in the spectrum as the constrained eigenvalues reached their typical value.

All these universal properties lie in the nature shown by the support of the constrained density $\rho^*(\lambda)$. For all three ensembles, when k differs from its typical value k_{typ} , there is no single support solution for $\rho^*(\lambda)$. The eigenvalues (particles) are constrained to split into two regions on the real line \mathbb{R} : a fraction k to the right and a fraction $1 - k$ to the left of the constraint $x \in \mathbb{R}$. As $k \rightarrow k_{\text{typ}}$, the two supports merge into a single support solution [123, 187, 216, 222, 224]. For example, for the Gaussian ensembles [123, 187, 216], $\rho^*(\lambda)$ divides into two supports, one to the left and one to the right of $x = 0$, presenting a singularity at such a value, i.e., an accumulation of eigenvalues at the threshold (Fig. 1 in Ref. [216]). As $k \rightarrow 1$ from below, the area formed by the constrained density at the left support decreases, leaving us with only one support to the right of zero. On the other hand, when k continuously decreases, the area of the left support grows and the upper edge increases. When $k = 1/2$, the two supports merge into a single support and reduce to the Wigner semicircle law (Fig. 2 in Ref. [216]). In the end, $\rho^*(\lambda)$ corresponds to the *equilibrium (or optimal) charge density* of the eigenvalue fluid given a fixed fraction k of positive charges [216].

Subsequent research to the invariant ensembles was conducted in Refs. [188, 189], where Allez et al. answered the question of how many eigenvalues lie outside an open disk of radius $R = 0.5$ in \mathbb{C} for the *complex* and *real* Ginibre ensembles. Defining the index N_R as the number of eigenvalues with modulus greater than R , the authors studied the probability distribution $\mathcal{P}(p, N)$ that a specific fraction of eigenvalues $p = N_R/N$ would lie outside the radius R disk for both ensembles. Resorting to the JPDE function for the complex ($\beta = 2$) and real ($\beta = 1$) Ginibre ensembles [25, 139, 225], and expressing $\mathcal{P}(p, N)$ as a functional path integral over the space of normalized densities $\rho_A(z)$, the authors demonstrated that in the $N \rightarrow \infty$ limit, $\mathcal{P}(p, N) \asymp \exp[-\beta/2\psi_R(p)]$ with ψ_R the rate function for both ensembles and $0 \leq p \leq 1$ the parameter controlling the number of eigenvalues outside the disk. Together with the analytical expressions for $\mathcal{P}(p, N)$ and ψ_R , Ref. [189] also proved that the constrained density $\rho^*(z)$ exhibited the following three features:

- (i) $\rho^*(z)$ was an asymptotic density supported by centred circles.
- (ii) Accumulation of eigenvalues at the border of the disk.
- (iii) An abrupt transition in the spectrum as the constrained eigenvalues reach their typical fluctuations.

To illustrate the above three points, let us take the case where we impose an atypically small amount of eigenvalues (charges) $p < p_{\text{typ}}$ outside the open ball $\mathcal{B}_R(0) = \{z \in \mathbb{C} \mid \|z\| < R\}$, that is, an abnormally large number of eigenvalues $1 - p > 1 - p_{\text{typ}}$ on the closed ball $\overline{\mathcal{B}}_R(0)$. Within $\mathcal{B}_R(0)$, the density of $\rho^*(z)$ is equal to $1/\pi$, which corresponds to a proportion R^2 of the charges. The charge excess $p_{\text{typ}} - p$ pulled inside $\mathcal{B}_R(0)$ has no choice but to lie exactly on the circle of radius R , where they allocate uniformly. Outside $\overline{\mathcal{B}}_R(0)$, we expect the charges to be allocated in one single annulus. Under no constraint, the CSD is regular on its full support, and we recover Girko's law (Fig. 1 in Ref. [189]). As with the invariant ensembles, $\rho^*(z)$ is the optimal charge density that minimizes the path integral action [189].

The above properties displayed by the constrained density ρ^* for the invariant and Ginibre ensembles are the same and result from the repulsive Coulomb interaction between eigenvalues shown by their corresponding JPDE functions (Eq. (1.26) and (1.27)). So, the first natural question would be whether or not all these properties of the constrained density on the invariant ensembles [123, 187, 216, 222, 224] will still be valid for SRMs now that we do not have a JPDE function. The answer to such a query appeared in Ref. [45], where Pérez Castillo and Metz computed the CSD for the adjacency matrix of the Erdős-Rényi random graphs and sparse Wishart random matrices, for which the traditional Coulomb fluid approach is unworkable. Establishing the index as the number of eigenvalues below a certain threshold $x \in \mathbb{R}$,

$$\mathcal{I}_N(x) \equiv \sum_{i=1}^N \Theta(x - \lambda_i), \quad (2.55)$$

the authors defined the CSD as

$$\rho(\lambda|k) = \lim_{N \rightarrow \infty} \frac{1}{N} \frac{\left\langle \sum_{i=1}^N \delta(\lambda - \lambda_i) \delta[kN - \mathcal{I}_N(x)] \right\rangle}{\langle \delta[kN - \mathcal{I}_N(x)] \rangle}, \quad (2.56)$$

where the symbol $\langle \dots \rangle$ denoted the average over the random matrix ensemble and $0 \leq k \leq 1$ was the adjustable parameter indicating the specific fraction of eigenvalues below x . Specifically, Eq. (2.56) corresponds to the conditional probability density for the eigenvalues in $[\lambda, \lambda + d\lambda]$, as long as there are precisely kN eigenvalues smaller than x [45]. As with Refs. [44] and [173], the authors solved the problem by means of self-consistent equations (details in Ref. [45]). Resorting to the replica method and replica-symmetric ansatz formalism, the authors found that in the limit of infinitely large matrices $N \rightarrow \infty$, the CSD, for both ensembles, displayed the following three outstanding properties, totally in contrast with the invariant cases:

1. $\rho(\lambda|k)$ had a compact support.
2. No accumulation of eigenvalues around x .
3. No transition in the spectrum as the constrained eigenvalues approach their typical value.

All these features seem to come from the weak or absent repulsion between the eigenvalues of SRMs, where they are allowed to be arbitrarily close to each other; we provide further details about this in Subsection 2.3.2. Added to the above features, $\rho(\lambda|k)$ for the infinitely large Erdős-Rényi random graphs also fulfilled with always being a

symmetric function. Depending on whether $k > k_{\text{typ}}$ or $k < k_{\text{typ}}$, the spectrum may have an excess or defect of eigenvalues to the left of the constraint, respectively. For the Erdős-Rényi random graphs case, as $k \rightarrow k_{\text{typ}}$, $\rho(\lambda|k)$ displayed a continuous change in its shape and a smooth decrease in the area formed by it (Fig. 1 in Ref. [45]). Since the CSD is always symmetric, the constrained graph ensemble should be empty for $k < 1/2$. Consequently, the authors glimpsed the possibility of a transition at some critical value k_c equal to or larger than $1/2$ [45].

In this section, we retake the previous question and tackle the CSD $\rho(z|\mathcal{R}_\gamma)$ for an ensemble of $N \times N$ sparse non-Hermitian random matrices in the $N \rightarrow \infty$ limit when the constraint $\mathcal{R}_\gamma \in [0, 1]$ fixing a specific fraction of eigenvalues within a smooth Jordan curve γ is imposed. As with the full counting statistics of the number \mathcal{N}_D [1] (Section 2.2), the strongest feature of our theory is the capacity to perform a formal analysis of the CSD in ensembles of arbitrarily large sparse non-Hermitian random matrices with real and complex entries, even when the corresponding JPDE functions are unknown. Resorting to the replica method and replica-symmetric formalism, we derive a general expression for $\rho(z|\mathcal{R}_\gamma)$, valid for any non-Hermitian random matrix in the $N \rightarrow \infty$ limit, and obtain explicit results for the diluted version of the real Ginibre ensemble considering symmetric adjacency matrices of Poisson random graphs with asymmetric couplings. We end with an effective expression for $\rho(z|\mathcal{R}_\gamma)$ in terms of a self-consistency equation and succeed in showing that, in the $N \rightarrow \infty$ limit, the CSD displays the following three striking features, which agree with the conclusions of Ref. [45] for the Erdős-Rényi random graphs:

- (i) $\rho(z|\mathcal{R}_\gamma)$ is a symmetric function on a connected compact support.
- (ii) There is no accumulation of eigenvalues at the boundaries of the γ curve.
- (iii) There is no abrupt transition in the spectrum as the constrained eigenvalues approach their typical fluctuations.

As with the Erdős-Rényi random graphs and Whisart random matrices, these features seem to emerge from the existing and absent eigenvalue repulsion in the delocalized and localized regions, respectively, in sparse and asymmetric random matrices [14, 32, 174, 210, 211, 226]. We compare all our results with Monte Carlo simulations for finite random matrices showing an excellent agreement.

We divide the calculation of the CSD into two parts: the analytical development (Subsection 2.3.1) and the numerical treatment (Subsection 2.3.2). While the latter focuses on providing a solution to the self-consistency equation through statistical numerical methods and presenting all our results for the diluted real Ginibre ensemble, the analytical procedure is further divided into two parts. In the first part, we define $\rho(z|\mathcal{R}_\gamma)$ and, by means of the CGF, achieve an analogy with statistical physics, obtaining the fully general expression for the CSD. Immediately after, we apply the general equation to the ensemble of symmetric Poisson graphs with asymmetric couplings and manage to rewrite $\rho(z|\mathcal{R}_\gamma)$ as a path integral. In the second part, we solve the integral equation via the saddle-point method and introduce a replica-symmetric ansatz assuming invariance of the equations under replica permutations. Finally, we combine all the expressions together and obtain the final equation for the CSD in terms of the self-consistency equation. We show in detail all the mathematical manipulations in Appendix B.

2.3.1 The analytical development

The path integral formalism

We commence by introducing $\mathbf{A} \in M_{N \times N}(\mathbb{C})$ a non-Hermitian random matrix drawn from some distribution $\mathcal{P}(\mathbf{A})$ with spectrum $\Lambda = \{\lambda_1, \dots, \lambda_N\}$ and $\{\lambda_i\}_{i=1}^N \in \mathbb{C}$. Subsequently, we take the ESD (Eq. (1.18)) and the number \mathcal{N}_A (Eq. (2.9)) with $\gamma = \partial D$ the smooth Jordan curve ($D \subseteq \mathbb{C}$) and define the CSD as

$$\rho(z|\mathcal{R}_\gamma) = \lim_{N \rightarrow \infty} \frac{\langle \rho_A(z) \delta[\mathcal{N}_A(\gamma) - N\mathcal{R}_\gamma] \rangle}{\langle \delta[\mathcal{N}_A(\gamma) - N\mathcal{R}_\gamma] \rangle}, \quad (2.57)$$

with $z = x + iy$, the symbol $\langle \dots \rangle$ the average over the distribution $\mathcal{P}(\mathbf{A})$, and $\mathcal{R}_\gamma \in [0, 1]$ the adjustable parameter controlling the number of eigenvalues within the γ curve. In order to compute the average of Eq. (2.57), we need to know the exact dependence of $\rho(z|\mathcal{R}_\gamma)$ with the \mathbf{A} matrix. Then, appealing to Eqs. (2.14) and (2.16), together with the Laplace representation of Dirac's δ , we rewrite the CSD as

$$\rho(z|\mathcal{R}_\gamma) = - \lim_{N \rightarrow \infty} \frac{1}{N\pi} \partial_z \partial_{z^*} \frac{\int \langle \ln Q_A(z, z^*) e^{-\mu \mathcal{N}_A(\gamma)} \rangle e^{\mu N \mathcal{R}_\gamma} d\mu}{\int \langle e^{-\mu \mathcal{N}_A(\gamma)} \rangle e^{\mu N \mathcal{R}_\gamma} d\mu}, \quad (2.58)$$

with $\partial_z = \frac{1}{2}(\partial_x - i\partial_y)$ and $\partial_{z^*} = \frac{1}{2}(\partial_x + i\partial_y)$ the derivatives over z and $z^* = x - iy$, respectively. Eq. (2.58) provides us with clues about the dependence of the CSD on the matrix \mathbf{A} by means of the equations of Section 2.2.1; however, we still cannot compute the average over $\mathcal{P}(\mathbf{A})$. Furthermore, we need to know the effects of the variable μ on $\rho(z|\mathcal{R}_\gamma)$. Specifically, the effects of μ on the number $\mathcal{N}_\mathbf{A}$.

We recall from Subsection 2.2.1 that the complete statistical information of $\mathcal{N}_\mathbf{A}$, typical and atypical fluctuations, is encoded within the CGF $\mathcal{F}_\gamma(\mu)$ (Eq. (2.10)). Then, to be able to express $\rho(z|\mathcal{R}_\gamma)$ in terms of $\mathcal{F}_\gamma(\mu)$, we resort to the following variation of Eq. (1.36)

$$\langle g(x) \ln f(x) \rangle = \lim_{n \rightarrow 0} \frac{1}{n} \langle g(x) \rangle \ln \left[\frac{\langle g(x) f^n(x) \rangle}{\langle g(x) \rangle} \right], \quad (2.59)$$

selecting $f = Q_\mathbf{A}(z, z^*)$ and $g = e^{-\mu \mathcal{N}_\mathbf{A}(\gamma)}$, and introduce $\mathcal{F}_\gamma(\mu)$ to the resulting expression (Eq. (B.1)). After a few algebraic manipulations and the use of the saddle-point method (Appendix B.1, Eqs. (B.1)-(B.3)), we rewrite Eq. (2.58) as

$$\rho(z|\mathcal{R}_\gamma) = - \lim_{N \rightarrow \infty} \lim_{n \rightarrow 0} \frac{1}{nN\pi} \partial_z \partial_{z^*} \ln \left\langle e^{-\mu_0 \mathcal{N}_\mathbf{A}(\gamma)} [Q_\mathbf{A}(z, z^*)]^n \right\rangle, \quad (2.60)$$

where the value μ_0 follows from the solution of the saddle-point equation

$$\mathcal{R}_\gamma = \partial_\mu \mathcal{F}_\gamma(\mu)|_{\mu=\mu_0}. \quad (2.61)$$

The effect of the parameter μ_0 over the spectrum is the following: $\mu_0 < 0$ (> 0) favours a major (lower) concentration of eigenvalues inside the γ curve. To keep the notation simple, we drop the zero subscript of parameter μ_0 for the subsequent developments. It is worth recalling that $\mathcal{F}_\gamma(\mu)$ is a concave function whose limit $N \rightarrow \infty$ exists and is different from zero or infinity since we assume that the Gärtner-Ellis result (Theorem 1.1) holds.

Invoking Eq. (2.15) and discretizing the γ curve into a set of points $\{\omega_\ell\}_{\ell=1}^L \subseteq \mathbb{C}$ such that $\omega_{L+1} \equiv \omega_1$ and $\omega_{\ell+1} \equiv \omega_\ell + \Delta\omega_\ell$, we arrive at the following exact identity for the number $\mathcal{N}_\mathbf{A}$

$$\mathcal{N}_\mathbf{A}(\gamma) = - \frac{1}{2\pi i} \lim_{L \rightarrow \infty} \sum_{\ell=1}^L [\ln Q_\mathbf{A}(\omega_{\ell+1}, \omega_\ell^*) - \ln Q_\mathbf{A}(\omega_\ell, \omega_\ell^*)], \quad (2.62)$$

transforming Eq. (2.60) into

$$\rho(z|\mathcal{R}_\gamma) = - \lim_{N \rightarrow \infty} \lim_{L \rightarrow \infty} \lim_{n \rightarrow 0} \frac{1}{nN\pi} \partial_z \partial_{z^*} \ln \left\langle [Q_\mathbf{A}(z, z^*)]^n \prod_{\ell=1}^L [Q_\mathbf{A}(\omega_{\ell+1}, \omega_\ell^*)]^{n+} [Q_\mathbf{A}(\omega_\ell, \omega_\ell^*)]^{n-} \right\rangle, \quad (2.63)$$

with n_\pm complex numbers defined as $n_\pm \equiv \pm\mu/2\pi i$.

Eq. (2.63) displays the specific dependence of the CSD on the non-Hermitian random matrix \mathbf{A} ; nonetheless, the computation of the average is far from easy. Then, we need to express $\rho(z|\mathcal{R}_\gamma)$ in a more suitable form. To do it, we resort to the matrix \mathbf{F}_η (Eq. (2.19)) [158, 176] and once more express $Q_\mathbf{A}$ as a Gaussian integral,

$$Q_\mathbf{A}(z, z^*) = \lim_{\eta \rightarrow 0^+} \int \left(\prod_{i=1}^N \frac{d\psi_i d\psi_i^\dagger}{\pi^2} \right) \exp \left[- \sum_{i=1}^N \psi_i^\dagger \mathbf{M}_\eta(z, z^*) \psi_i + i \sum_{i,j=1}^N \psi_i^\dagger \mathbf{B}_{ij} \psi_j \right],$$

over a set of spinors $\psi_i \in \mathbb{C}^2$, for $i = 1, \dots, N$, maintaining the previous definitions of the matrices \mathbf{M}_η , \mathbf{B}_{ij} , σ_+ , and σ_- (Eqs. (2.21) and (2.22)). We recall that in its integral form, $Q_\mathbf{A}$ represents the partition function of a system of N spinors placed over a graph and coupled through the 2×2 set of complex matrices $\{\mathbf{B}_{ij}\}_{i,j=1}^N$. Owing to the imaginary nature of the numbers n_\pm in Eq. (2.63), we are required to invoke once more the replica method assuming $n_\pm \in \mathbb{N}^+$, to subsequently calculate the $N \rightarrow \infty$ limit and finally perform the analytical continuation of the CSD to their values $n_\pm \rightarrow \pm\mu/2\pi i$. As a consequence of assuming the Gärtner-Ellis theorem to be valid, the thermodynamic limit $N \rightarrow \infty$ exists and differs from zero or infinity. Analogous to the full counting statistics of the number $\mathcal{N}_\mathbf{A}$ (Section 2.2), the remaining limits in Eq. (2.63) and the analytical continuation of $\rho(z|\mathcal{R}_\gamma)$ are not rigorously proven. Nevertheless, at all moments, we assume the CSD is such that all the remaining limits to exist and to be interchangeable. We verify these assumptions later during the numerical procedure.

Inserting the integral representation of $Q_{\mathbf{A}}(z, z^*)$ into Eq. (2.63), we obtain a general expression, valid for any contour $\gamma \in \mathbb{C}$ and non-Hermitian random matrix ensemble, for the CSD

$$\begin{aligned} \rho(z|\mathcal{R}_\gamma) = & - \lim_{N \rightarrow \infty} \lim_{L \rightarrow \infty} \lim_{n \rightarrow 0} \lim_{n_\pm \rightarrow \frac{\pm \mu}{2\pi i}} \lim_{\eta \rightarrow 0^+} \frac{1}{nN\pi} \partial_z \partial_{z^*} \ln \int \left(\prod_{i=1}^N \prod_{\ell=1}^L \prod_{a=1}^{n_+} d\Psi_{i\ell a} \right) \left(\prod_{i=1}^N \prod_{\ell=1}^L \prod_{b=1}^{n_-} d\Phi_{i\ell b} \right) \left(\prod_{i=1}^N \prod_{c=1}^n d\Omega_{ic} \right) \\ & \times \exp \left[- \sum_{i=1}^N \left(\sum_{c=1}^n \Omega_{ic}^\dagger \mathbf{M}_\eta(z, z^*) \Omega_{ic} + \sum_{\ell=1}^L \left\{ \sum_{a=1}^{n_+} \psi_{i\ell a}^\dagger \mathbf{M}_\eta(\omega_{\ell+1}, \omega_\ell^*) \psi_{i\ell a} + \sum_{b=1}^{n_-} \phi_{i\ell b}^\dagger \mathbf{M}_\eta(\omega_\ell, \omega_\ell^*) \phi_{i\ell b} \right\} \right) \right] \\ & \times \left\langle \exp \left[i \sum_{i < j} \left(\sum_{c=1}^n \left\{ \Omega_{ic}^\dagger \mathbf{B}_{ij} \Omega_{jc} + \Omega_{jc}^\dagger \mathbf{B}_{ij}^\dagger \Omega_{ic} \right\} + \sum_{\ell=1}^L \left[\sum_{a=1}^{n_+} \left\{ \psi_{i\ell a}^\dagger \mathbf{B}_{ij} \psi_{j\ell a} + \psi_{j\ell a}^\dagger \mathbf{B}_{ij}^\dagger \psi_{i\ell a} \right\} \right. \right. \right. \right. \\ & \left. \left. \left. + \sum_{b=1}^{n_-} \left\{ \phi_{i\ell b}^\dagger \mathbf{B}_{ij} \phi_{j\ell b} + \phi_{j\ell b}^\dagger \mathbf{B}_{ij}^\dagger \phi_{i\ell b} \right\} \right] \right) \right] \right\rangle, \end{aligned} \quad (2.64)$$

where we have written the measures over the spinors as $d\Psi_i \equiv d\psi_i d\psi_i^\dagger / \pi^2$ (analogous for $d\Phi_i$ and $d\Omega_i$) to simplify the notation. As with $\mathcal{F}_\gamma(\mu)$ (Eq. (2.23)), the success in computing the average of Eq. (2.64), and consequently in obtaining a final expression for $\rho(z|\mathcal{R}_\gamma)$, depends on the $\mathcal{P}(\mathbf{A})$ choice.

We test the exactness of our theory with \mathbf{A} , the adjacency matrix of a weighted random graph with directed edges following a Poisson distribution. Hence, we express the elements of \mathbf{A} as $A_{ij} = c_{ij} J_{ij}$ [31], with $\{c_{ij}\}_{i,j=1}^N$ the entries of the adjacency matrix \mathbf{C} (Definition 1.8) drawn from Eq. (1.17), with $c \in \mathbb{R}^+$ the average connectivity independent of N , and $\{J_{ij}\}_{i,j=1}^N$ real-valued i.i.d. random variables drawn from a probability distribution p_J . Whereas the entries $\{c_{ij}\}_{i,j=1}^N$ encode the topology of the graph, the elements $\{J_{ij}\}_{i,j=1}^N$ correspond to the system quenched variables and represent the asymmetric interactions between sites. Performing the average over \mathbf{C} in Eq. (2.64) leads us to

$$\begin{aligned} \rho(z|\mathcal{R}_\gamma) = & - \lim_{N \rightarrow \infty} \lim_{L \rightarrow \infty} \lim_{n \rightarrow 0} \lim_{n_\pm \rightarrow \frac{\pm \mu}{2\pi i}} \lim_{\eta \rightarrow 0^+} \frac{1}{nN\pi} \partial_z \partial_{z^*} \ln \int \left(\prod_{i=1}^N \prod_{\ell=1}^L \prod_{a=1}^{n_+} d\Psi_{i\ell a} \right) \left(\prod_{i=1}^N \prod_{\ell=1}^L \prod_{b=1}^{n_-} d\Phi_{i\ell b} \right) \left(\prod_{i=1}^N \prod_{c=1}^n d\Omega_{ic} \right) \\ & \times \exp \left[- \sum_{i=1}^N \left\{ \sum_{c=1}^n \Omega_{ic}^\dagger \mathbf{M}_\eta(z, z^*) \Omega_{ic} + \sum_{\ell=1}^L \left(\sum_{a=1}^{n_+} \psi_{i\ell a}^\dagger \mathbf{M}_\eta(\omega_{\ell+1}, \omega_\ell^*) \psi_{i\ell a} + \sum_{b=1}^{n_-} \phi_{i\ell b}^\dagger \mathbf{M}_\eta(\omega_\ell, \omega_\ell^*) \phi_{i\ell b} \right) \right\} \right] \\ & \times \exp \left[\frac{c}{2N} \sum_{i,j=1}^N \left\langle \exp \left[i \left\{ \sum_{c=1}^n \left(\Omega_{ic}^\dagger \mathbf{J} \Omega_{jc} + \Omega_{jc}^\dagger \mathbf{J}^\dagger \Omega_{ic} \right) + \sum_{\ell=1}^L \left[\sum_{a=1}^{n_+} \left(\psi_{i\ell a}^\dagger \mathbf{J} \psi_{j\ell a} + \psi_{j\ell a}^\dagger \mathbf{J}^\dagger \psi_{i\ell a} \right) \right. \right. \right. \right. \right. \right. \\ & \left. \left. \left. + \sum_{b=1}^{n_-} \left(\phi_{i\ell b}^\dagger \mathbf{J} \phi_{j\ell b} + \phi_{j\ell b}^\dagger \mathbf{J}^\dagger \phi_{i\ell b} \right) \right] \right\} - 1 \right\rangle_J \right], \end{aligned} \quad (2.65)$$

with $\langle \dots \rangle_J$ the average over the quenched disorder $\mathbf{J} = \mathbf{J}\sigma_+ + \mathbf{J}'\sigma_-$ and \mathbf{J}, \mathbf{J}' real-valued interaction strengths drawn independently from the distribution p_J .

To decouple the sites of Eq. (2.65), we follow the procedure of Refs. [41–43] and introduce the equivalent to the replicated density $\rho(\phi)$ (Eq. (2.6)) via the next order parameter

$$P(\Psi, \Phi, \Omega) \equiv \frac{1}{N} \sum_{i=1}^N \left[\prod_{c=1}^n \delta(\Omega_c - \Omega_{ic}) \right] \prod_{\ell=1}^L \left[\prod_{a=1}^{n_+} \delta(\psi_{\ell a} - \psi_{i\ell a}) \prod_{b=1}^{n_-} \delta(\phi_{\ell b} - \phi_{i\ell b}) \right], \quad (2.66)$$

with the shorthand notation $P(\Psi, \Phi, \Omega) \equiv P(\Psi, \Phi, \Omega; \{\Psi_i, \Phi_i, \Omega_i\}_{i=1}^N)$, $\Psi \equiv \{\psi_{\ell a}\}$, $\Phi \equiv \{\phi_{\ell b}\}$, and $\Omega \equiv \{\Omega_c\}_{c=1}^n$, for $\ell = 1, \dots, L$, $a = 1, \dots, n_+$, and $b = 1, \dots, n_-$. Analogously, $\Psi_i \equiv \{\psi_{i\ell a}\}$, $\Phi_i \equiv \{\phi_{i\ell b}\}$, and $\Omega_i \equiv \{\Omega_{ic}\}$ for $i = 1, \dots, N$.

After a series of manipulations (Appendix B.1, Eqs. (B.5)–(B.8)), we express Eq. (2.65) as the logarithm of a path integral over the order parameter P and its conjugated parameter \hat{P}

$$\rho(z|\mathcal{R}_\gamma) = - \lim_{N \rightarrow \infty} \lim_{L \rightarrow \infty} \lim_{n \rightarrow 0} \lim_{n_\pm \rightarrow \frac{\pm \mu}{2\pi i}} \lim_{\eta \rightarrow 0^+} \frac{1}{nN\pi} \partial_z \partial_{z^*} \ln \int e^{-NS[\{P, \hat{P}\}]} \mathcal{D}[\{P, \hat{P}\}], \quad (2.67)$$

with the action $\mathcal{S} \left[\left\{ P, \hat{P} \right\} \right]$ given by

$$\begin{aligned} \mathcal{S} \left[\left\{ P, \hat{P} \right\} \right] &= -\ln \left(\int e^{-\tau(\Psi, \Phi, \Omega) - i\hat{P}(\Psi, \Phi, \Omega)} d\Psi d\Phi d\Omega \right) - i \int P(\Psi, \Phi, \Omega) \hat{P}(\Psi, \Phi, \Omega) d\Psi d\Phi d\Omega \\ &\quad - \frac{c}{2} \int \left\langle e^{i\Xi(\Psi, \Phi, \Omega, \Psi', \Phi', \Omega')} - 1 \right\rangle_J P(\Psi, \Phi, \Omega) \hat{P}(\Psi', \Phi', \Omega') d\Psi d\Phi d\Omega d\Psi' d\Phi' d\Omega'. \end{aligned} \quad (2.68)$$

To facilitate the handling of Eq. (2.67), we have introduced the auxiliary functions

$$\tau(\Psi, \Phi, \Omega) \equiv \sum_{c=1}^n \Omega_c^\dagger M_\eta(z, z^*) \Omega_c + \sum_{\ell=1}^L \left(\sum_{a=1}^{n_+} \psi_{\ell a}^\dagger M_\eta(\omega_{\ell+1}, \omega_\ell^*) \psi_{\ell a} + \sum_{b=1}^{n_-} \phi_{\ell b}^\dagger M_\eta(\omega_\ell, \omega_\ell^*) \phi_{\ell b} \right) \quad (2.69)$$

and

$$\begin{aligned} \Xi(\Psi, \Phi, \Omega, \Psi', \Phi', \Omega') &\equiv \sum_{\ell=1}^L \left[\sum_{a=1}^{n_+} \left(\psi_{\ell a}^\dagger J \psi'_{\ell a} + \psi'_{\ell a} J^\dagger \psi_{\ell a} \right) + \sum_{b=1}^{n_-} \left(\phi_{\ell b}^\dagger J \phi'_{\ell b} + \phi'_{\ell b} J^\dagger \phi_{\ell b} \right) \right] \\ &\quad + \sum_{c=1}^n \left(\Omega_c^\dagger J \Omega'_c + \Omega'_c J^\dagger \Omega_c \right), \end{aligned} \quad (2.70)$$

maintaining the notation employed for Eq. (2.27).

Replica-symmetric ansatz and the auto-consistent equations

To solve the integral of Eq. (2.67), we resort to the saddle-point method. Hence, the asymptotic convergence shown in Eq. (2.30) still holds with the corresponding action given by Eq. (2.68); for notation purposes, we drop the zero subscript from the order parameter P and its conjugated variable \hat{P} . Then, the stationary conditions for P and \hat{P} obey the following saddle-point equations

$$i\hat{P}(\Psi, \Phi, \Omega) = -c \int \left\langle e^{i\Xi(\Psi, \Phi, \Omega, \Psi', \Phi', \Omega')} - 1 \right\rangle_J P(\Psi', \Phi', \Omega') d\Psi' d\Phi' d\Omega' \quad (2.71)$$

and

$$P(\Psi, \Phi, \Omega) = \frac{e^{-\tau(\Psi, \Phi, \Omega) - i\hat{P}(\Psi, \Phi, \Omega)}}{\int e^{-\tau(\Psi', \Phi', \Omega') - i\hat{P}(\Psi', \Phi', \Omega')} d\Psi' d\Phi' d\Omega'}. \quad (2.72)$$

To proceed with the derivation, with a modest amount of foresight, we assume that the state in which the system is trapped corresponds to the global minimum of Eq. (2.67) and propose the next replica-symmetric (RS) ansatz concerning the functional form of the order parameter $P(\Psi, \Phi, \Omega)$ that appears in the effective replica theory

$$\begin{aligned} P(\Psi, \Phi, \Omega) &= \int d\Delta \left[\prod_{\ell=1}^L d\Sigma_\ell d\Gamma_\ell \right] \omega \left(\Delta, \{ \Sigma_\ell, \Gamma_\ell \}_{\ell=1}^L \right) \\ &\quad \times \left(\prod_{c=1}^n \frac{e^{-\Omega_c^\dagger \Delta^{-1} \Omega_c}}{\det \Delta} \right) \prod_{\ell=1}^L \left[\prod_{a=1}^{n_+} \frac{e^{-\psi_{\ell a}^\dagger \Sigma_\ell^{-1} \psi_{\ell a}}}{\det \Sigma_\ell} \prod_{b=1}^{n_-} \frac{e^{-\phi_{\ell b}^\dagger \Gamma_\ell^{-1} \phi_{\ell b}}}{\det \Gamma_\ell} \right], \end{aligned} \quad (2.73)$$

with $\Delta, \Sigma_\ell, \Gamma_\ell \in M_{2 \times 2}(\mathbb{C})$ and the set of matrices $\{ \Sigma_\ell, \Gamma_\ell \}_{\ell=1}^L$ defined for each point ω_ℓ on the γ curve. The function $\omega \left(\Delta, \{ \Sigma_\ell, \Gamma_\ell \}_{\ell=1}^L \right)$ corresponds to the joint probability distribution for the complete set of matrices and complies with being normalized to unity, i.e.,

$$\int d\Delta \left(\prod_{\ell=1}^L d\Sigma_\ell d\Gamma_\ell \right) \omega \left(\Delta, \{ \Sigma_\ell, \Gamma_\ell \}_{\ell=1}^L \right) = 1. \quad (2.74)$$

Inserting the RS ansatz into the saddle-point equations and action (Eqs. (2.71), (2.72), and (2.68), respectively), and after a sequence of algebraic manipulations (Appendix B.2, Eqs. (B.9)-(B.14)), we find the exact expression for

the joint probability distribution,

$$\begin{aligned} \omega\left(\Delta, \{\Sigma_\ell, \Gamma_\ell\}_{\ell=1}^L\right) &= \frac{1}{\mathfrak{N}} \sum_{k=0}^{\infty} \frac{e^{-c} c^k}{k!} \int \left[\prod_{r=1}^k \left(d\Delta_r \prod_{\ell=1}^L d\Sigma_{r\ell} d\Gamma_{r\ell} \right) \omega\left(\Delta_r, \{\Sigma_{r\ell}, \Gamma_{r\ell}\}_{\ell=1}^L\right) \right] \left\langle \delta\left(\Delta - \mathfrak{F}^{-1}\right) \right. \\ &\quad \left. \times e^{-n \ln \det \mathfrak{F} - \frac{\mu}{2\pi i} \sum_{\ell=1}^L (\ln \det \Upsilon_\ell - \ln \det \zeta_\ell)} \prod_{\ell=1}^L \delta\left(\Gamma_\ell - \zeta_\ell^{-1}\right) \delta\left(\Sigma_\ell - \Upsilon_\ell^{-1}\right) \right\rangle_{\mathbf{J}_{1,\dots,k}}, \end{aligned} \quad (2.75)$$

and action,

$$\begin{aligned} \mathcal{S} &= -\ln \left(\sum_{k=0}^{\infty} \frac{e^{-c} c^k}{k!} \int \left[\prod_{r=1}^k \left(d\Delta_r \prod_{\ell=1}^L d\Sigma_{r\ell} d\Gamma_{r\ell} \right) \omega\left(\Delta_r, \{\Sigma_{r\ell}, \Gamma_{r\ell}\}_{\ell=1}^L\right) \right] \right. \\ &\quad \left. \times \left\langle \exp \left[-n \ln \det \mathfrak{F} - \frac{\mu}{2\pi i} \sum_{\ell=1}^L (\ln \det \Upsilon_\ell - \ln \det \zeta_\ell) \right] \right\rangle_{\mathbf{J}_{1,\dots,k}} \right) \\ &\quad + \frac{c}{2} \int \left(d\Delta d\Delta' \left[\prod_{\ell=1}^L d\Sigma_\ell d\Gamma_\ell d\Sigma'_\ell d\Gamma'_\ell \right] \right) \omega\left(\Delta, \{\Sigma_\ell, \Gamma_\ell\}_{\ell=1}^L\right) \omega\left(\Delta', \{\Sigma'_\ell, \Gamma'_\ell\}_{\ell=1}^L\right) \\ &\quad \times \left\langle \exp \left[-n \ln \det \mathfrak{K} - \frac{\mu}{2\pi i} \sum_{\ell=1}^L (\ln \det \nu_\ell - \ln \det \xi_\ell) \right] \right\rangle_{\mathbf{J}} - \frac{c}{2}, \end{aligned} \quad (2.76)$$

with \mathfrak{N} in Eq. (2.75) a normalization constant and the symbol $\langle \dots \rangle_{\mathbf{J}_{1,\dots,k}}$ in both expressions the average over the set $\mathbf{J}_1, \dots, \mathbf{J}_k$. Due to the similarity of the joint probability distribution $\omega\left(\Delta, \{\Sigma_\ell, \Gamma_\ell\}_{\ell=1}^L\right)$ and action \mathcal{S} with Eqs. (2.35) and (2.36), respectively, we have resorted to the previous auxiliary matrices Υ_ℓ , ζ_ℓ , ν_ℓ , and ξ_ℓ of Eqs. (2.37) and (2.38), and defined a new pair of 2×2 complex auxiliary matrices

$$\mathfrak{F} \equiv M_\eta(z, z^*) + \sum_{r=1}^k \mathbf{J}_r \Delta_r \mathbf{J}_r^\dagger \quad \text{and} \quad \mathfrak{K} \equiv I_2 + \Delta \mathbf{J} \Delta' \mathbf{J}^\dagger, \quad (2.77)$$

so that we can keep the notation for both expressions as simple as possible.

In both equations, (2.75) and (2.76), we have computed the replica limits $n_\pm \rightarrow \pm\mu/2\pi i$ assuming that they yield the correct results. The remaining steps are the calculation of the continuum limit $L \rightarrow \infty$, the replica limit $n \rightarrow 0$, and the partial derivatives ∂_{z^*} and ∂_z . Although the calculation of the first two limits and the first derivative ∂_{z^*} are straightforward (the continuum limit $L \rightarrow \infty$ procedure is analogous to that of the CGF), the second derivative ∂_z calculation requires further analysis. We assume the both derivatives ∂_z and ∂_{z^*} to exist, and the CSD is such that both are interchangeable. We have also corroborated this last assumption in our numerical analysis.

After computing the continuum limit $L \rightarrow \infty$, the resulting functional density $\omega[\Delta, \{\Gamma, \mathbf{R}\}]$ (Eq. (B.15)) and action \mathcal{S} (Eq. (B.16)) are such that the calculation of the replica limit $n \rightarrow 0$ requires no further effort. The evaluation of the first derivative ∂_{z^*} is also immediate thanks to the inherent characteristics of the saddle-point expressions, Eq. (B.20) and (B.21), leaving us with an equation for $\rho(z|\mathcal{R}_\gamma)$ in terms of the $\eta \rightarrow 0^+$ limit and the second derivative ∂_z (Eq. (B.22)). However, the evaluation of ∂_z represents a non-trivial task. Assuming a dependence of the functional density $\omega[\Delta, \{\Gamma, \mathbf{R}\}]$ on ∂_z (Appendix B.3, Eqs. (B.22)-(B.26)), and after some algebraic manipulations, we obtain the final expression for the CSD

$$\rho(z|\mathcal{R}_\gamma) = \frac{1}{\pi} \lim_{\eta \rightarrow 0^+} \langle \text{Tr} [i\sigma_- \partial_z \Delta(z)] \rangle_{\Delta, \partial_z \Delta, \{\Gamma, \mathbf{R}\}}, \quad (2.78)$$

where the symbol $\langle \dots \rangle_{\Delta, \partial_z \Delta, \{\Gamma, \mathbf{R}\}}$ denotes the average over all possible paths $\{\Gamma, \mathbf{R}\}$ in the γ curve and all z points within the complex plane $\Delta(z)$ and $\partial_z \Delta(z)$. As with $\mathcal{F}_\gamma(\mu)$, any path $\{\Gamma, \mathbf{R}\}$ can be thought of as the limit $L \rightarrow \infty$ of a sequence $\{\Gamma(\omega_\ell), \mathbf{R}(\omega_\ell)\}_{\ell=1}^L$, with $\omega_\ell \in \gamma$ for all ℓ . Hence, the path integration measure formally reads $d\{\Gamma, \mathbf{R}\} = \lim_{L \rightarrow \infty} \prod_{\ell=1}^L d\Gamma(\omega_\ell) d\mathbf{R}(\omega_\ell)$. Invoking the auxiliary matrices $\chi_k(\omega)$ and $\Pi_k(\omega)$ from Eq. (2.45),

and defining the pair of 2×2 complex matrices

$$\hat{\chi}_k(z) = \left[\mathbf{M}_\eta(z, z^*) + \sum_{r=1}^k \mathbf{J}_r \Delta_r(z) \mathbf{J}_r^\dagger \right]^{-1} \quad \text{and} \quad \hat{\Pi}_k(z) = -\hat{\chi}_k \left(i\sigma_+ + \sum_{r=1}^k \mathbf{J}_r \partial_z \Delta_r(z) \mathbf{J}_r^\dagger \right) \hat{\chi}_k, \quad (2.79)$$

the average $\langle \cdots \rangle_{\Delta, \partial_z \Delta, \{\Gamma, \mathbf{R}\}}$ for any functional $\mathcal{S}[\Delta, \partial_z \Delta, \{\Gamma, \mathbf{R}\}]$ is formally read

$$\langle \mathcal{S}[\Delta, \partial_z \Delta, \{\Gamma, \mathbf{R}\}] \rangle_{\Delta, \partial_z \Delta, \{\Gamma, \mathbf{R}\}} = \int \omega[\Delta, \partial_z \Delta, \{\Gamma, \mathbf{R}\}] \mathcal{S}[\Delta, \partial_z \Delta, \{\Gamma, \mathbf{R}\}] d\Delta d(\partial_z \Delta) d\{\Gamma, \mathbf{R}\}, \quad (2.80)$$

with $\omega[\Delta, \partial_z \Delta, \{\Gamma, \mathbf{R}\}]$ the resulting functional density following from the solution of the self-consistency equation

$$\begin{aligned} \omega[\Delta, \partial_z \Delta, \{\Gamma, \mathbf{R}\}] &= \frac{1}{\mathfrak{N}} \sum_{k=0}^{\infty} \frac{e^{-c} c^k}{k!} \int \left[\prod_{r=1}^k d\Delta_r d(\partial_z \Delta_r) d\{\Gamma_r, \mathbf{R}_r\} \omega[\Delta_r, \partial_z \Delta_r, \{\Gamma_r, \mathbf{R}_r\}] \right] e^{\mu W[\{\Gamma, \mathbf{R}\}]} \\ &\quad \times \left\langle \delta[\Delta(z) - \hat{\chi}_k(z)] \delta[\partial_z \Delta(z) - \hat{\Pi}_k(z)] \delta_F[\Gamma(\omega) - \chi_k(\omega)] \delta_F[\mathbf{R}(\omega) - \mathbf{\Pi}_k(\omega)] \right\rangle_{\mathcal{J}_{1, \dots, k}}. \end{aligned} \quad (2.81)$$

Note that in Eq. (2.81), we explicitly indicate the dependence of the functional density on the second partial derivative ∂_z . The symbol δ_F within the average $\langle \cdots \rangle_{\mathcal{J}_{1, \dots, k}}$ represents the functional Dirac δ over the path space and the normalization constant \mathfrak{N} takes the form

$$\mathfrak{N} = \left(\int e^{-\mu W[\{\Gamma, \mathbf{R}\}]} \omega[\Delta, \partial_z \Delta, \{\Gamma, \mathbf{R}\}] d\Delta d(\partial_z \Delta) d\{\Gamma, \mathbf{R}\} \right)^{-1}. \quad (2.82)$$

As for the CGF case, the statistical contribution of each path is weighted by the exponential factor of Eq. (2.81) and the $W[\{\Gamma, \mathbf{R}\}]$ term of Eq. (2.44); both equations (2.78) and (2.81) ought to be solved in the $\eta \rightarrow 0^+$ limit. The Eq. (2.78) for the conditioned spectral density $\rho(z|\mathcal{R}_\gamma)$ and Eq. (2.81) for the functional density $\omega[\Delta, \partial_z \Delta, \{\Gamma, \mathbf{R}\}]$ are the principal outcomes of this second research. From them, we derive all the possible features that the spectrum of an ensemble of sparse non-Hermitian random matrices undergoes when the constraint $\mathcal{R}_\gamma \in [0, 1]$ fixing the number of eigenvalues \mathcal{N}_A within the smooth Jordan curve γ is placed.

2.3.2 Numerical analysis and results

As it happened with the path probability $\omega[\{\Gamma, \mathbf{R}\}]$ (Eq. (2.42)), the functional density $\omega[\Delta, \partial_z \Delta, \{\Gamma, \mathbf{R}\}]$ has no known analytical solution; then, we anew appeal to the weighted population dynamics algorithm. Firstly, we discretize the γ curve into a finite collection of points $\{\omega_1, \dots, \omega_L\}$ and define the finite set of 2×2 complex random matrices $\{\Gamma(\omega_\ell), \mathbf{R}(\omega_\ell)\}_{\ell=1}^L$ sampled consistently with Eq. (2.81) via a Monte Carlo scheme. Then, once again we make a switch from the functional density $\omega[\Delta, \partial_z \Delta, \{\Gamma, \mathbf{R}\}]$ to the joint distribution $\omega[\Delta, \partial_z \Delta, \{\Gamma(\omega_\ell), \mathbf{R}(\omega_\ell)\}_{\ell=1}^L]$. Since $\omega[\Delta, \partial_z \Delta, \{\Gamma, \mathbf{R}\}]$ contains all the possible correlations for any collection of points, both $\omega[\Delta, \partial_z \Delta, \{\Gamma, \mathbf{R}\}]$ and $\omega[\Delta, \partial_z \Delta, \{\Gamma(\omega_\ell), \mathbf{R}(\omega_\ell)\}_{\ell=1}^L]$ do not factorize.

To move forward, we introduce a population of a total number of M sets of matrices

$$\{\Delta_\alpha, \partial_z \Delta_\alpha, \Gamma_\alpha(\omega_1), \dots, \Gamma_\alpha(\omega_L), \mathbf{R}_\alpha(\omega_1), \dots, \mathbf{R}_\alpha(\omega_L)\}_{\alpha=1}^M,$$

with Δ_α and $\partial_z \Delta_\alpha \in \mathbb{M}_{2 \times 2}(\mathbb{C})$ for all $\alpha = 1, \dots, M$. Therefore, the joint probability distribution formally reads

$$\begin{aligned} \omega[\Delta, \partial_z \Delta, \{\Gamma(\omega_\ell), \mathbf{R}(\omega_\ell)\}_{\ell=1}^L] &\sim \frac{1}{M} \sum_{\alpha=1}^M e^{\mu W[\{\Gamma(\omega_\ell), \mathbf{R}(\omega_\ell)\}_{\ell=1}^L]} \left(\delta[\Delta - \Delta_\alpha(z)] \delta[\partial_z \Delta - \partial_z \Delta_\alpha(z)] \right. \\ &\quad \left. \times \prod_{\ell=1}^L \delta[\Gamma(\omega_\ell) - \Gamma_\alpha(\omega_\ell)] \delta[\mathbf{R}(\omega_\ell) - \mathbf{R}_\alpha(\omega_\ell)] \right) \end{aligned} \quad (2.83)$$

where the weighted factor $e^{\mu W[\{\Gamma(\omega_\ell), \mathbf{R}(\omega_\ell)\}_{\ell=1}^L]} = \Theta[\{\Gamma(\omega_\ell), \mathbf{R}(\omega_\ell)\}_{\ell=1}^L]$ indicates the number of population

elements that are updated according to Eq. (2.50). To demonstrate the exactness of the theory, we have chosen as γ curve the boundary of a disk of radius $R = 0.5$ centred at the origin of \mathbb{C} and divided our findings into three figures: Figs. 2.4, 2.5, and 2.6. While Figs. 2.4 and 2.5 show the results obtained by numerical diagonalization and theory, separately, Fig. 2.6 displays the comparison between both schemes exhibiting excellent agreement.

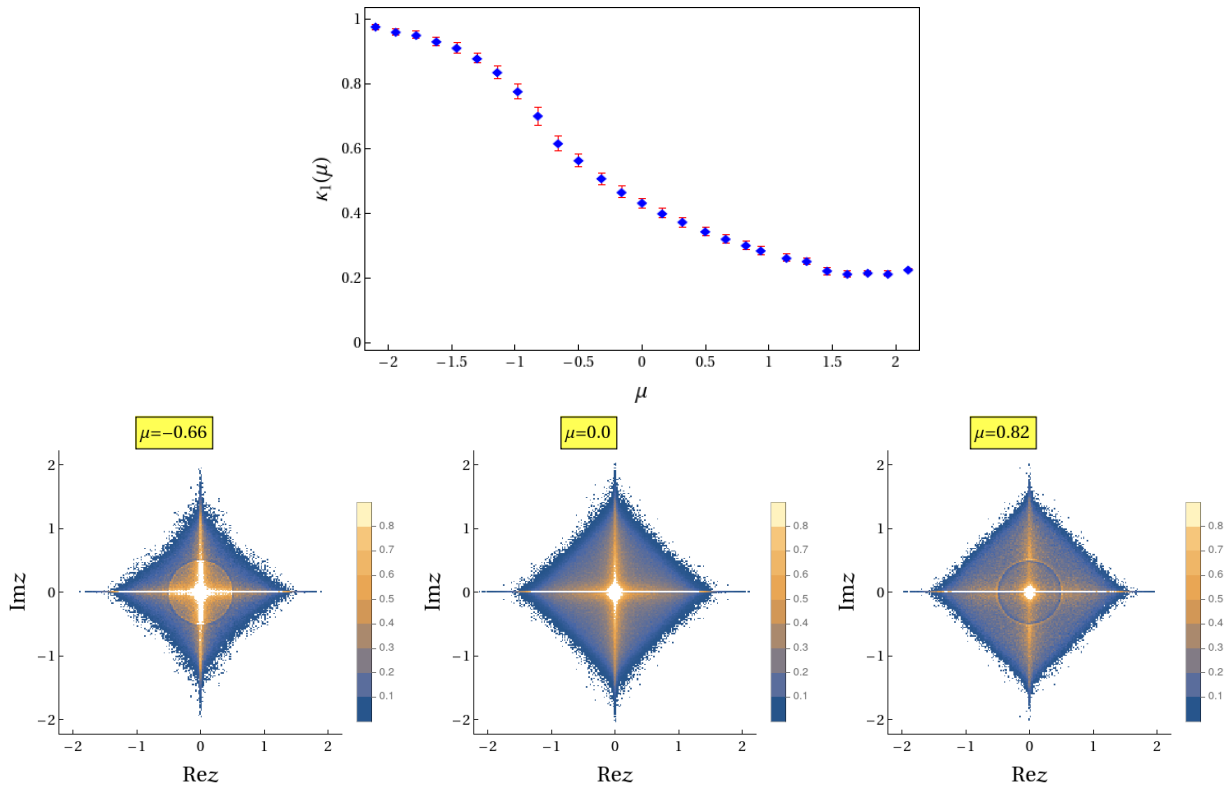


Figure 2.4: Numerical diagonalization for the spectral density constrained to have a specific fraction of eigenvalues inside a disk of radius $R = 0.5$ centred at the origin of the complex plane for different values of μ . The matrix \mathbf{A} corresponds to the adjacency matrix of a Poisson random graph with average connectivity $c = 4$ and asymmetric Gaussian weights of zero mean and variance $1/c$. **Top:** fraction of eigenvalues inside the disk of radius $R = 0.5$ as a function of the parameter μ for a range of values $\mu \in [-2.1, 2.1]$. **Bottom:** density plots of the CSD for the disk of radius $R = 0.5$ and values of $\mu = -0.66$ (left panel), $\mu = 0.0$ (central panel), and $\mu = 0.82$ (right panel). For the diagonalization procedure, 10^3 samples are averaged and the process is repeated 400 times for matrices of 800×800 .

Fig. 2.4 depicts the results obtained by numerical diagonalization employing the Metropolis algorithm (Appendix D) for \mathbf{A} the adjacency matrix of a Poisson random graph with Gaussian directed edges of mean value equal zero and variance $1/c$, the diluted real Ginibre ensemble, using as γ curve a disk of radius $R = 0.5$ centred at the origin of \mathbb{C} . The upper row of Fig. 2.4 shows the first cumulant κ_1 , with its corresponding error bars, for the fraction of eigenvalues inside the disk as a function of the parameter μ for a range of values $-2.1 \leq \mu \leq 2.1$, passing through its typical fluctuations at $\mu = 0.0$. On the other hand, the lower row of Fig. 2.4 displays three density plots of the CSD for the values $\mu = -0.66$ (left panel), $\mu = 0.0$ (central panel), and $\mu = 0.82$ (right panel). All graphs in Fig. 2.4 portray the changes the spectrum undergoes depending on the value of the μ parameter: $\mu < 0$ (> 0) will favour a major (minor) concentration of eigenvalues inside the γ curve (as we had predicted in Eq. (2.60)). In both rows, we observe how the transition from the atypical to the typical fluctuations occurs in a smooth-continuous form, i.e., there is no abrupt transition as the number of constrained eigenvalues approaches its typical value at $\mu = 0.0$. Furthermore, and contrary to the spectral density displayed in Fig. 1 of Ref. [189], the support of the constrained density for the diluted real Ginibre ensemble shown in the lower row of Fig. 2.4 corresponds to a connected compact set in the complex plane whether μ is positive or negative.

In Fig. 2.5, we display the principal outcome of the theory: the theoretical results from Eqs. (2.78) and (2.81) via the population dynamics algorithm for the diluted real Ginibre ensemble considering symmetric values of μ around $\mu = 0$ of $\mu = (-1.62, 1.62)$, $(-1.14, 1.14)$, and $(-0.5, 0.5)$, indicating, for each value, the fraction of eigenvalues

\mathcal{R}_γ within the selected smooth Jordan curve. To demonstrate the accuracy of the method, we have settled as γ curve the border of a disk of radius $R = 0.5$, represented by a yellow plane at $\text{Im}z = 0.5$, centred at the origin of \mathbb{C} and have plotted the CSD at the cut $\text{Re}z = 0.10$ for the different μ colouring the positive values as *blue curves*, the negative values as *green curves*, and the typical case $\mu = 0$ as a *red curve*. We observe how effectively, for every μ , the spectrum goes through a continuous-smooth shift in its curvature as the value of $\text{Im}z$ approaches the radius of the disk, supporting our previous conclusions of Fig. 2.4 that the CSD possesses a compact support and that there is no sudden transition as the conditioned eigenvalues get close to their typical fluctuations. Also, we notice how the theoretical results faithfully reproduce the behaviour of the constrained eigenvalues when the μ value is either negative (major concentration) or positive (less concentration); Fig. 2.5 also deploys another crucial fact concerning the behaviour of the eigenvalues at the border of the disk. From the lower row of Fig. 2.4, we observe how the eigenvalues seem to concentrate at the boundary of the disk; nevertheless, such an effect is no longer visible for the different values of μ in Fig. 2.5. Effectively, Fig. 2.5 proves that such a perception is due to finite size effects that disappear as the matrix dimension becomes infinitely large, i.e., in the $N \rightarrow \infty$ limit; the same effect was also perceptible in Fig. 2 of Ref. [45] for the Erdős-Rényi random graphs and Wishart random matrices. The reader will have noticed that the CSD in Fig. 2.5 corresponds, for each μ , to a symmetric function around the origin; this is because the spectrum of infinitely large random graphs ought to be symmetric since these are bipartite graphs [31, 44, 110, 112].

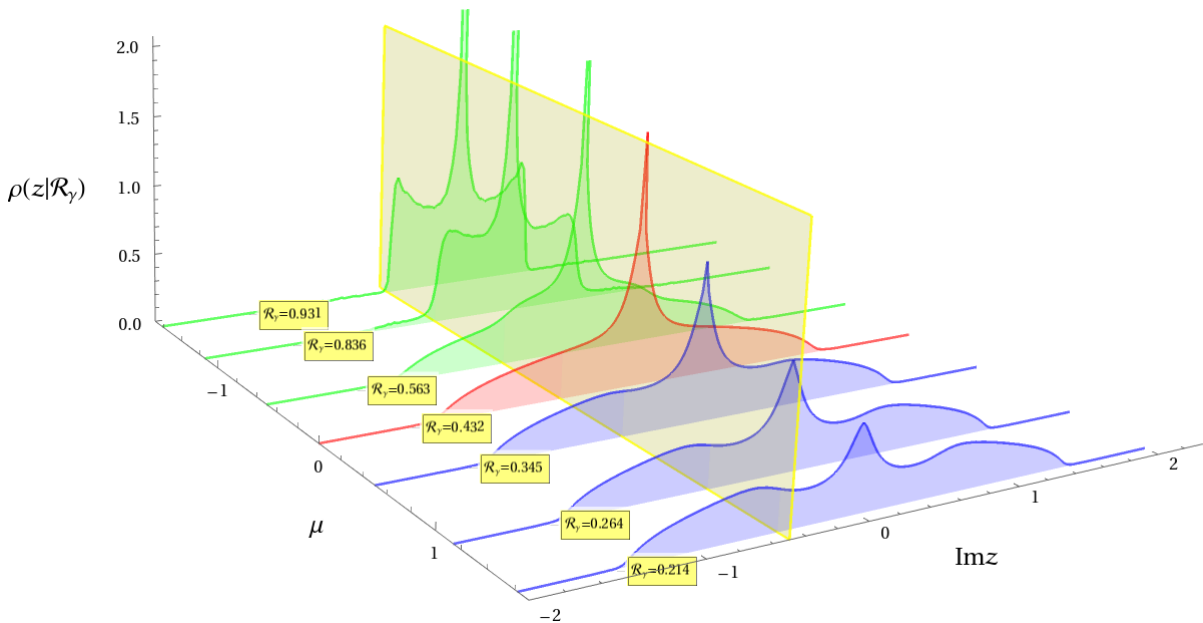


Figure 2.5: Theoretical results for the spectral density at the cut $\text{Re}z = 0.10$ conditioned to have a fixed fraction of eigenvalues \mathcal{R}_γ inside a disks of radius $R = 0.5$ for several positive (*blue curves*) and negative (*green curves*) values of μ . The matrix \mathbf{A} corresponds to the adjacency matrix of a weighted random graph of directed edges with average connectivity $c = 4$, where the asymmetric interactions are independently drawn from a Gaussian distribution p_J with zero mean and variance $1/c$. The cuts for the several values of μ illustrate the continuous-smooth shift the CSD undergoes in its curvature and the absence of a sudden phase transition as the constrained eigenvalues approximate their typical fluctuations at $\mu = 0$ (*red curve*). All the results were obtained using a population of 3.5×10^3 with an iteration of 16625×10^3 times and a discretization of 300 points over the disk.

Finally, in Fig. 2.6, we compare the theoretical findings from Eqs. (2.78) and (2.81) with the results obtained by numerical diagonalization for the adjacency matrix of a weighted random graph of directed edges with average connectivity $c = 4$ for the several μ values of Fig. 2.5 at the cut $\text{Re}z = 0.10$. While in the left panels, we display the CSD for the negative values of μ , in the right panels we show their positive counterparts, exhibiting, in all cases, excellent agreement between results. The few existing discrepancies amid the red grid lines (numerical diagonalization) and the continuous blue lines (theoretical results) in the tails of the spectrum and throughout the curvature shifts for the different values of μ were previously reported in Ref. [44] and are due to the discretization the histogram introduces. Moreover, the behaviour induced by the red grid lines in both panels permits us to observe more in detail the false-eigenvalue-concentration-effect at the disk border, precisely around the values of $\text{Im}z$ where the curvature of the spectral density changes. This effect is easily noticeable for $\mu = 1.62$, where the many shifts in the curvature

make it difficult for the numerical diagonalization to accurately display the constrained density. Clearly, this false impression disappears when the limit $N \rightarrow \infty$ is considered and which is correctly represented by the continuous blue lines.

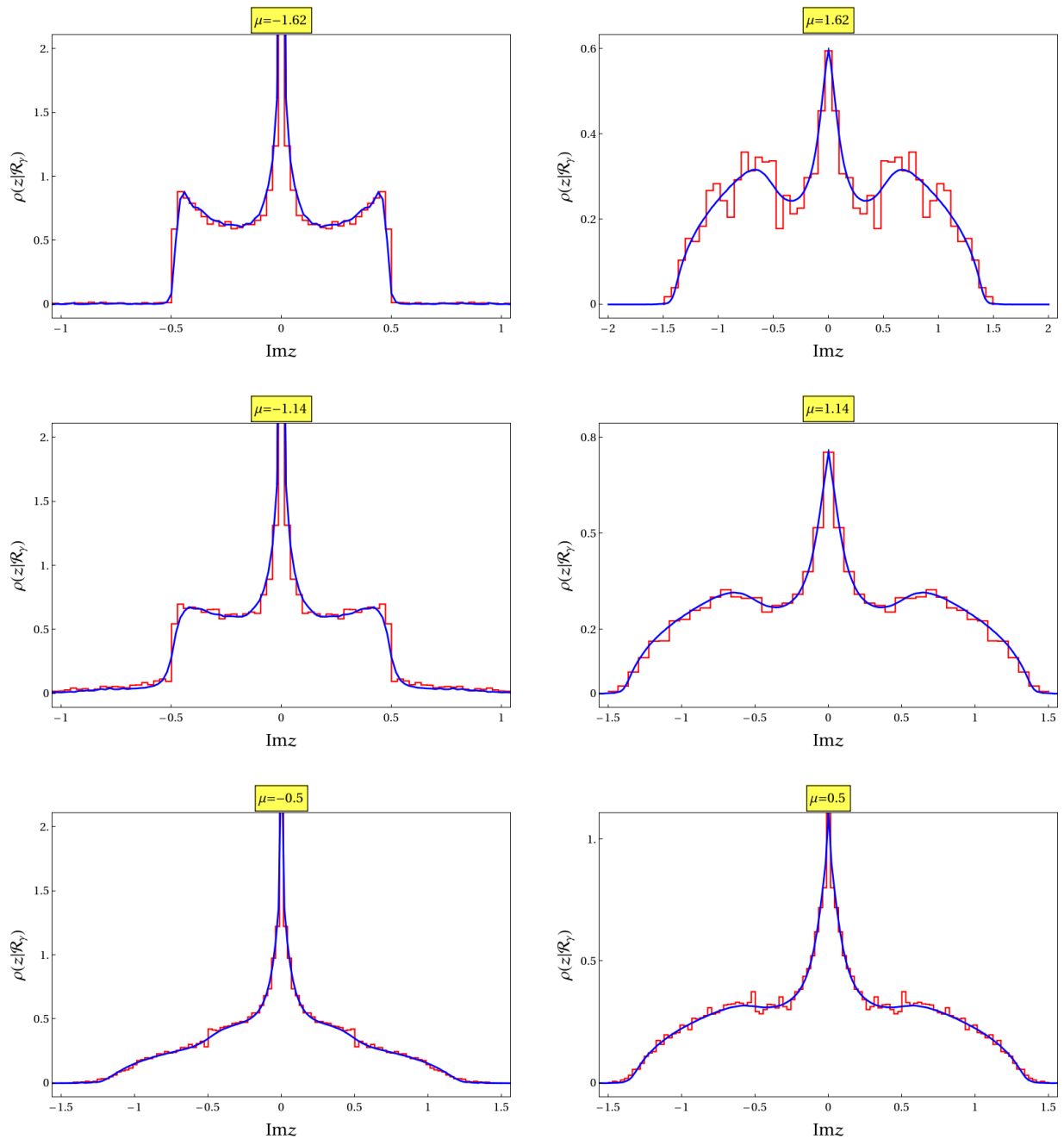


Figure 2.6: Comparison between the exact theoretical and diagonalization results of the CSD for a disk of radius $R = 0.5$ centred at the origin of \mathbb{C} . The matrix \mathbf{A} corresponds to the adjacency matrix of a Poisson random graph with average connectivity $c = 4$ and asymmetric Gaussian weights of zero mean and variance $1/c$. Solid blue lines are the theoretical findings, while red grid lines (histogram) are the exact diagonalization results for values of $\mu = -1.66, -1.14, -0.5$ (left panels) and $\mu = 1.66, 1.14, 0.5$ (right panels), both at $\text{Re}z = 0.10$. For the diagonalization, 10^3 samples are averaged and the process is repeated 400 times for matrices of 800×800 ; for the exact theoretical results, a population of 3500 with a discretization of 300 points over the γ curve and 16625×10^3 iterations is employed.

The authors in Ref. [189] demonstrated that the CSD for a number of eigenvalues outside a disk of radius $R = 0.5$ for the complex and real Ginibre ensembles exhibited (i) an asymptotic density supported on either balls, annuli, or

circles centred at the origin of \mathbb{C} (Fig. 1 and Eq. (9) in Ref. [189]), (ii) a concentration of the eigenvalues at the border of the disk (Fig. 1 in Ref. [189]), and (iii) a phase transition of the Coulomb gas as the constrained eigenvalues reach their typical fluctuations, all of them derived from the Coulomb gas picture of Eq. (1.27). Interestingly, the phase transition of the Coulomb gas leads to a third-order phase transition in the corresponding rate function [189]. Due to the similarity between the Coulomb gas picture for the classical (Eq. (1.26)) and Ginibre ensembles (Eq. (1.27)), the results obtained for the constrained density in both cases agree and display the same universal features [123, 187, 216, 222, 224]. On the other hand, Ref. [44] proved that introducing sparsity within the invariant ensembles breaks the usual scheme and leads to contrasting results for the CSD.

Our findings of the CSD for the diluted real Ginibre ensemble in the limit of infinitely large matrices $N \rightarrow \infty$ highlight the results of Ref. [44] and can be summarized in the following three features:

- (i) $\rho(z|\mathcal{R}_\gamma)$ is a symmetric function over a connected compact support.
- (ii) No accumulation of eigenvalues at the border of the disk.
- (iii) No abrupt transition as the constrained eigenvalues reach their typical fluctuations.

All these astonishing features seem to result from the weak or absent repulsion among the eigenvalues of sparse non-Hermitian random matrices. We know, thanks to Ref. [211], that, in general, the spectrum of non-Hermitian random matrices near the origin (delocalized region) displays significant eigenvalue repulsion while at the borders (localized zone), the eigenvalues behave as an *ideal gas*. Previous research has demonstrated that for both the Erdős-Rényi random graphs [210] and sparse symmetric random matrices [32], the fluctuations $\langle [\delta n(\lambda)]^2 \rangle$ of the number of eigenvalues $n(\lambda)$ are proportional to the mean $\langle n(\lambda) \rangle$ for localized states and to the logarithm $\ln \langle n(\lambda) \rangle$ for delocalized states. These features seem also to occur for sparse non-Hermitian random matrices, where the eigenvalues are allowed to be arbitrarily close to each other [211]. All these arguments lead us to conjecture that properties (i), (ii), and (iii) are universal for sparse random matrices, whether they are Hermitian or non-Hermitian.

Chapter 3

Concluding remarks

I would rather have questions that can't be answered than answers that can't be questioned.

Richard Phillips Feynman (1918-1988)

In this thesis, we departed from the previous research conducted in Refs. [44,45] for symmetric and non-Hermitian SRMs, and resorting to various RMT mathematical techniques such as the Hermitization [158] and replica methods [149], and by means of the so-called replica-symmetric formalism, we developed new and powerful methods capable of studying (i) the complete statistics surrounding the number \mathcal{N}_D of eigenvalues within a smooth Jordan curve contained inside a domain $D \subseteq \mathbb{C}$, and (ii) the spectral properties of the so-called conditioned spectral density $\rho(z|\mathcal{R}_\gamma)$, that is, the spectral density $\rho(z)$ constrained to have a specific fraction \mathcal{R}_γ of eigenvalues inside the Jordan curve. The ultimate goal of our research was to extend the scarce knowledge we have concerning sparse non-Hermitian random matrices in the limit of infinitely large matrix dimensions and verify whether or not new universal properties arise under the introduction of sparsity together with their range of validity. To demonstrate the exactness of our methods, we selected the diluted version of the real Ginibre ensemble as the sparse ensemble and confirmed our theoretical findings with finite numerical diagonalization, obtaining excellent results.

For both methods, the most outstanding features were that they did not rely on the knowledge of the JPDE function for sparse non-Hermitian random matrices and that they can be applied, in principle, to any non-Hermitian random matrix ensemble of the mean-field type, i.e., ensembles where the coupling strengths do not depend on the distance between the components. Another significant achievement was the capacity of the theories to calculate the complete statistical information of the number \mathcal{N}_D and the spectral features of $\rho(z|\mathcal{R}_\gamma)$, taking into account the weights characterizing the diverse δ peaks throughout the spectra for small and moderate values of the average connectivity c ; a fact where the approximate methods EMA, SDA, SEMA, and DEMA failed [41–43].

Regarding the full counting statistics of the number \mathcal{N}_D , we observed that, while the first cumulant κ_1 showed excellent agreement between the exact theoretical findings and the results by numerical diagonalization for small and moderate values of c , the second cumulant κ_2 displayed a stronger dependence with the matrix dimensions N used in the numerical diagonalization. Whereas the complex Ginibre ensemble exhibits three different regimes for the variance of \mathcal{N}_D in the large N limit [180], κ_2 for the diluted real Ginibre ensemble only presented a unique regime and a linear scaling behaviour with N . This difference was due to the distinctive eigenvalue repulsion present in each ensemble. For both cumulants, κ_1 and κ_2 , the results shown in Fig. 2.2 varying the radius of the disk from $R = 0.05$ to $R \approx 1.58$ for the diluted real Ginibre ensemble resembles those displayed by the complex Ginibre ensemble (Fig. 2 in Ref. [180]) when we consider larger values of the average connectivity c . This, indeed, reflects the level of dilution present in the sparse ensemble. So, it is natural to expect that in the zero dilution case, i.e., in the fully connected limit $c \rightarrow \infty$ [44], we will fully recover the results of Fig. 2 in Ref. [180] for the complex Ginibre ensemble. While for the latter, the eigenvalues undergo a strong repulsion given by Eq. (1.27), the eigenvalue repulsion for the diluted real Ginibre ensemble is considerably weaker [211]. The effects of such a remarkable difference were also visible in the asymmetry of the rate function $\phi_\gamma(n)$ compared to the complex Ginibre ensemble rate function [180]. Previous research evidenced that it was possible to recover the scaling behaviour of the variance for Gaussian Hermitian random matrices from their diluted version by including finite-size corrections in their corresponding saddle-point

integrals [227]. For Gaussian non-Hermitian random matrices, we expect an analogous situation, i.e., we look forward to recovering the results for the Ginibre ensemble [180] by taking into account finite-size corrections to the saddle-point integral of Eq. (2.26).

Regarding the CSD for the diluted real Ginibre ensemble considering the border of the disk of radius $R = 0.5$ centred at the origin of \mathbb{C} as the smooth Jordan curve γ , we observed a completely contrasting behaviour with respect to its non-diluted counterpart. Contrary to the real and complex Ginibre ensembles [189], we discovered that $\rho(z|\mathcal{R}_\gamma)$ was (i) a symmetric function on a connected compact support with (ii) no accumulation of eigenvalues at the border of the disk and (iii) no phase transition as the eigenvalues approach their typical fluctuations. While the connected compact support, along with points (ii) and (iii), was displayed for both the Erdős-Rényi random graphs and Wishart random matrices in the limit $N \rightarrow \infty$ [45], we only observed the symmetry of $\rho(z|\mathcal{R}_\gamma)$ for the infinitely large random graphs. As we have pointed out, this last feature is because random graphs are bipartite graphs [31, 44, 110, 112]. As with the full counting statistics of \mathcal{N}_D , these outstanding characteristics follow from the weak and absent eigenvalue repulsion of the spectrum [211]. Whereas the eigenvalue repulsion for the complex Ginibre ensemble, for instance, follows Eq. (1.27), the relative variance $\langle [\delta n(\lambda)]^2 \rangle / \langle n(\lambda) \rangle$ for symmetric sparse random matrices is equal to one for localized states (absent eigenvalue repulsion) and much smaller than one for delocalized states (significant eigenvalue repulsion) [32]. Since both states appear in the spectrum of non-Hermitian matrices, and hence in sparse non-Hermitian matrices, that feature seems to be also present in the diluted real Ginibre ensemble spectrum, permitting the eigenvalues to be arbitrarily close to each other. Since our findings agree with the results displayed by Ref. [45] for the CSD of noninvariant ensembles, they lead us to conjecture that properties (i), (ii), and (iii) stand as new universal features for the diverse ensembles of sparse random matrices whether they are Hermitian or non-Hermitian.

The results obtained in both studies highlight the efficiency and capacity of the theories to compute the statistical and spectral properties of infinitely large sparse non-Hermitian random matrices. Had we stayed only with finite numerical diagonalization, we would not have provided an accurate description of such properties. For instance, while finite numerical diagonalization for the CSD indicated the accumulation of eigenvalues at the borders of the disk of radius $R = 0.5$ (Fig. 2.4), the theory corrected such a misinterpretation and lets us conclude that they were only finite-size effects.

In the end, we fulfilled the objectives we had set for ourselves. We provided an accurate description of the typical and atypical fluctuations surrounding the random variable \mathcal{N}_D for the diluted real Ginibre ensemble and discovered new universal features for the conditioned spectral density $\rho(z|\mathcal{R}_\gamma)$ that emerge when we add the sparsity condition to non-Hermitian ensembles. Nevertheless, there are still many questions to be answered and properties to be discovered. For instance, we desire a formal picture of the localization and delocalization properties for sparse non-Hermitian random matrices as the one of Ref. [226]; in addition, we also wish to apply our method to different physical systems that allow us to provide a more complete physical interpretation to the diverse results we have presented throughout this thesis. All these are questions and objectives we intend to treat in future research.

Appendix A

Mathematical procedure for the full counting statistics of \mathcal{N}_D

In this first appendix, we provide in detail the mathematical manipulations required for Chapter 2, Section 2.2, dividing them into four parts: firstly, the path integral formulation of the CGF $\mathcal{F}_\gamma(\mu)$; secondly, the implementation of the replica-symmetric ansatz; thirdly, the calculation of the continuous limit $L \rightarrow \infty$; and lastly, the derivation of the parametric rate function. The first Section A.1 covers from Eq. (2.14), the alternative expression for the ESD, to the path integral representation of the CGF, Eq. (2.26); the second Section A.2 departs from the replica-symmetric ansatz (Eq. (2.33)) implementation on the saddle-point equations of section 2.2.1 and arrives to Eqs. (2.35) and (2.36), the explicit expressions for the joint probability distribution function ω and action \mathcal{S} , respectively. The third Section A.3 focuses on obtaining the final expressions for the cumulant generating function $\mathcal{F}_\gamma(\mu)$ and path probability $\omega[\{\Gamma, \mathbf{R}\}]$ through the computation of the continuous limit $L \rightarrow \infty$ and, finally, the last Section A.4 displays the necessary mathematical handlings to obtain the parametric form of the rate function $\phi_\gamma(n)$, Eq. (2.48).

A.1 Constructing the path integral

Contrary to the well-known cases of symmetric and Hermitian random matrices [151], where the δ function appearing in the spectral density is rewritten using the *Sokhotski–Plemelj theorem* [157] and immediately after the resulting equation is formulated in terms of multivariate Gaussian integrals [10, 150], the treatment of Eq. (1.18) requires further algebraic manipulations.

Given any number $z \in \mathbb{C}$ such that $z = x + iy$, we obtain

$$\partial_z = \frac{1}{2}(\partial_x - i\partial_y) \quad \text{and} \quad \partial_{z^*} = \frac{1}{2}(\partial_x + i\partial_y), \quad (\text{A.1})$$

with $z^* = x - iy$ the complex conjugate of z ; hence, for any well-behaved function f , we have that $\partial_{z^*}\partial_z f = \frac{1}{4}\nabla^2 f$. Recalling from electrostatics the fundamental solution to Poisson's two-dimensional differential equation for a point source electric potential (Green's function) [228], $\nabla^2 \ln \|\mathbf{x} - \mathbf{x}_0\|^2 = 4\pi\delta(\mathbf{x} - \mathbf{x}_0)$, and using the equality between the Laplacian and the partial derivatives of z and z^* , we have that

$$\partial_{z^*}\partial_z \ln [(z - z_0)(z - z_0)^*] = \pi\delta(z - z_0). \quad (\text{A.2})$$

Inserting Eq. (A.2) into Eq. (1.18), we rewrite the ESD

$$\rho_A(z, z^*) = \frac{1}{N\pi} \partial_{z^*}\partial_z \ln \left(\left[\prod_{i=1}^N (z - \lambda_i) \right] \left[\prod_{i=1}^N (z - \lambda_i)^* \right] \right), \quad (\text{A.3})$$

permitting us to arrive at Eq. (2.14).

Appealing to the definition of the *wedge product* $\wedge_{j=1}^N du_j = J \wedge_{j=1}^N dv_j$ with J the Jacobian [9], we find that

$\int dz dz^* = -2i \int dx dy$. Consequently, from Eq. (2.14), we have that

$$\mathcal{N}_{\mathbf{A}}(\gamma) = -\frac{1}{2\pi i} \int_D \partial_{z^*} \partial_z \ln \det \left[(z\mathbf{I}_N - \mathbf{A})(z\mathbf{I}_N - \mathbf{A})^\dagger \right] dz^* dz, \quad (\text{A.4})$$

which, resorting to Green's theorem

$$\oint_{\partial\Omega} (f_1 dz + f_2 dz^*) = \iint_{\Omega} (\partial_z f_2 - \partial_{z^*} f_1) dz dz^* \quad (\text{A.5})$$

($\Omega \subseteq \mathbb{C}$ a connected compact set), placing $f_1 = \partial_z \ln \det \left[(z\mathbf{I}_N - \mathbf{A})(z\mathbf{I}_N - \mathbf{A})^\dagger \right]$, $f_2 = 0$ derives in Eq. (2.15).

To arrive at Eq. (2.26), we need to decouple the sites i and j of Eq. (2.24). Then, using the well-known properties of the Dirac δ function, we express the argument of the exponential function in the last row of Eq. (2.24) as

$$\begin{aligned} & \frac{c}{2N} \sum_{i,j=1}^N \int \prod_{\ell=1}^L \left[\left(\prod_{a=1}^{n_+} d\Psi_{\ell a} d\Psi'_{\ell a} \prod_{b=1}^{n_-} d\Phi_{\ell b} d\Phi'_{\ell b} \right) \prod_{a=1}^{n_+} \delta(\psi_{\ell a} - \psi_{i\ell a}) \delta(\psi'_{\ell a} - \psi_{j\ell a}) \prod_{b=1}^{n_-} \delta(\phi_{\ell b} - \phi_{i\ell b}) \delta(\phi'_{\ell b} - \phi_{j\ell b}) \right] \\ & \times \left\langle \exp \left[i \sum_{\ell=1}^L \left\{ \sum_{a=1}^{n_+} (\psi_{\ell a}^\dagger \mathbf{J} \psi'_{\ell a} + \psi'_{\ell a} \mathbf{J}^\dagger \psi_{\ell a}) + \sum_{b=1}^{n_-} (\phi_{\ell b}^\dagger \mathbf{J} \phi'_{\ell b} + \phi'_{\ell b} \mathbf{J}^\dagger \phi_{\ell b}) \right\} \right] - 1 \right\rangle_J, \end{aligned} \quad (\text{A.6})$$

which we rewrite in terms of the order parameter $P(\Psi, \Phi)$ (Eq. (2.25))

$$\begin{aligned} & \frac{c}{2} N \int \prod_{\ell=1}^L \left(\prod_{a=1}^{n_+} d\Psi_{\ell a} d\Psi'_{\ell a} \prod_{b=1}^{n_-} d\Phi_{\ell b} d\Phi'_{\ell b} \right) P(\Psi, \Phi) P(\Psi', \Phi') \\ & \times \left\langle \exp \left[i \sum_{\ell=1}^L \left\{ \sum_{a=1}^{n_+} (\psi_{\ell a}^\dagger \mathbf{J} \psi'_{\ell a} + \psi'_{\ell a} \mathbf{J}^\dagger \psi_{\ell a}) + \sum_{b=1}^{n_-} (\phi_{\ell b}^\dagger \mathbf{J} \phi'_{\ell b} + \phi'_{\ell b} \mathbf{J}^\dagger \phi_{\ell b}) \right\} \right] - 1 \right\rangle_J. \end{aligned} \quad (\text{A.7})$$

To make easier the ensuing manipulations for Eq. (A.7), we introduce the short notation $d\Psi \equiv \prod_{\ell=1}^L \prod_{a=1}^{n_+} d\Psi_{\ell a}$ and $d\Phi \equiv \prod_{\ell=1}^L \prod_{b=1}^{n_-} d\Phi_{\ell b}$ for the measures. Recalling the auxiliary functions

$$\tau(\Psi_i, \Phi_i) = \sum_{\ell=1}^L \left(\sum_{a=1}^{n_+} \psi_{i\ell a}^\dagger \mathbf{M}_\eta(z_{\ell+1}, z_\ell^*) \psi_{i\ell a} + \sum_{b=1}^{n_-} \phi_{i\ell b}^\dagger \mathbf{M}_\eta(z_\ell, z_\ell^*) \phi_{i\ell b} \right) \quad (\text{A.8})$$

and

$$\Xi(\Psi, \Phi, \Psi', \Phi') = \sum_{\ell=1}^L \left[\sum_{a=1}^{n_+} (\psi_{\ell a}^\dagger \mathbf{J} \psi'_{\ell a} + \psi'_{\ell a} \mathbf{J}^\dagger \psi_{\ell a}) + \sum_{b=1}^{n_-} (\phi_{\ell b}^\dagger \mathbf{J} \phi'_{\ell b} + \phi'_{\ell b} \mathbf{J}^\dagger \phi_{\ell b}) \right], \quad (\text{A.9})$$

together with Fourier's functional form of Dirac's δ [229], we write the last row of Eq. (2.24) as

$$\begin{aligned} & \int \mathcal{D} \left[\{P, \hat{P}\} \right] \exp \left(\frac{c}{2} N \int d\Psi d\Psi' d\Phi d\Phi' P(\Psi, \Phi) P(\Psi', \Phi') \left\langle e^{i\Xi(\Psi, \Phi, \Psi', \Phi')} - 1 \right\rangle_J \right) \\ & \times \exp \left[iN \int d\Psi d\Phi \hat{P}(\Psi, \Phi) \left(P(\Psi, \Phi) - \frac{1}{N} \sum_{i=1}^N \delta(\Psi - \Psi_i) \delta(\Phi - \Phi_i) \right) \right]. \end{aligned} \quad (\text{A.10})$$

Placing Eq. (A.10) into Eq. (2.24), we reformulate the cumulant generating function

$$\begin{aligned} \mathcal{F}_\gamma(\mu) = & - \lim_{N \rightarrow \infty} \lim_{L \rightarrow \infty} \lim_{n_\pm \rightarrow \frac{\pm\mu}{2\pi i}} \lim_{\eta \rightarrow 0^+} \frac{1}{N} \ln \int \mathcal{D} \left[\{P, \hat{P}\} \right] \int \prod_{i=1}^N \left[d\Psi_i d\Phi_i \exp \left(-\tau(\Psi_i, \Phi_i) - i\hat{P}(\Psi_i, \Phi_i) \right) \right] \\ & \times \exp \left[\frac{c}{2} N \int d\Psi d\Psi' d\Phi d\Phi' P(\Psi, \Phi) P(\Psi', \Phi') \left\langle e^{i\Xi(\Psi, \Phi, \Psi', \Phi')} - 1 \right\rangle_J + iN \int d\Psi d\Phi P(\Psi, \Phi) \hat{P}(\Psi, \Phi) \right], \end{aligned} \quad (\text{A.11})$$

permitting us to arrive at the path integral expression of the CGF (Eq. (2.26)).

A.2 The replica-symmetric ansatz and the path probability function

Using the Maclaurin series of the exponential together with the replica-symmetric ansatz, we rewrite Eq. (2.31) as

$$e^{-i\hat{P}(\Psi, \Phi)} = \sum_{k=0}^{\infty} \frac{e^{-c} c^k}{k!} \int \left(\prod_{r=1}^k \prod_{\ell=1}^L d\mathbf{\Sigma}_{r\ell} d\mathbf{\Gamma}_{r\ell} \right) \left[\prod_{r=1}^k \omega \left(\{\mathbf{\Sigma}_{r\ell}, \mathbf{\Gamma}_{r\ell}\}_{\ell=1}^L \right) \right] \int \left(\prod_{r=1}^k d\Psi'_r d\Phi'_r \right) \left\langle \prod_{r=1}^k \prod_{\ell=1}^L \frac{e^{-\psi'_{r\ell a} \Sigma_{r\ell}^{-1} \psi'_{r\ell a} + i(\psi'_{r\ell a} \mathbf{J}_r \psi'_{r\ell a} + \psi'_{r\ell a} \mathbf{J}_r^\dagger \psi_{r\ell a})}}{\det \mathbf{\Sigma}_{r\ell}} \prod_{b=1}^{n_-} \frac{e^{-\phi'_{r\ell b} \Gamma_{r\ell}^{-1} \phi'_{r\ell b} + i(\phi'_{r\ell b} \mathbf{J}_r \phi'_{r\ell b} + \phi'_{r\ell b} \mathbf{J}_r^\dagger \phi_{r\ell b})}}{\det \mathbf{\Gamma}_{r\ell}} \right\rangle_{\mathbf{J}_1, \dots, \mathbf{J}_k}, \quad (\text{A.12})$$

which, using the well-known Gaussian integrals, can be reexpressed as

$$e^{-i\hat{P}(\Psi, \Phi)} = \sum_{k=0}^{\infty} \frac{e^{-c} c^k}{k!} \int \left(\prod_{r=1}^k \prod_{\ell=1}^L d\mathbf{\Sigma}_{r\ell} d\mathbf{\Gamma}_{r\ell} \right) \left[\prod_{r=1}^k \omega \left(\{\mathbf{\Sigma}_{r\ell}, \mathbf{\Gamma}_{r\ell}\}_{\ell=1}^L \right) \right] \times \left\langle \prod_{r=1}^k \prod_{\ell=1}^L \left[\prod_{a=1}^{n_+} \exp \left(-\psi'_{r\ell a} \mathbf{J}_r \mathbf{\Sigma}_{r\ell} \mathbf{J}_r^\dagger \psi_{r\ell a} \right) \prod_{b=1}^{n_-} \exp \left(-\phi'_{r\ell b} \mathbf{J}_r \mathbf{\Gamma}_{r\ell} \mathbf{J}_r^\dagger \phi_{r\ell b} \right) \right] \right\rangle_{\mathbf{J}_1, \dots, \mathbf{J}_k}. \quad (\text{A.13})$$

Placing Eq. (A.13) into Eq. (2.32) and recognizing its denominator as a constant Λ , we rewrite the second-saddle point equation

$$P(\Psi, \Phi) = \frac{1}{\Lambda} \sum_{k=0}^{\infty} \frac{e^{-c} c^k}{k!} \int \left(\prod_{r=1}^k \prod_{\ell=1}^L d\mathbf{\Sigma}_{r\ell} d\mathbf{\Gamma}_{r\ell} \right) \left[\prod_{r=1}^k \omega \left(\{\mathbf{\Sigma}_{r\ell}, \mathbf{\Gamma}_{r\ell}\}_{\ell=1}^L \right) \right] \times \left\langle \prod_{\ell=1}^L \left(\prod_{a=1}^{n_+} e^{-\psi'_{r\ell a} [\mathbf{M}_\eta(z_{\ell+1}, z_\ell^*) + \sum_{r=1}^k \mathbf{J}_r \mathbf{\Sigma}_{r\ell} \mathbf{J}_r^\dagger] \psi_{r\ell a}} \prod_{b=1}^{n_-} e^{-\phi'_{r\ell b} [\mathbf{M}_\eta(z_\ell, z_\ell^*) + \sum_{r=1}^k \mathbf{J}_r \mathbf{\Gamma}_{r\ell} \mathbf{J}_r^\dagger] \phi_{r\ell b}} \right) \right\rangle_{\mathbf{J}_1, \dots, \mathbf{J}_k}, \quad (\text{A.14})$$

where, appealing to the Dirac δ function, we reformulate as

$$P(\Psi, \Phi) = \frac{1}{\Lambda} \sum_{k=0}^{\infty} \frac{e^{-c} c^k}{k!} \int \left(\prod_{\ell=1}^L d\mathbf{\Sigma}_\ell d\mathbf{\Gamma}_\ell \right) \int \left(\prod_{r=1}^k \prod_{\ell=1}^L d\mathbf{\Sigma}_{r\ell} d\mathbf{\Gamma}_{r\ell} \right) \left[\prod_{r=1}^k \omega \left(\{\mathbf{\Sigma}_{r\ell}, \mathbf{\Gamma}_{r\ell}\}_{\ell=1}^L \right) \right] \times \left\langle \exp \left[-\sum_{\ell=1}^L \left\{ n_+ \ln \det \left(\mathbf{M}_\eta(z_{\ell+1}, z_\ell^*) + \sum_{r=1}^k \mathbf{J}_r \mathbf{\Sigma}_{r\ell} \mathbf{J}_r^\dagger \right) + n_- \ln \det \left(\mathbf{M}_\eta(z_\ell, z_\ell^*) + \sum_{r=1}^k \mathbf{J}_r \mathbf{\Gamma}_{r\ell} \mathbf{J}_r^\dagger \right) \right\} \right] \right. \\ \times \prod_{\ell=1}^L \delta \left[\mathbf{\Sigma}_\ell - \frac{1}{\mathbf{M}_\eta(z_{\ell+1}, z_\ell^*) + \sum_{r=1}^k \mathbf{J}_r \mathbf{\Sigma}_{r\ell} \mathbf{J}_r^\dagger} \right] \delta \left[\mathbf{\Gamma}_\ell - \frac{1}{\mathbf{M}_\eta(z_\ell, z_\ell^*) + \sum_{r=1}^k \mathbf{J}_r \mathbf{\Gamma}_{r\ell} \mathbf{J}_r^\dagger} \right] \left. \right\rangle_{\mathbf{J}_1, \dots, \mathbf{J}_k} \\ \times \prod_{\ell=1}^L \left(\prod_{a=1}^{n_+} \frac{e^{-\psi'_{r\ell a} \Sigma_\ell^{-1} \psi_{r\ell a}}}{\det \mathbf{\Sigma}_\ell} \prod_{b=1}^{n_-} \frac{e^{-\phi'_{r\ell b} \Gamma_\ell^{-1} \phi_{r\ell b}}}{\det \mathbf{\Gamma}_\ell} \right). \quad (\text{A.15})$$

From Eqs. (A.15) and (2.33), we deduce that

$$\omega \left(\{\mathbf{\Sigma}_\ell, \mathbf{\Gamma}_\ell\}_{\ell=1}^L \right) = \frac{1}{\Lambda} \sum_{k=0}^{\infty} \frac{e^{-c} c^k}{k!} \int \left(\prod_{r=1}^k \prod_{\ell=1}^L d\mathbf{\Sigma}_{r\ell} d\mathbf{\Gamma}_{r\ell} \right) \left[\prod_{r=1}^k \omega \left(\{\mathbf{\Sigma}_{r\ell}, \mathbf{\Gamma}_{r\ell}\}_{\ell=1}^L \right) \right] \\ \times \left\langle e^{-\sum_{\ell=1}^L [n_+ \ln \det (\mathbf{M}_\eta(z_{\ell+1}, z_\ell^*) + \sum_{r=1}^k \mathbf{J}_r \mathbf{\Sigma}_{r\ell} \mathbf{J}_r^\dagger) + n_- \ln \det (\mathbf{M}_\eta(z_\ell, z_\ell^*) + \sum_{r=1}^k \mathbf{J}_r \mathbf{\Gamma}_{r\ell} \mathbf{J}_r^\dagger)]} \right. \\ \times \prod_{\ell=1}^L \delta \left[\mathbf{\Sigma}_\ell - \frac{1}{\mathbf{M}_\eta(z_{\ell+1}, z_\ell^*) + \sum_{r=1}^k \mathbf{J}_r \mathbf{\Sigma}_{r\ell} \mathbf{J}_r^\dagger} \right] \delta \left[\mathbf{\Gamma}_\ell - \frac{1}{\mathbf{M}_\eta(z_\ell, z_\ell^*) + \sum_{r=1}^k \mathbf{J}_r \mathbf{\Gamma}_{r\ell} \mathbf{J}_r^\dagger} \right] \left. \right\rangle_{\mathbf{J}_1, \dots, \mathbf{J}_k}, \quad (\text{A.16})$$

which, with the replica limits $n_\pm \rightarrow \pm\mu/2\pi i$ computed and the implementation of the 2×2 complex auxiliary matrices Υ_ℓ and ζ_ℓ from Eq. (2.37), turns into Eq. (2.35). The procedure to arrive at Eq. (2.36) is quite similar to the one carried out for the joint probability $\omega \left(\{\mathbf{\Sigma}_\ell, \mathbf{\Gamma}_\ell\}_{\ell=1}^L \right)$, i.e., it is based on the same mathematical manipulations.

Resorting to Eqs. (A.8) and (A.9), together with the first saddle-point equation (Eq. (2.31)), we rewrite the action $\mathcal{S} \left[\left\{ P, \hat{P} \right\} \right]$ (Eq. (2.27)) as

$$\mathcal{S} \left[\left\{ P, \hat{P} \right\} \right] = -\ln \int d\boldsymbol{\Psi} d\boldsymbol{\Phi} e^{-\tau(\boldsymbol{\Psi}, \boldsymbol{\Phi}) - i\hat{P}(\boldsymbol{\Psi}, \boldsymbol{\Phi})} + \frac{c}{2} \int d\boldsymbol{\Psi} d\boldsymbol{\Phi} d\boldsymbol{\Psi}' d\boldsymbol{\Phi}' P(\boldsymbol{\Psi}, \boldsymbol{\Phi}) \hat{P}(\boldsymbol{\Psi}', \boldsymbol{\Phi}') \left\langle e^{i\Xi(\boldsymbol{\Psi}, \boldsymbol{\Phi}, \boldsymbol{\Psi}', \boldsymbol{\Phi}')} \right\rangle_{\mathcal{J}} - \frac{c}{2}. \quad (\text{A.17})$$

The remaining procedure encompasses solving the two integrals appearing in Eq. (A.17). For the term involving the logarithm, we appeal to Eq. (A.13) and compute the Gaussian integrals, arriving at the expression

$$\begin{aligned} & -\ln \sum_{k=0}^{\infty} \frac{e^{-c} c^k}{k!} \int \left(\prod_{r=1}^k \prod_{\ell=1}^L d\boldsymbol{\Sigma}_{r\ell} d\boldsymbol{\Gamma}_{r\ell} \right) \left[\prod_{r=1}^k \omega \left(\left\{ \boldsymbol{\Sigma}_{r\ell}, \boldsymbol{\Gamma}_{r\ell} \right\}_{\ell=1}^L \right) \right] \\ & \times \left\langle \exp \left[-\sum_{\ell=1}^L \left\{ n_+ \ln \det \left(\mathbf{M}_{\eta}(z_{\ell+1}, z_{\ell}^*) + \sum_{r=1}^k \mathbf{J}_r \boldsymbol{\Sigma}_{r\ell} \mathbf{J}_r^{\dagger} \right) + n_- \ln \det \left(\mathbf{M}_{\eta}(z_{\ell}, z_{\ell}^*) + \sum_{r=1}^k \mathbf{J}_r \boldsymbol{\Gamma}_{r\ell} \mathbf{J}_r^{\dagger} \right) \right\} \right] \right\rangle_{\mathcal{J}_{1, \dots, k}}. \end{aligned} \quad (\text{A.18})$$

For the missing term, we introduce the replica-symmetric ansatz into the second integral of Eq. (A.17) and solving the Gaussian integrals we obtain

$$\begin{aligned} & \frac{c}{2} \int \left[\prod_{\ell=1}^L d\boldsymbol{\Sigma}_{\ell} d\boldsymbol{\Gamma}_{\ell} d\boldsymbol{\Sigma}'_{\ell} d\boldsymbol{\Gamma}'_{\ell} \right] \omega \left(\left\{ \boldsymbol{\Sigma}_{\ell}, \boldsymbol{\Gamma}_{\ell} \right\}_{\ell=1}^L \right) \omega \left(\left\{ \boldsymbol{\Sigma}'_{\ell}, \boldsymbol{\Gamma}'_{\ell} \right\}_{\ell=1}^L \right) \\ & \times \left\langle \exp \left[-\sum_{\ell=1}^L \left\{ n_+ \ln \det \left(\mathbf{I}_2 + \boldsymbol{\Sigma}_{\ell} \mathbf{J} \boldsymbol{\Sigma}'_{\ell} \mathbf{J}^{\dagger} \right) + n_- \ln \det \left(\mathbf{I}_2 + \boldsymbol{\Gamma}_{\ell} \mathbf{J} \boldsymbol{\Gamma}'_{\ell} \mathbf{J}^{\dagger} \right) \right\} \right] \right\rangle_{\mathcal{J}}. \end{aligned} \quad (\text{A.19})$$

Adding both terms, (A.18) and (A.19), together with the 2×2 complex auxiliary matrices Υ_{ℓ} , ζ_{ℓ} and ν_{ℓ} , ξ_{ℓ} from Eqs. (2.37) and (2.38), respectively, and after computing the replica limit $n_{\pm} \rightarrow \pm\mu/2\pi i$ assuming it yield the correct results, we arrive at Eq. (2.36).

A.3 The continuous limit throughout the γ contour

Recalling the definition of the \mathbf{M}_{η} matrix (Eq. (2.21)), we find

$$\mathbf{M}_{\eta}(z_{\ell+1}, z_{\ell}^*) = \mathbf{M}_{\eta}(z_{\ell}, z_{\ell}^*) + i\Delta z_{\ell} \boldsymbol{\sigma}_+ + O(\Delta z_{\ell}^2), \quad (\text{A.20})$$

for $\Delta z_{\ell} \ll 1$. Then, expanding all quantities in powers of Δz_{ℓ} up to the leading term, we obtain the equality

$$\left(\mathbf{M}_{\eta}(z_{\ell+1}, z_{\ell}^*) + \sum_{r=1}^k \mathbf{J}_r \boldsymbol{\Sigma}_{r\ell} \mathbf{J}_r^{\dagger} \right)^{-1} = \frac{1}{\mathbf{M}_{\eta}(z_{\ell}, z_{\ell}^*) + \sum_{r=1}^k \mathbf{J}_r \boldsymbol{\Sigma}_{r\ell} \mathbf{J}_r^{\dagger}} \left(\mathbf{I}_2 - \boldsymbol{\sigma}_+ \frac{i\Delta z_{\ell}}{\mathbf{M}_{\eta}(z_{\ell}, z_{\ell}^*) + \sum_{r=1}^k \mathbf{J}_r \boldsymbol{\Sigma}_{r\ell} \mathbf{J}_r^{\dagger}} \right). \quad (\text{A.21})$$

Looking at the δ arguments of Eq. (2.35), it turns out convenient to perform the change of variable $\boldsymbol{\Sigma}_{\ell} \rightarrow \boldsymbol{\Gamma}_{\ell} + \Delta z_{\ell} \mathbf{R}_{\ell}$, with $\mathbf{R}_{\ell} \in \mathbb{M}_{2 \times 2}(\mathbb{C})$ for all $\ell \in \{1, \dots, L\}$, leading us to write the right-hand side of Eq. (A.21)

$$\begin{aligned} & \frac{1}{\mathbf{M}_{\eta}(z_{\ell}, z_{\ell}^*) + \sum_{r=1}^k \mathbf{J}_r \boldsymbol{\Gamma}_{r\ell} \mathbf{J}_r^{\dagger}} + \Delta z_{\ell} \left[\frac{1}{\mathbf{M}_{\eta}(z_{\ell}, z_{\ell}^*) + \sum_{r=1}^k \mathbf{J}_r \boldsymbol{\Gamma}_{r\ell} \mathbf{J}_r^{\dagger}} i\boldsymbol{\sigma}_+ + \frac{1}{\mathbf{M}_{\eta}(z_{\ell}, z_{\ell}^*) + \sum_{r=1}^k \mathbf{J}_r \boldsymbol{\Gamma}_{r\ell} \mathbf{J}_r^{\dagger}} + \right. \\ & \left. \frac{1}{\mathbf{M}_{\eta}(z_{\ell}, z_{\ell}^*) + \sum_{r=1}^k \mathbf{J}_r \boldsymbol{\Gamma}_{r\ell} \mathbf{J}_r^{\dagger}} \sum_{r=1}^k \mathbf{J}_r \mathbf{R}_{r\ell} \mathbf{J}_r^{\dagger} \frac{1}{\mathbf{M}_{\eta}(z_{\ell}, z_{\ell}^*) + \sum_{r=1}^k \mathbf{J}_r \boldsymbol{\Gamma}_{r\ell} \mathbf{J}_r^{\dagger}} \right], \end{aligned} \quad (\text{A.22})$$

where we did use that terms of order $O(\Delta z_{\ell}^2)$ vanish and that under the proposed change of variable

$$\frac{1}{\mathbf{M}_{\eta}(z_{\ell+1}, z_{\ell}^*) + \sum_{r=1}^k \mathbf{J}_r \boldsymbol{\Sigma}_{r\ell} \mathbf{J}_r^{\dagger}} \rightarrow \frac{1}{\mathbf{M}_{\eta}(z_{\ell}, z_{\ell}^*) + \sum_{r=1}^k \mathbf{J}_r \boldsymbol{\Gamma}_{r\ell} \mathbf{J}_r^{\dagger}} \left[\mathbf{I}_2 - \Delta z_{\ell} \frac{\sum_{r=1}^k \mathbf{J}_r \mathbf{R}_{r\ell} \mathbf{J}_r^{\dagger}}{\mathbf{M}_{\eta}(z_{\ell}, z_{\ell}^*) + \sum_{r=1}^k \mathbf{J}_r \boldsymbol{\Gamma}_{r\ell} \mathbf{J}_r^{\dagger}} \right]. \quad (\text{A.23})$$

Rewriting the measure of Eq. (2.35) throughout the computation of the Jacobian, using that for $\mathbf{A} \in \mathbb{M}_{N \times N}(\mathbb{C})$

$\det e^{\mathbf{A}} = e^{\text{Tr}\mathbf{A}}$, and computing the limit $L \rightarrow \infty$ in the resulting equations, we arrive at the expressions

$$\begin{aligned} \omega[\{\mathbf{\Gamma}, \mathbf{R}\}] &= \frac{1}{\Lambda} \sum_{k=0}^{\infty} \frac{e^{-c} c^k}{k!} \int \left(\prod_{r=1}^k d\{\mathbf{\Gamma}_r, \mathbf{R}_r\} \omega[\{\mathbf{\Gamma}_r, \mathbf{R}_r\}] \right) \left\langle \delta_F \left[\mathbf{R}(z) + \mathbf{\Gamma}(z) \left(i\sigma_+ + \sum_{r=1}^k \mathbf{J}_r \mathbf{R}_r(z) \mathbf{J}_r \right) \mathbf{\Gamma}(z) \right] \right. \\ &\quad \left. \times \delta_F \left[\mathbf{\Gamma}(z) - \frac{1}{M_\eta(z, z^*) + \sum_{r=1}^k \mathbf{J}_r \mathbf{\Gamma}_r(z) \mathbf{J}_r^\dagger} \right] e^{-\frac{\mu}{2\pi i} \oint_\gamma dz \text{Tr} \left(\frac{i\sigma_+ + \sum_{r=1}^k \mathbf{J}_r \mathbf{R}_r(z) \mathbf{J}_r}{M_\eta(z, z^*) + \sum_{r=1}^k \mathbf{J}_r \mathbf{\Gamma}_r(z) \mathbf{J}_r^\dagger} \right)} \right\rangle_{\mathbf{J}_{1, \dots, k}} \end{aligned} \quad (\text{A.24})$$

and

$$\begin{aligned} \mathcal{S} &= -\frac{c}{2} - \ln \sum_{k=0}^{\infty} \frac{e^{-c} c^k}{k!} \int \left(\prod_{r=1}^k d\{\mathbf{\Gamma}_r, \mathbf{R}_r\} \omega[\{\mathbf{\Gamma}_r, \mathbf{R}_r\}] \right) \left\langle e^{-\frac{\mu}{2\pi i} \oint_\gamma dz \text{Tr} \left(\frac{i\sigma_+ + \sum_{r=1}^k \mathbf{J}_r \mathbf{R}_r(z) \mathbf{J}_r}{M_\eta(z, z^*) + \sum_{r=1}^k \mathbf{J}_r \mathbf{\Gamma}_r(z) \mathbf{J}_r^\dagger} \right)} \right\rangle_{\mathbf{J}_{1, \dots, k}} \\ &\quad + \frac{c}{2} \int d\{\mathbf{\Gamma}, \mathbf{R}\} d\{\mathbf{\Gamma}', \mathbf{R}'\} \omega(\{\mathbf{\Gamma}, \mathbf{R}\}) \omega(\{\mathbf{\Gamma}', \mathbf{R}'\}) \left\langle e^{-\frac{\mu}{2\pi i} \oint_\gamma dz \text{Tr} \left(\frac{\mathbf{\Gamma}(z) \mathbf{J} \mathbf{R}'(z) \mathbf{J}^\dagger + \mathbf{R}(z) \mathbf{J} \mathbf{\Gamma}'(z) \mathbf{J}^\dagger}{I_2 + \mathbf{\Gamma}(z) \mathbf{J} \mathbf{\Gamma}'(z) \mathbf{J}^\dagger} \right)} \right\rangle_{\mathbf{J}} \end{aligned} \quad (\text{A.25})$$

for the path probability and action, respectively.

Appealing to the complex auxiliary matrices of Eqs. (2.40) and (2.45), together with the average $\langle \dots \rangle_{\{\mathbf{\Gamma}, \mathbf{R}\}}$ defined in Eq. (2.41) and the fact that under integration

$$\mathbf{\Gamma}(z) \rightarrow \left(M_\eta(z, z^*) + \sum_{r=1}^k \mathbf{J}_r \mathbf{\Gamma}_r(z) \mathbf{J}_r^\dagger \right)^{-1} \quad (\text{A.26})$$

and

$$\mathbf{R}(z) \rightarrow -\mathbf{\Gamma}(z) \left(i\sigma_+ + \sum_{r=1}^k \mathbf{J}_r \mathbf{R}_r(z) \mathbf{J}_r \right) \mathbf{\Gamma}(z), \quad (\text{A.27})$$

we arrive at Eqs. (2.39) and (2.42) for the cumulant generating function $\mathcal{F}_\gamma(\mu)$ and path probability $\omega[\{\mathbf{\Gamma}, \mathbf{R}\}]$, respectively. Note that throughout the development of the present section, we have dropped the auxiliary matrix notation and worked directly with the full-length equations so that we could correctly display the calculations.

A.4 Computing the rate function

Resorting to Eq. (1.7), we write the rate function ϕ_γ in terms of the probability density \mathfrak{P}_A of \mathcal{N}_A

$$\mathfrak{P}_A(\mathcal{N}_A) \asymp e^{-N\phi_\gamma(n)}, \quad (\text{A.28})$$

making possible to formulate the cumulant generating function as

$$\mathcal{F}_\gamma(\mu) = -\lim_{N \rightarrow \infty} \frac{1}{N} \ln \int \exp \left[-\mu \mathcal{N}_A - N \Phi \left(\frac{\mathcal{N}_A}{N} \right) \right] d\mathcal{N}_A. \quad (\text{A.29})$$

Employing the saddle-point method, we obtain that

$$\mathcal{F}_\gamma(\mu) \asymp -\sup_{n \in \mathbb{R}} \{-\mu n - \Phi(n)\} \equiv -\tilde{\Phi}(-\mu). \quad (\text{A.30})$$

Thanks to having assumed the Gärtner-Ellis theorem to hold, we know that the rate function $\phi_\gamma(n)$ is convex regardless of the CGF form [78, 84]. Assuming that $\phi_\gamma(n)$ is also differentiable, and observing that $n = \tilde{\Phi}'(\mu)$ and $\Phi(n) = \mu \tilde{\Phi}'(\mu) - \tilde{\Phi}(\mu)$, we arrive finally at Eq. (2.48).

Appendix B

Mathematical handlings of the CSD for the diluted real Ginibre ensemble

In this second appendix, we display, in detail, all the mathematical handlings of Section 2.3, Chapter 2. As we did in Appendix A, we have divided the handling into three sections: firstly, the path integral formulation of the CSD; secondly, the implementation of the replica-symmetry ansatz; and, finally, the computation of the partial derivatives ∂_{z^*} and ∂_z . For the first Section B.1, we commence from Eq. (2.14), the alternative expression of the ESD, and build the path integral equation for the CSD (Eq. (2.67)); immediately after, in Section B.2, we implement the replica-symmetry ansatz on the resulting saddle point equations of Section 2.3.1 and obtain explicit expressions for the joint probability function ω and action \mathcal{S} (Eqs. (2.75) and (2.76), respectively). Owing to the calculation of the $L \rightarrow \infty$ limit is analogous to the one carried out in Section A.3, we skip it and present directly in Section B.3 the explicit computation of the ∂_{z^*} and ∂_z derivatives.

B.1 Building the path integral

Appealing to Eq. (2.59) and the CGF (Eq. (2.10)), we rewrite the CSD (Eq. (2.58)) as

$$\rho(z|\mathcal{R}_\gamma) = - \lim_{N \rightarrow \infty} \lim_{n \rightarrow 0} \frac{1}{nN\pi} \partial_z \partial_{z^*} \frac{\int e^{-N[\mathcal{F}_\gamma(\mu) - \mu\mathcal{R}_\gamma]} \ln \left\langle e^{-\mu\mathcal{N}_A(\gamma)} [Q_A(z, z^*)]^n \right\rangle / e^{-N\mathcal{F}_\gamma(\mu)} d\mu}{\int e^{-N[\mathcal{F}_\gamma(\mu) - \mu\mathcal{R}_\gamma]} d\mu}. \quad (\text{B.1})$$

Utilizing that by the saddle-point method

$$\int e^{-N[\mathcal{F}_\gamma(\mu) - \mu\mathcal{R}_\gamma]} \ln \left\langle e^{-\mu\mathcal{N}_A(\mu)} [Q_A(z, z^*)]^n \right\rangle d\mu \simeq e^{-N[\mathcal{F}_\gamma(\mu_0) - \mu_0\mathcal{R}_\gamma]} \ln \left\langle e^{-\mu_0\mathcal{N}_A(\mu)} [Q_A(z, z^*)]^n \right\rangle \quad (\text{B.2})$$

and

$$\int e^{-N[\mathcal{F}_\gamma(\mu) - \mu\mathcal{R}_\gamma]} d\mu \simeq e^{-N[\mathcal{F}_\gamma(\mu_0) - \mu_0\mathcal{R}_\gamma]}, \quad (\text{B.3})$$

with μ_0 the point where the function $\mathcal{F}_\gamma(\mu) - \mu\mathcal{R}_\gamma$ attains its minimum, we arrive at Eq. (2.60) with Eq. (2.61), the resulting saddle-point condition.

To arrive at Eq. (2.67), we need to decouple the sites i and j of the general expression of $\rho(z|\mathcal{R}_\gamma)$ (Eq. (2.65)). Then, analogous to Eq. (A.6), we rewrite the term involving the average $\langle \dots \rangle_{\mathcal{J}}$ of Eq. (2.65) as

$$\begin{aligned} & \frac{c}{2N} \sum_{i,j=1}^N \int \prod_{\ell=1}^L \left[\prod_{a=1}^{n_+} \delta(\psi_{\ell a} - \psi_{i\ell a}) \delta(\psi'_{\ell a} - \psi_{j\ell a}) \prod_{b=1}^{n_-} \delta(\phi_{\ell b} - \phi_{i\ell b}) \delta(\phi'_{\ell b} - \phi_{j\ell b}) \right] \left[\prod_{c=1}^n \delta(\Omega_c - \Omega_{ic}) \delta(\Omega'_c - \Omega_{jc}) \right] \\ & \times \left\langle e^{i \left\{ \sum_{c=1}^n (\Omega_c^\dagger \mathcal{J} \Omega_c + \Omega_c'^\dagger \mathcal{J} \Omega_c) + \sum_{\ell=1}^L \left[\sum_{a=1}^{n_+} (\psi_{\ell a}^\dagger \mathcal{J} \psi'_{\ell a} + \psi_{\ell a}'^\dagger \mathcal{J} \psi_{\ell a}) + \sum_{b=1}^{n_-} (\phi_{\ell b}^\dagger \mathcal{J} \phi'_{\ell b} + \phi_{\ell b}'^\dagger \mathcal{J} \phi_{\ell b}) \right] \right\}} - 1 \right\rangle_{\mathcal{J}} d\Psi d\Phi d\Omega d\Psi' d\Phi' d\Omega', \end{aligned} \quad (\text{B.4})$$

which, by means of the order parameter $P(\Psi, \Phi, \Omega)$ of Eq. (2.66), transforms into

$$\frac{c}{2}N \int d\Psi d\Phi d\Omega d\Psi' d\Phi' d\Omega' P(\Psi, \Phi, \Omega) P(\Psi', \Phi', \Omega') \times \left\langle e^{i\left\{\sum_{c=1}^n (\Omega_c^\dagger J \Omega_c' + \Omega_c'^\dagger J^\dagger \Omega_c) + \sum_{\ell=1}^L \left[\sum_{a=1}^{n_+} (\psi_{\ell a}^\dagger J \psi'_{\ell a} + \psi'_{\ell a}{}^\dagger J^\dagger \psi_{\ell a}) + \sum_{b=1}^{n_-} (\phi_{\ell b}^\dagger J \phi'_{\ell b} + \phi'_{\ell b}{}^\dagger J^\dagger \phi_{\ell b}) \right] \right\}} - 1 \right\rangle_J. \quad (\text{B.5})$$

To facilitate the handling of the subsequent equations, we have introduced the shorthand notation $d\Omega \equiv \prod_{c=1}^n d\Omega_c$, $d\Psi \equiv \prod_{\ell=1}^L \prod_{a=1}^{n_+} d\Psi_{\ell a}$, and $d\Phi \equiv \prod_{\ell=1}^L \prod_{b=1}^{n_-} d\Phi_{\ell b}$. Inserting Eq. (B.5) into Eq. (2.65) and using the auxiliary functions

$$\tau(\Psi_i, \Phi_i, \Omega_i) = \sum_{c=1}^n \Omega_{ic}^\dagger M_\eta(z, z^*) \Omega_{ic} + \sum_{\ell=1}^L \left(\sum_{a=1}^{n_+} \psi_{i\ell a}^\dagger M_\eta(\omega_{\ell+1}, \omega_\ell^*) \psi_{i\ell a} + \sum_{b=1}^{n_-} \phi_{i\ell b}^\dagger M_\eta(\omega_\ell, \omega_\ell^*) \phi_{i\ell b} \right) \quad (\text{B.6})$$

and

$$\Xi(\Psi, \Phi, \Omega, \Psi', \Phi', \Omega') = \sum_{\ell=1}^L \left[\sum_{a=1}^{n_+} (\psi_{\ell a}^\dagger J \psi'_{\ell a} + \psi'_{\ell a}{}^\dagger J^\dagger \psi_{\ell a}) + \sum_{b=1}^{n_-} (\phi_{\ell b}^\dagger J \phi'_{\ell b} + \phi'_{\ell b}{}^\dagger J^\dagger \phi_{\ell b}) \right] + \sum_{c=1}^n (\Omega_c^\dagger J \Omega_c' + \Omega_c'^\dagger J^\dagger \Omega_c), \quad (\text{B.7})$$

together with the Fourier representation of the functional Dirac δ for the exponential term of Eq. (2.65) involving the average over the disorder $\langle \dots \rangle_J$, we arrive at the expression

$$\rho(z|\mathcal{R}_\gamma) = \lim_{N \rightarrow \infty} \lim_{L \rightarrow \infty} \lim_{n \rightarrow 0} \lim_{n_\pm \rightarrow \frac{\pm n}{2\pi i}} \lim_{\eta \rightarrow 0^+} \frac{-1}{nN\pi} \partial_z \partial_{z^*} \ln \int \mathcal{D} \left[\{P, \hat{P}\} \right] \int \prod_{i=1}^N \left[d\Psi_i d\Phi_i d\Omega_i e^{-\tau(\Psi_i, \Phi_i, \Omega_i) - i\hat{P}(\Psi_i, \Phi_i, \Omega_i)} \right] \times \exp \left(\frac{c}{2}N \int d\Psi d\Phi d\Omega d\Psi' d\Phi' d\Omega' P(\Psi, \Phi, \Omega) P(\Psi', \Phi', \Omega') \left\langle e^{i\Xi(\Psi, \Phi, \Omega, \Psi', \Phi', \Omega')} - 1 \right\rangle_J \right) \times \exp \left[iN \int d\Psi d\Phi d\Omega \hat{P}(\Psi, \Phi, \Omega) P(\Psi, \Phi, \Omega) \right], \quad (\text{B.8})$$

from which the path integral formulation for the CSD detaches (Eq. (2.67)) with its action provided by Eq. (2.68).

B.2 The replica-symmetric ansatz and the joint probability distribution

Following the same path carried out for Eq. (A.12), we rewrite Eq. (2.71) as

$$e^{-i\hat{P}(\Psi, \Phi, \Omega)} = \sum_{k=0}^{\infty} \frac{e^{-c} c^k}{k!} \int \left[\prod_{r=1}^k \left(d\Delta_r \prod_{\ell=1}^L d\Sigma_{r\ell} d\Gamma_{r\ell} \right) \omega(\Delta_r, \{\Sigma_{r\ell}, \Gamma_{r\ell}\}_{\ell=1}^L) \right] \int \left(\prod_{r=1}^k d\Psi_r d\Phi_r d\Omega_r \right) \times \left\langle \prod_{r=1}^k \left[\prod_{c=1}^n \frac{e^{-\Omega_{rc}^\dagger \Delta_r^{-1} \Omega_{rc}' + i(\Omega_c^\dagger J_r \Omega_{rc}' + \Omega_{rc}'^\dagger J_r^\dagger \Omega_c)}}{\det \Delta_r} \prod_{\ell=1}^L \left(\prod_{a=1}^{n_+} \frac{e^{-\psi_{r\ell a}^\dagger \Sigma_{r\ell}^{-1} \psi'_{r\ell a} + i(\psi_{\ell a}^\dagger J_r \psi'_{r\ell a} + \psi'_{r\ell a}{}^\dagger J_r^\dagger \psi_{\ell a})}}{\det \Sigma_{r\ell}} \right) \times \prod_{b=1}^{n_-} \frac{e^{-\phi_{r\ell b}^\dagger \Gamma_{r\ell}^{-1} \phi'_{r\ell b} + i(\phi_{\ell b}^\dagger J_r \phi'_{r\ell b} + \phi'_{r\ell b}{}^\dagger J_r^\dagger \phi_{\ell b})}}{\det \Gamma_{r\ell}} \right) \right] \right\rangle_{J_1, \dots, k}; \quad (\text{B.9})$$

solving the integrals for the variables (Ψ', Φ', Ω') , we obtain an equivalent expression to Eq. (A.13),

$$e^{-i\hat{P}(\Psi, \Phi, \Omega)} = \sum_{k=0}^{\infty} \frac{e^{-c} c^k}{k!} \int \left[\prod_{r=1}^k \left(d\Delta_r \prod_{\ell=1}^L d\Sigma_{r\ell} d\Gamma_{r\ell} \right) \omega(\Delta_r, \{\Sigma_{r\ell}, \Gamma_{r\ell}\}_{\ell=1}^L) \right] \times \left\langle \prod_{r=1}^k \left(\prod_{c=1}^n e^{-\Omega_c J_r \Delta_r J_r^\dagger \Omega_c} \prod_{\ell=1}^L \left[\prod_{a=1}^{n_+} e^{-\psi_{\ell a}^\dagger J_r \Sigma_{r\ell} J_r^\dagger \psi_{\ell a}} \prod_{b=1}^{n_-} e^{-\phi_{\ell b}^\dagger J_r \Gamma_{r\ell} J_r^\dagger \phi_{\ell b}} \right] \right) \right\rangle_{J_1, \dots, k}. \quad (\text{B.10})$$

Inserting Eq. (B.10) into Eq. (2.72), we get an analogous expression to Eq. (A.15) for the CSD, where we identify

$$\begin{aligned} \omega\left(\Delta, \{\Sigma_\ell, \Gamma_\ell\}_{\ell=1}^L\right) &= \frac{1}{\mathfrak{N}} \sum_{k=0}^{\infty} \frac{e^{-c} c^k}{k!} \int \left[\prod_{r=1}^k \left(d\Delta_r \prod_{\ell=1}^L d\Sigma_{r\ell} d\Gamma_{r\ell} \right) \prod_{r=1}^k \omega\left(\Delta_r, \{\Sigma_{r\ell}, \Gamma_{r\ell}\}_{\ell=1}^L\right) \right] \\ &\times \left\langle \delta \left[\Delta - \frac{1}{M_\eta(z, z^*) + \sum_{r=1}^k \mathbf{J}_r \Delta_r \mathbf{J}_r^\dagger} \right] e^{-n \ln \det(M_\eta(z, z^*) + \sum_{r=1}^k \mathbf{J}_r \Delta_r \mathbf{J}_r^\dagger)} \right. \\ &\times e^{-\sum_{\ell=1}^L [n_+ \ln \det(M_\eta(z_{\ell+1}, z_\ell^*) + \sum_{r=1}^k \mathbf{J}_r \Sigma_{r\ell} \mathbf{J}_r^\dagger) + n_- \ln \det(M_\eta(z_\ell, z_\ell^*) + \sum_{r=1}^k \mathbf{J}_r \Gamma_{r\ell} \mathbf{J}_r^\dagger)]} \\ &\times \left. \prod_{\ell=1}^L \delta \left[\Sigma_\ell - \frac{1}{M_\eta(z_{\ell+1}, z_\ell^*) + \sum_{r=1}^k \mathbf{J}_r \Sigma_{r\ell} \mathbf{J}_r^\dagger} \right] \delta \left[\Gamma_\ell - \frac{1}{M_\eta(z_\ell, z_\ell^*) + \sum_{r=1}^k \mathbf{J}_r \Gamma_{r\ell} \mathbf{J}_r^\dagger} \right] \right\rangle_{\mathbf{J}_{1, \dots, k}} \end{aligned} \quad (\text{B.11})$$

as the joint probability distribution function. Identifying the expressions within the arguments of the exponential and δ functions as the ones appearing in the 2×2 complex auxiliary matrices Υ_ℓ , ζ_ℓ , and \mathfrak{F} of Eqs. (2.37) and (2.77), we successfully arrive at Eq. (2.75).

As we did for $\mathcal{F}_\gamma(\mu)$, we express the CSD action in terms of the functions τ and Ξ (Eqs. (B.6) and (B.7)),

$$\begin{aligned} \mathcal{S} \left[\{P, \hat{P}\} \right] &= -\frac{c}{2} + \frac{c}{2} \int d\Psi d\Phi d\Omega d\Psi' d\Phi' d\Omega' P(\Psi, \Phi, \Omega) \hat{P}(\Psi', \Phi', \Omega') \left\langle e^{i\Xi(\Psi, \Phi, \Omega, \Psi', \Phi', \Omega')} \right\rangle_{\mathbf{J}} \\ &- \ln \int d\Psi d\Phi d\Omega e^{-\tau(\Psi, \Phi, \Omega) - i\hat{P}(\Psi, \Phi, \Omega)}, \end{aligned} \quad (\text{B.12})$$

solving the first and second integrals, we obtain

$$\begin{aligned} &\frac{c}{2} \int \left[d\Delta d\Delta' \prod_{\ell=1}^L d\Sigma_\ell d\Gamma_\ell d\Sigma'_\ell d\Gamma'_\ell \right] \omega\left(\Delta, \{\Sigma_\ell, \Gamma_\ell\}_{\ell=1}^L\right) \omega\left(\Delta', \{\Sigma'_\ell, \Gamma'_\ell\}_{\ell=1}^L\right) \\ &\times \left\langle \exp \left[-n \ln \det \left(\mathbf{I}_2 + \Delta \mathbf{J} \Delta' \mathbf{J}^\dagger \right) - \sum_{\ell=1}^L \left\{ n_+ \ln \det \left(\mathbf{I}_2 + \Sigma_\ell \mathbf{J} \Sigma'_\ell \mathbf{J}^\dagger \right) + n_- \ln \det \left(\mathbf{I}_2 + \Gamma_\ell \mathbf{J} \Gamma'_\ell \mathbf{J}^\dagger \right) \right\} \right] \right\rangle_{\mathbf{J}} \end{aligned} \quad (\text{B.13})$$

and

$$\begin{aligned} &\ln \sum_{k=0}^{\infty} \frac{e^{-c} c^k}{k!} \int \left(\prod_{r=1}^k \left[d\Delta_r \prod_{\ell=1}^L d\Sigma_{r\ell} d\Gamma_{r\ell} \right] \right) \left[\prod_{r=1}^k \omega\left(\Delta_r, \{\Sigma_{r\ell}, \Gamma_{r\ell}\}_{\ell=1}^L\right) \right] \left\langle e^{-n \ln \det(M_\eta(z, z^*) + \sum_{r=1}^k \mathbf{J}_r \Delta_r \mathbf{J}_r^\dagger)} \right. \\ &\times \exp \left[-\sum_{\ell=1}^L \left\{ n_+ \ln \det \left(M_\eta(\omega_{\ell+1}, \omega_\ell^*) + \sum_{r=1}^k \mathbf{J}_r \Sigma_{r\ell} \mathbf{J}_r^\dagger \right) + n_- \ln \det \left(M_\eta(\omega_\ell, \omega_\ell^*) + \sum_{r=1}^k \mathbf{J}_r \Gamma_{r\ell} \mathbf{J}_r^\dagger \right) \right\} \right] \right\rangle_{\mathbf{J}_{1, \dots, k}}, \end{aligned} \quad (\text{B.14})$$

respectively. Resorting to the complex matrices Υ_ℓ , ζ_ℓ , \mathfrak{F} and \mathfrak{R} , we manage to arrive finally at Eq. (2.76).

B.3 Computing ∂_{z^*} and ∂_z for the conditioned spectral density

The calculation of the continuum limit $L \rightarrow \infty$ in Eqs. (2.75) and (2.76) is analogous to the one carried out for the CGF (Eqs. (A.20)-(A.25)), leading us to an exact equation for the functional density,

$$\begin{aligned} \omega[\Delta, \{\Gamma, \mathbf{R}\}] &= \frac{1}{\mathfrak{N}} \sum_{k=0}^{\infty} \frac{e^{-c} c^k}{k!} \int \left(\prod_{r=1}^k d\Delta_r d\{\Gamma_r, \mathbf{R}_r\} \right) \omega[\Delta_r, \{\Gamma_r, \mathbf{R}_r\}] \left\langle \exp(\mu W[\{\Gamma, \mathbf{R}\}] + n \ln \det \Delta) \right. \\ &\times \delta \left[\Delta - \frac{1}{M_\eta(z, z^*) + \sum_{r=1}^k \mathbf{J}_r \Delta_r \mathbf{J}_r^\dagger} \right] \delta_F \left[\Gamma(\omega) - \frac{1}{M_\eta(\omega, \omega^*) + \sum_{r=1}^k \mathbf{J}_r \Gamma_r(\omega) \mathbf{J}_r^\dagger} \right] \\ &\times \delta_F \left[\mathbf{R}(\omega) + \Gamma(\omega) \left(i\sigma_+ + \sum_{r=1}^k \mathbf{J}_r \mathbf{R}_r(\omega) \mathbf{J}_r^\dagger \right) \Gamma(\omega) \right] \right\rangle_{\mathbf{J}_{1, \dots, k}}, \end{aligned} \quad (\text{B.15})$$

and action,

$$\mathcal{S} = \frac{c}{2} \left\langle \left\langle \exp \left[-n \ln \det \left(\mathbf{I}_2 + \Delta \mathbf{J} \Delta' \mathbf{J}^\dagger \right) - \frac{\mu}{2\pi i} \oint_{\gamma} \text{Tr} [\mathbf{G}(\omega) \mathbf{H}(\omega)] d\omega \right] \right\rangle \right\rangle_{\mathbf{J}, \Delta, \{\Gamma, \mathbf{R}\}, \Delta', \{\Gamma', \mathbf{R}'\}} \quad (\text{B.16})$$

$$- \frac{c}{2} - \ln \left\langle \exp \left[-n \ln \det \left(\mathbf{M}_\eta(z, z^*) + \sum_{r=1}^k \mathbf{J}_r \Delta_r \mathbf{J}_r^\dagger \right) - W[\{\Gamma, \mathbf{R}\}] \right] \right\rangle_{\Delta, \{\Gamma, \mathbf{R}\}},$$

where $W[\{\Gamma, \mathbf{R}\}]$ is given by Eq. (2.44) and $\mathbf{G}(\omega), \mathbf{H}(\omega) \in \mathbb{M}_{2 \times 2}(\mathbb{C})$ are the auxiliary matrices defined in Eq. (2.40). For both expressions, (B.15) and (B.16), we have used the fact that under integration,

$$\Delta \rightarrow \left(\mathbf{M}_\eta(z, z^*) + \sum_{r=1}^k \mathbf{J}_r \Delta_r \mathbf{J}_r^\dagger \right)^{-1}, \quad (\text{B.17})$$

$$\Gamma(\omega) \rightarrow \left(\mathbf{M}_\eta(\omega, \omega^*) + \sum_{r=1}^k \mathbf{J}_r \Gamma_r(\omega) \mathbf{J}_r^\dagger \right)^{-1}, \quad (\text{B.18})$$

and

$$\mathbf{R}(\omega) \rightarrow -\Gamma(\omega) \left(i\sigma_+ + \sum_{r=1}^k \mathbf{J}_r \mathbf{R}_r(\omega) \mathbf{J}_r^\dagger \right) \Gamma(\omega); \quad (\text{B.19})$$

note that in (B.18) and (B.19), the continuum limit $L \rightarrow \infty$ has already been computed. In order to correctly display the subsequent manipulations, we momentarily abandon the auxiliary matrices notation and work with the full-length expressions.

From the asymptotic convergence of $\rho(z|\mathcal{R}_\gamma)$ (Eq. (2.30)), we observe that calculating the first derivative ∂_{z^*} on the logarithm of the path integral translates into computing ∂_{z^*} directly on the action \mathcal{S} . Since we expressed the latter in terms of averages over the functional density $\omega[\Delta, \{\Gamma, \mathbf{R}\}]$, we have

$$\frac{\partial \mathcal{S}}{\partial z^*} = \frac{\partial \omega}{\partial z^*} \frac{\partial \mathcal{S}}{\partial \omega} + \frac{\partial \mathcal{S}}{\partial z^*}. \quad (\text{B.20})$$

In other words, to obtain $\partial_{z^*} \mathcal{S}$, we need to calculate the partial derivative of $\omega[\Delta, \{\Gamma, \mathbf{R}\}]$, which, by its expression, seems like a complicated task. Fortunately, appealing to the saddle-point equations, Eqs. (2.71) and (2.72), we manage to write

$$\frac{\partial \mathcal{S}}{\partial \omega} = \frac{\partial \mathcal{S}}{\partial P} \frac{\partial P}{\partial \omega} + \frac{\partial \mathcal{S}}{\partial \hat{P}} \frac{\partial \hat{P}}{\partial \omega}, \quad (\text{B.21})$$

where both $\partial_P \mathcal{S}$ and $\partial_{\hat{P}} \mathcal{S}$ are equal to zero. Therefore, post calculation, we express $\rho(z|\mathcal{R}_\gamma)$ in terms of the partial derivative ∂_z and the limit $\eta \rightarrow 0^+$,

$$\rho(z|\mathcal{R}_\gamma) = \frac{1}{\pi} \lim_{\eta \rightarrow 0^+} \partial_z \langle \text{Tr} [i\sigma_- \Delta(z)] \rangle_{\Delta, \{\Gamma, \mathbf{R}\}}, \quad (\text{B.22})$$

with

$$\omega[\Delta, \{\Gamma, \mathbf{R}\}] = \frac{1}{\mathfrak{N}} \sum_{k=0}^{\infty} \frac{e^{-c} c^k}{k!} \int \left(\prod_{r=1}^k d\Delta_r d\{\Gamma_r, \mathbf{R}_r\} \omega[\Delta_r, \{\Gamma_r, \mathbf{R}_r\}] \right) \left\langle \exp \left(\frac{\mu}{2\pi i} \oint_{\gamma} \text{Tr} [\Gamma^{-1}(z) \mathbf{R}(z)] dz \right) \right.$$

$$\times \delta \left[\Delta(z) - \frac{1}{\mathbf{M}_\eta(z, z^*) + \sum_{r=1}^k \mathbf{J}_r \Delta_r \mathbf{J}_r^\dagger} \right] \delta_F \left[\Gamma(\omega) - \frac{1}{\mathbf{M}_\eta(\omega, \omega^*) + \sum_{r=1}^k \mathbf{J}_r \Gamma_r(\omega) \mathbf{J}_r^\dagger} \right] \quad (\text{B.23})$$

$$\times \delta_F \left[\mathbf{R}(\omega) + \Gamma(\omega) \left(i\sigma_+ + \sum_{r=1}^k \mathbf{J}_r \mathbf{R}_r(\omega) \mathbf{J}_r^\dagger \right) \Gamma(\omega) \right] \Bigg\rangle_{\mathbf{J}_{1, \dots, k}}.$$

the corresponding functional density. Noteworthy is that in Eq. (B.23), in contrast with Eq. (B.15), we have already calculated the replica limit $n \rightarrow 0$.

As mentioned in Subsection 2.3.1, calculating both the partial derivative ∂_{z^*} and the replica limit $n \rightarrow 0$ was a straightforward procedure. To compute the remaining derivative ∂_z , we must proceed with a deeper analysis. We assume a dependence of the functional density of Eq. (B.23) on ∂_z of the form

$$\delta \left(\partial_z \Delta - \partial_z \frac{1}{M_\eta(z, z^*) + \sum_{r=1}^k \mathbf{J}_r \Delta_r \mathbf{J}_r^\dagger} \right). \quad (\text{B.24})$$

Realizing the change of variable $z \rightarrow z + \Delta z$ so $\Delta \rightarrow \Delta + \Delta z \partial_z \Delta$, we obtain

$$\frac{1}{M_\eta(z, z^*) + \sum_{r=1}^k \mathbf{J}_r \Delta_r \mathbf{J}_r^\dagger} \rightarrow \frac{1}{M_\eta(z, z^*) + \sum_{r=1}^k \mathbf{J}_r \Delta_r \mathbf{J}_r^\dagger} \left[\mathbf{I}_2 - \Delta z \frac{i\sigma_+ + \sum_{r=1}^k \mathbf{J}_r \partial_z \Delta_r \mathbf{J}_r^\dagger}{M_\eta(z, z^*) + \sum_{r=1}^k \mathbf{J}_r \Delta_r \mathbf{J}_r^\dagger} \right], \quad (\text{B.25})$$

from where we identify

$$\partial_z \Delta = - \frac{1}{M_\eta(z, z^*) + \sum_{r=1}^k \mathbf{J}_r \Delta_r \mathbf{J}_r^\dagger} \left(\frac{i\sigma_+ + \sum_{r=1}^k \mathbf{J}_r \partial_z \Delta_r \mathbf{J}_r^\dagger}{M_\eta(z, z^*) + \sum_{r=1}^k \mathbf{J}_r \Delta_r \mathbf{J}_r^\dagger} \right). \quad (\text{B.26})$$

Combining all the above expressions, we arrive at the final equation of the conditioned spectral density $\rho(z|\mathcal{R}_\gamma)$ for the diluted real Ginibre ensemble (Eq. (2.78)) with the functional density $\omega[\Delta, \partial_z \Delta, \{\Gamma, \mathbf{R}\}]$ given by Eq. (2.81).

Appendix C

Population dynamics algorithm

For this third appendix, we depict the bases of the population dynamics algorithm and, by two simple schemes, we illustrate its implementation in Eqs. (2.42) and (2.81).

In general, equations such as (2.42) and (2.81) cannot be solved in closed form; consequently, one must appeal to numerical methods to estimate the functional densities $\omega[\{\mathbf{\Gamma}, \mathbf{R}\}]$ and $\omega[\mathbf{\Delta}, \partial_z \mathbf{\Delta}, \{\mathbf{\Gamma}, \mathbf{R}\}]$, respectively. The method we use to estimate both distributions is known in statistical physics as the *population dynamics algorithm* [96]. This algorithm efficiently generates samples of random variables whose distribution closely approximates the so-called *special endogeneous*¹ *solution to a stochastic fixed-point equation* [230]. In general, stochastic fixed-point equations can possess various solutions; nevertheless, one is commonly interested in the so-called *endogenous solutions*, that is, solutions obtained via *weighted branching processes* [230, 231]. It could happen that the endogenous solution is not unique, but it is still possible to characterize all endogenous solutions via *the special endogenous solution*, which is the only attracting solution constructed by iterating the stochastic fixed-point equation [230].

The idea behind this method is to approximate the target distribution through a sample of N i.i.d. copies of the random variables, called *population*, on which the distribution evolves [96]. The algorithm performance is based on sampling with a constant replacement of the random variables from the population as iterations advance, i.e., the next level of recursion samples with replacement from the population previously replaced according to the target distribution [230]. As N becomes large, the empirical distributions should converge to the actual desired distribution [96].

For Subsection 2.2, the distribution to approximate corresponds to Eq. (2.42),

$$\omega[\{\mathbf{\Gamma}, \mathbf{R}\}] = \frac{1}{\Lambda} \sum_{k=0}^{\infty} \frac{e^{-c} c^k}{k!} \int \left(\prod_{r=1}^k d\{\mathbf{\Gamma}_r, \mathbf{R}_r\} \omega[\{\mathbf{\Gamma}_r, \mathbf{R}_r\}] \right) e^{\mu W[\{\mathbf{\Gamma}, \mathbf{R}\}]} \langle \delta_F[\mathbf{R}(z) - \mathbf{\Pi}_k(z)] \delta_F[\mathbf{\Gamma}(z) - \mathbf{\chi}_k(z)] \rangle_{\mathbf{J}_1, \dots, \mathbf{J}_k}, \quad (\text{C.1})$$

which, as we have explained, is discretized into a finite collection of points $\{z_1, \dots, z_L\}$ with the 2×2 complex matrices $\{\mathbf{\Gamma}(z_\ell), \mathbf{R}(z_\ell)\}_{\ell=1}^L$ (Eq. (2.49)). Now, we illustrate how $\omega[\{\mathbf{\Gamma}, \mathbf{R}\}]$ is solved numerically through the population dynamics algorithm:

1. Firstly, we introduce a population of the form $\{\mathbf{R}_\alpha(z_1), \dots, \mathbf{R}_\alpha(z_L), \mathbf{\Gamma}_\alpha(z_1), \dots, \mathbf{\Gamma}_\alpha(z_L)\}_{\alpha=1}^M$.
2. Immediately after, we draw a random number $k \in \mathbb{Z}^+$ from a Poisson distribution $e^{-c} c^k / k!$ with average c . We randomly pick k elements $\{\mathbf{\Gamma}_\beta(z_1), \dots, \mathbf{\Gamma}_\beta(z_L), \mathbf{R}_\beta(z_1), \dots, \mathbf{R}_\beta(z_L)\}_{\beta=1}^k$ from the initial population and create the set of 2×2 complex matrices $\{\mathbf{J}_1, \dots, \mathbf{J}_k\}$ to compute the Dirac δ operations of Eq. (C.1).
3. Next, we calculate the weighted factor $W[\{\mathbf{\Gamma}, \mathbf{R}\}]$ via the Eq. (2.50) and replace n_p members of the original population according to the following procedure: for each value of n_p , we draw a random number r_{n_p} from a uniform distribution between 1 and M such that

$$\{\mathbf{\Gamma}_{r_j}(z_1), \dots, \mathbf{\Gamma}_{r_j}(z_L)\}_{j=1}^{n_p} \rightarrow \{\mathbf{\chi}_k(z_1), \dots, \mathbf{\chi}_k(z_L)\}$$

and

$$\{\mathbf{R}_{r_j}(z_1), \dots, \mathbf{R}_{r_j}(z_L)\}_{j=1}^{n_p} \rightarrow \{-\mathbf{\Pi}_k(z_1), \dots, -\mathbf{\Pi}_k(z_L)\}.$$

¹An endogeneous variable is a random variable in a statistical model that is determined by its relation with the other variables within the model.

4. Finally, we return to the second step until we have achieved convergence.

For subsection 2.3 the probability distribution to approximate is more complicated and corresponds to Eq. (2.81),

$$\begin{aligned} \omega[\Delta, \partial_z \Delta, \{\Gamma, \mathbf{R}\}] &= \frac{1}{\mathfrak{N}} \sum_{k=0}^{\infty} \frac{e^{-c} c^k}{k!} \int \left(\prod_{r=1}^k d\Delta_r d(\partial_z \Delta_r) d\{\Gamma_r, \mathbf{R}_r\} \omega[\Delta_r, \partial_z \Delta_r, \{\Gamma_r, \mathbf{R}_r\}] \right) e^{\mu W[\{\Gamma, \mathbf{R}\}]} \\ &\times \left\langle \delta[\Delta(z) - \hat{\chi}_k(z)] \delta[\partial_z \Delta(z) - \hat{\Pi}_k(z)] \delta_F[\Gamma(\omega) - \chi_k(\omega)] \delta_F[\mathbf{R}(\omega) - \Pi_k(\omega)] \right\rangle_{\mathbf{J}_{1, \dots, k}}; \end{aligned} \quad (\text{C.2})$$

nonetheless, the algorithm's base remains the same.

1. We introduce the population $\{\Delta_\alpha, \partial_z \Delta_\alpha, \mathbf{R}_\alpha(\omega_1), \dots, \mathbf{R}_\alpha(\omega_L), \Gamma_\alpha(\omega_1), \dots, \Gamma_\alpha(\omega_L)\}_{\alpha=1}^M$.
2. Subsequently, we draw a number $k \in \mathbb{Z}^+$ according to a Poisson distribution with average c . We randomly select k elements $\{\Delta_\beta, \partial_z \Delta_\beta, \mathbf{R}_\beta(\omega_1), \dots, \mathbf{R}_\beta(\omega_L), \Gamma_\beta(\omega_1), \dots, \Gamma_\beta(\omega_L)\}_{\beta=1}^M$ from the initial population and create the set of matrices $\{\mathbf{J}_1, \dots, \mathbf{J}_k\}$, with $\mathbf{J}_\beta \in \text{M}_{2 \times 2}(\mathbb{C})$ for all $\beta = 1, \dots, k$.
3. We evaluate the weight factor $W[\{\Gamma, \mathbf{R}\}]$ via the Eq. (2.50) and replace n_p members of the original population according to

$$\{\Delta_{r_j}(z)\}_{j=1}^{n_p} \rightarrow \hat{\chi}_k(z), \quad \{\partial_z \Delta_{r_j}(z)\}_{j=1}^{n_p} \rightarrow \hat{\Pi}_k(z),$$

$$\{\Gamma_{r_j}(\omega_1), \dots, \Gamma_{r_j}(\omega_L)\}_{j=1}^{n_p} \rightarrow \{\chi_k(\omega_1), \dots, \chi_k(\omega_L)\},$$

and

$$\{\mathbf{R}_{r_j}(\omega_1), \dots, \mathbf{R}_{r_j}(\omega_L)\}_{j=1}^{n_p} \rightarrow \{-\Pi_k(\omega_1), \dots, -\Pi_k(\omega_L)\},$$

with r_j a random number drawn from a uniform distribution between 1 and M for all $j = 1, \dots, n_p$.

4. To conclude, we return to step 2 until we have achieved convergence.

As we can see, the population dynamics algorithm is a highly efficient procedure to obtain the probability distribution of cases when an analytical solution seems hopeless. The effectiveness of the algorithm can be observed through the different figures displayed within the main text.

Appendix D

Monte Carlo methods

In this last appendix, we present a concise overview of the Monte Carlo methods (MCM), centring our attention on the Metropolis algorithm; to provide an appropriate description, we have partitioned the appendix into six parts. We begin in Section D.1 by introducing the general motivations behind the MCM; immediately after, we move to Section D.2, displaying the concepts of simple and importance sampling. In Section D.3, we introduce the basic definitions of Markov processes, and in Sections D.4 and D.5, we present the conditions of ergodicity, detailed balance, and acceptance ratios. Finally, in Section D.6 we place all the previous concepts together and introduce the Metropolis algorithm.

D.1 Bases

Many of the calculations performed on statistical mechanics focus on the properties of condensed matter systems. The problem in these calculations is the fact that such systems are composed of atoms and molecules; even when these components follow quite simple equations of motion or are generally all the same, it is the large number of equations (the magnitude of the problem) that is responsible for the lacking of exact solutions. In other words, *while the formal developments of statistical mechanics are commonly quite elegant, the computation of properties for some models turns out to be highly complicated*. For instance, let us say we wish to calculate the partition function Z of a specific system. To carry out it, we must perform a sum over a large number of states; moreover, if we are interested in the thermodynamic limit, the sum has to run over an infinite number of states, which undoubtedly is far more complicated. Indeed, for most models, finding an exact analytical expression for the partition function Z or any other equivalent thermodynamic quantity still seems far away. To overcome the difficulties, several computational methods have been developed [232].

The most straightforward computational form for solving problems in statistical physics is to take the model under study and place it on a finite-size lattice so that the partition function becomes a sum over a finite number of terms; one of the numerical methods capable of calculating such a partition function is known as *Monte Carlo simulation* [232]. Strictly speaking, a Monte Carlo simulation generates random objects or processes utilizing a computer. These objects can arise naturally, like complex road networks, transport of neutrons, and evolution of the stock market (to mention a few), or (as in many cases) being artificially introduced to provide solutions to deterministic problems. For these last, Monte Carlo simulations involve random samplings from certain probability distributions [233]. Whether the objects arise naturally or artificially, the idea behind Monte Carlo techniques is to repeat the experiments a large number of times to obtain many quantities of interest using the *law of large numbers* [49, 234, 235] and other statistical inference methods [233].

Hence, *Monte Carlo methods* are a broad of computational algorithms relying on repeated random sampling to obtain numerical results [236]. We can think of them as techniques whose main characteristic is the use of random numbers as *raw material*. There are commonly three uses for the MCM [232–234, 236–238]: *numerical integration*, *optimization*, and *generation of probability sample distributions*. Nonetheless, dealing with MCM frequently means calculating the expected value of an observable Q (this could be the internal energy, magnetization, etc.). The ideal path to perform such a calculation is averaging the observable over all states μ of the system, weighting each one with

its Boltzmann probability through the equation [232]

$$\langle Q \rangle = \frac{\sum_{\mu} Q_{\mu} e^{-\beta E_{\mu}}}{\sum_{\mu} e^{-\beta E_{\mu}}}. \quad (\text{D.1})$$

Unfortunately, the computation of Eq. (D.1) is viable only on small systems; generally, such a task is numerically impossible. In larger systems, the best option is to pick a subset of states and perform the calculation. It is here when Monte Carlo techniques appear, randomly selecting states from a certain distribution p_{μ} [232, 237].

D.2 Simple and importance sampling

The immediate option to deal with the computation of $\langle Q \rangle$ is to select a set of states $\{\mu_1, \mu_2, \dots, \mu_M\}$ with probability p_{μ_i} for all $i = 1, 2, \dots, M$. Consequently, we rewrite Eq. (D.1) as [232, 237]

$$Q_M = \frac{\sum_{i=1}^M Q_{\mu_i} p_{\mu_i}^{-1} e^{-\beta E_{\mu_i}}}{\sum_{i=1}^M e^{-\beta E_{\mu_i}} p_{\mu_i}^{-1}}; \quad (\text{D.2})$$

Eq. (D.2) is called *the estimator* and has the property that in the limit $M \rightarrow \infty$, $Q_M = \langle Q \rangle$. But then, *what kind of states must be selected for an accurate estimate of $\langle Q \rangle$?* In other words, *who p_{μ_i} must be?* The easiest choice would be placing all states with the same probability p_{μ} ,

$$Q_M = \frac{\sum_{i=1}^M Q_{\mu_i} e^{-\beta E_{\mu_i}}}{\sum_{i=1}^M e^{-\beta E_{\mu_i}}}. \quad (\text{D.3})$$

This procedure is known as *simple sampling*. Formally speaking, *simple sampling consists of a subset of individuals (sample) chosen from a larger set (a population) in which each element has the same probability of being picked at any stage during the sampling process, and each subset of k individuals possesses the same probability of being chosen for the sample as any other subset of k individuals* [239].

Despite the advances this procedure could represent in calculating $\langle Q \rangle$, it faces the following problems [232, 237]:

1. Practically, it is only possible to sample a small fraction of the total number of states. Consequently, Q_M stands as a poor guide to evaluating $\langle Q \rangle$.
2. Not all states produce significant contributions to Eq. (D.3). I.e., it is very unlikely that the selected states $\{\mu_1, \dots, \mu_M\}$ coincide with the foremost states of the system.

It would be efficient to select those states in charge of the main contributions, ignore the rest, and perform the sums of Eq. (D.3). Following such a path would provide an excellent estimate of $\langle Q \rangle$ occupying only a small number of states. This procedure of selecting only the important states from an immense number of possibilities is known as *importance sampling* and stands as the essence of thermal MCM [232]. Hence, instead of selecting M states in such a way that every state is as likely to get picked out as every other, states are chosen so that the probability for a particular state μ is $p_{\mu} = Z^{-1} \exp(-\beta E_{\mu})$ [232, 237],

$$Q_M = \frac{\sum_{i=1}^M Q_{\mu_i} (Z^{-1} e^{\beta E_{\mu_i}}) e^{-\beta E_{\mu_i}}}{\sum_{i=1}^M (Z^{-1} e^{\beta E_{\mu_i}}) e^{-\beta E_{\mu_i}}} = \frac{1}{M} \sum_{i=1}^M Q_{\mu_i}. \quad (\text{D.4})$$

The reason behind the selection of p_{μ} is that systems are not sampling all states with equal probability; instead, they sample according to the *Boltzmann probability distribution* [232].

Undoubtedly, Eq. (D.4) turns out to be simpler and works better than Eq. (D.3). Principally, when systems spend the majority of their time in a small number of states (such as the lowest-lying states at low temperatures) since these will be precisely the states that will be chosen more often, and the relative frequency with which they will be picked out will correspond exactly to the amount of time systems would spend in those states. Then, how exactly do we select these states? States with their correct Boltzmann probability. A standard solution is via the *Markov processes*; almost all Monte Carlo schemes rely on Markov processes as the generating engine for the set of states used [232].

D.3 Markov processes

All definitions within this section are taken from Refs. [240–242].

Definition D.1. A *stochastic process* is a collection of random variables $\{X_t | t \in T\}$ on a common probability space, parametrized by the set T known as the *index set* (*parameter set* or *time set*). Each X_t in the collection takes values from the set S called *state space*.

Commonly, we identify the index set as time. Hence, we talk about *past* and *future states* within the stochastic process. If T is countable, the stochastic process is called a *stochastic sequence* or *discrete parameter stochastic process*; if S is countable, the process is named a *discrete state* (space) *process*. If $S \subseteq \mathbb{R}$, the stochastic process is known as a *real-valued process*.

Strictly speaking, a *Markov process* is a stochastic process that satisfies the so-called *Markov property*. This last establishes that for any integer $n \geq 0$, if $t_0 < t_1 < \dots < t_n$ are parameter values, the conditional X_{t_n} probabilities relative to $X_{t_0}, \dots, X_{t_{n-1}}$ are the same as those relative only to $X_{t_{n-1}}$. In other words, a Markov process is a process for which predictions can be made based solely on its present; furthermore, such predictions are as good as the ones that could be made knowing the process's complete history. From this point, we can define the case when the Markov process has either a discrete state space or a discrete index set, known as the Markov chain.

Definition D.2. A *Markov chain* is a stochastic process $\{X_t | t \in T\}$ such that the probability distribution of the future state X_{t+1} depends only on the current state X_t ,

$$P(X_{t+1} = x_{t+1} | X_0 = x_0, \dots, X_t = x_t) = P(X_{t+1} = x_{t+1} | X_t = x_t). \quad (\text{D.5})$$

Definition D.3. Let μ and ν be states over the space of states. The *transition probability* between such states is defined as the probability of generating the state ν given that the process is in the state μ , $P(X_{t+1} = \nu | X_t = \mu)$. Such a probability is denoted as $P(\mu \rightarrow \nu)$ and fulfills

$$i) P(\mu \rightarrow \nu) \leq 1 \quad ii) \sum_{\nu} P(\mu \rightarrow \nu) = 1. \quad (\text{D.6})$$

All transition probabilities should not vary over time and should depend only on the properties of the states μ and ν . These two conditions assure that the probability for the Markov process generating the state ν from state μ is regardless of anything that had happened. We point out that $P(\mu \rightarrow \mu) \neq 0$, that is, there is a finite probability that the Markov process stays in the state μ . Hence, departing from the state μ , the new second state ν is generated; later, such state is used to produce a new third state λ , and so on. Formally speaking [232],

in a Monte Carlo simulation, a Markov process is employed repeatedly to generate a Markov chain of states.

The Markov process is such that when it has run long enough, starting from any state of the system, it will eventually produce a succession of states appearing with probability given by the Boltzmann distribution. This process is known as *coming to equilibrium*. Additionally, for the Markov chain to produce states with the required probability, two more conditions are needed: *ergodicity* and *detailed balance* [232, 237].

D.4 Ergodicity and detailed balance

The request of ergodicity assures us that after some time, the process will have visited all possible states of the system. In other words, ergodicity makes it possible for the Markov process to reach any state within the system from any other state if it runs long enough. To be more accurate, let us place the following example: every state ν in the system appears with some non-zero probability p_ν within the Boltzmann distribution. Now, let us suppose there is a state μ such that ν is inaccessible from μ no matter how long the process runs. If we intend to commence the process from the state μ , we will fail since the probability of finding ν will be zero and not p_ν as we require. *The ergodicity condition establishes that it is allowed to make some transition probabilities zero, but there must be at least one path of non-zero transition probabilities between any two states* [232].

On the other hand, the detailed balance condition guarantees us that the Boltzmann distribution is generated after the system has come to equilibrium rather than any other distribution. For the Markov chain to reach equilibrium, *the*

rate at which the system realizes transitions into and out of any state μ must be equal [232],

$$\sum_{\nu} p_{\mu} P(\mu \rightarrow \nu) = \sum_{\nu} p_{\nu} P(\nu \rightarrow \mu) \Rightarrow p_{\mu} = \sum_{\nu} p_{\nu} P(\nu \rightarrow \mu). \quad (\text{D.7})$$

Eq. (D.7) indicates that for any set of transition probabilities, the probability distribution p_{μ} will be an equilibrium of the dynamics of the Markov process. Sadly, this condition does not guarantee that the probability distribution tends to p_{μ} from any system state if the process runs long enough. We place an additional requirement on the previous probabilities transitions to solve this inconvenience [232, 235, 237, 238],

$$p_{\mu} P(\mu \rightarrow \nu) = p_{\nu} P(\nu \rightarrow \mu). \quad (\text{D.8})$$

Eq. (D.8) is none other than the detailed balance condition, which indicates that on average, the system should go from μ to ν just as often as it goes from ν to μ . The left-hand side of Eq. (D.8) stands as the probability of being in the state μ multiplied by the probability of making a transition to another state ν , i.e., it is the overall rate at which shifts from μ to ν happen. Consequently, the right-hand side corresponds to the overall rate for the reverse transition [232]; the fulfillment of Eq. (D.7) follows from Eq. (D.8).

Hence, selecting the set of transition probabilities to satisfy Eq. (D.8) makes it possible for the Markov chain to tend to any distribution p_{μ} . Since the Boltzmann probability is the desired distribution, the detailed balance condition must make the transition probabilities to satisfy [232, 237]

$$\frac{P(\mu \rightarrow \nu)}{P(\nu \rightarrow \mu)} = \frac{p_{\nu}}{p_{\mu}} = e^{-\beta(E_{\nu} - E_{\mu})}. \quad (\text{D.9})$$

Eqs. (D.8) and (D.9), together with ergodicity, guarantee that the equilibrium distribution within the Markov process will be none other than the Boltzmann distribution. One last refinement is still required to efficiently construct a Monte Carlo calculation; nonetheless, all previous concepts constitute the bases on which all modern equilibrium Monte Carlo calculations are based [232].

D.5 Acceptance ratios

So far, throughout the previous sections, we have explained how to produce an appropriate Monte Carlo calculation, arriving at the requirements of ergodicity and detailed balance. However, finding the required set of transition probabilities can become an arduous task. We could suggest many candidates that create new states ν from previous states μ and yet, not find those with the correct transition probabilities. So, as we mentioned before, a final refinement called *acceptance ratio* or *acceptance probability* is needed [232].

The transition probabilities are divided into two parts [232]:

$$P(\mu \rightarrow \nu) = g(\mu \rightarrow \nu) A(\mu \rightarrow \nu); \quad (\text{D.10})$$

- $g(\mu \rightarrow \nu)$ is called the *selection probability* and indicates the probability that at a given initial state μ , the algorithm generates a new state ν .
- $A(\mu \rightarrow \nu)$ is the acceptance ratio, which establishes that when departing from a state μ and having generated a new state ν , the new state must be accepted and the system modified to it a fraction of the time $A(\mu \rightarrow \nu)$; the rest of the time, the system should remain in μ .

The advantage of Eq. (D.10) is the freedom to set $A(\mu \rightarrow \nu) \in [0, 1]$ and $g(\mu \rightarrow \nu)$ any desired value. Placing $A(\mu \rightarrow \nu) = 0$ indicates the algorithm always stays in the departing state; in other words, $P(\mu \rightarrow \mu) = 1$. Appealing to Eq. (D.10), we rewrite Eq. (D.9)

$$\frac{P(\mu \rightarrow \nu)}{P(\nu \rightarrow \mu)} = \frac{g(\mu \rightarrow \nu) A(\mu \rightarrow \nu)}{g(\nu \rightarrow \mu) A(\nu \rightarrow \mu)}, \quad (\text{D.11})$$

allowing us to choose freely the selection probabilities $g(\mu \rightarrow \nu)$ and $g(\nu \rightarrow \mu)$ since Eq. (D.9) only fixes the ratio; the rate $A(\mu \rightarrow \nu) / A(\nu \rightarrow \mu)$ takes values within the interval $[0, \infty)$. Hence, appealing to all previous discussions, the idea would be to construct an algorithm that creates a state ν starting from a specific state μ with some set of

probabilities $g(\mu \rightarrow \nu)$ and then accept or reject the change with acceptance ratios $A(\mu \rightarrow \nu)$ satisfying Eq. (D.11). Indeed, this procedure will satisfy all previous requirements for the transition probabilities and produce a string of states where, when the system reaches equilibrium, each one will appear with the Boltzmann probability [232].

What would happen if the acceptance ratios were too slow? Should that situation occur, the algorithm would pass most of the time in the state it is in and would not go anywhere. To prevent this from happening, we select the acceptance ratios to be as close to unity as possible. Eq. (D.11) fixes the ratio of the acceptance ratios; then, it is viable to multiply both of them by the same factor, and the equation would still be true. The only condition is that $A(\mu \rightarrow \nu)$ and $A(\nu \rightarrow \mu) \in [0, 1]$. In practice, we set the larger of the acceptance ratios to one and have the other take whatever necessary value to fulfill the detailed balance condition. In this way, we ensure the acceptance ratios to be as large as they can be while still satisfying the relevant conditions and, indeed, that the ratio in one direction will be unity. Thus, movements in that direction will always be accepted [232].

D.6 The Metropolis algorithm

The algorithm was first introduced in 1953 by *Nicholas Metropolis* et al. [243] and later extended in 1970 by *W. K. Hastings* [244]; nowadays, stands as one of the most widely used algorithms in statistical physics [232, 238]. Strictly speaking, the Metropolis algorithm generates a Markov chain on a state space S , such that its stationary distribution corresponds to a target distribution P [235]. The basic architecture of the algorithm lies within the concepts discussed in the previous sections [232]. We select a set of selection probabilities $g(\mu \rightarrow \nu)$ fulfilling the ergodicity condition, a set of acceptance ratios $A(\mu \rightarrow \nu)$ such that Eq. (D.11) satisfies Eq. (D.9), and then, the algorithm accepts or rejects the new state with our chosen acceptance probability.

In the Metropolis algorithm, the selection probabilities $g(\mu \rightarrow \nu)$ for each possible state ν are all chosen to be equal. Consequently, Eq. (D.11) takes the form [232]

$$\frac{P(\mu \rightarrow \nu)}{P(\nu \rightarrow \mu)} = \frac{A(\mu \rightarrow \nu)}{A(\nu \rightarrow \mu)}. \quad (\text{D.12})$$

To maximize the acceptance ratios, and produce a most efficient algorithm, we set the acceptance ratio $\mu \rightarrow \nu$ to be [232, 235, 237, 238]

$$A(\mu \rightarrow \nu) = \min \left\{ 1, \frac{P(\mu \rightarrow \nu)}{P(\nu \rightarrow \mu)} \right\}; \quad (\text{D.13})$$

Eq. (D.13) is known as the *Metropolis function* [237]. In order to sample a probability distribution P , the Metropolis algorithm follows the next scheme [238, 245]:

1. *Select an initial state $\mu \in S$.*
2. *Propose a new state $\nu \in S$ throughout a Markov chain, equalizing the selection probabilities.*
3. *Accept the new state ν with acceptance probability*

$$A(\mu \rightarrow \nu) = \min \left\{ 1, \frac{P(\mu \rightarrow \nu)}{P(\nu \rightarrow \mu)} \right\};$$

should the new state be rejected, add it to the Markov chain.

4. *Return to the second step until the Markov chain is long enough.*

To ensure the Markov chain has reached a steady state (fluctuations around the target density are minimal), we divide the algorithm into two parts. The first part corresponds to the thermalization process, where we let the Markov chain reach its stationary state; the second part, on the other hand, stands as the generator and collector of samples of the desired distribution [245].

Bibliography

- [1] I. Pérez Castillo, E. Guzmán-González, A. T. Ramos Sánchez, and F. L. Metz, “Analytic approach for the number statistics of non-hermitian random matrices,” *Physical Review E*, vol. 103, p. 062108, Jun 2021.
- [2] L. P. Kadanoff, “Scaling and universality in statistical physics,” *Physica A: Statistical Mechanics and its Applications*, vol. 163, pp. 1–14, Feb. 1990.
- [3] R. Baxter, *Exactly Solved Models in Statistical Mechanics*. Elsevier Science, 2016.
- [4] T. Spencer, *Universality, Phase Transitions and Statistical Mechanics*, pp. 839–858. Basel: Birkhäuser Basel, 2010.
- [5] V. Weberruß, *Universality in Statistical Physics and Synergetics: A Comprehensive Approach to Modern Theoretical Physics*. Vieweg+Teubner Verlag, 2013.
- [6] J. Wishart, “The generalised product moment distribution in samples from a normal multivariate population,” *Biometrika*, vol. 20A, pp. 32–52, Jul. 1928.
- [7] E. P. Wigner, “Characteristic vectors of bordered matrices with infinite dimensions,” *Annals of Mathematics*, vol. 62, pp. 548–564, Nov. 1955.
- [8] E. P. Wigner, “Characteristics vectors of bordered matrices with infinite dimensions II,” *Annals of Mathematics*, vol. 65, no. 2, pp. 203–207, 1957.
- [9] P. Forrester, *Log-Gases and Random Matrices (LMS-34)*. London Mathematical Society Monographs, Princeton University Press, 2010.
- [10] G. Akemann, J. Baik, and P. D. Francesco, eds., *The Oxford Handbook of Random Matrix Theory*. Oxford University Press, Aug. 2018.
- [11] M. L. Mehta, *Random Matrices*. Pure and Applied Mathematics 142, Academic Press, Elsevier, 2004.
- [12] M. Mehta, *Random Matrices and the Statistical Theory of Energy Levels* D M.L. Mehta. Academic Press, 1967.
- [13] F. Luo, J. Zhong, Y. Yang, R. H. Scheuermann, and J. Zhou, “Application of random matrix theory to biological networks,” *Physics Letters A*, vol. 357, pp. 420–423, May 2006.
- [14] A. Amir, N. Hatano, and D. R. Nelson, “Non-hermitian localization in biological networks,” *Physical Review E*, vol. 93, p. 042310, Apr. 2016.
- [15] Z. Fang, Y. Liang, and Z. Bai, *Spectral Theory Of Large Dimensional Random Matrices And Its Applications To Wireless Communications And Finance Statistics: Random Matrix Theory And Its Applications*. World Scientific Publishing Company, 2014.
- [16] J. P. Bouchaud and M. Potters, “Financial Applications of Random Matrix Theory: a short review,” *arXiv e-prints*, p. arXiv:0910.1205, Oct. 2009.
- [17] T. Guhr, A. Müller–Groeling, and H. A. Weidenmüller, “Random-matrix theories in quantum physics: common concepts,” *Physics Reports*, vol. 299, pp. 189–425, Jun. 1998.

- [18] V. Kota, *Embedded Random Matrix Ensembles in Quantum Physics*. Lecture Notes in Physics, Springer International Publishing, 2014.
- [19] O. Bohigas, M. J. Giannoni, and C. Schmit, “Characterization of chaotic quantum spectra and universality of level fluctuation laws,” *Physical Review Letters*, vol. 52, pp. 1–4, Jan. 1984.
- [20] P. Bourgade and J. P. Keating, “Quantum chaos, random matrix theory, and the riemann ζ -function,” in *Chaos*, pp. 125–168, Springer, 2013.
- [21] L. Mersini-Houghton, “Can we predict Λ for the non-SUSY sector of the landscape?,” *Classical and Quantum Gravity*, vol. 22, pp. 3481–3490, Aug. 2005.
- [22] A. Aazami and R. Easther, “Cosmology from random multifield potentials,” *Journal of Cosmology and Astroparticle Physics*, vol. 2006, pp. 013–013, Mar. 2006.
- [23] T. C. Bachlechner, “On Gaussian random supergravity,” *Journal of High Energy Physics*, vol. 2014, Apr. 2014.
- [24] E. P. Wigner, “On the distribution of the roots of certain symmetric matrices,” *Annals of Mathematics*, vol. 67, pp. 325–327, Mar. 1958.
- [25] J. Ginibre, “Statistical ensembles of complex, quaternion, and real matrices,” *Journal of Mathematical Physics*, vol. 6, pp. 440–449, Mar. 1965.
- [26] V. L. Girko, “Circular law,” *Teor. Veroyatnost. i. Primenen*, vol. 29, no. 4, pp. 669–679, 1984.
- [27] V. L. Girko, “Circular law,” *Theory of Probability & Its Applications*, vol. 29, pp. 694–706, Jan. 1985.
- [28] V. L. Girko, *Theory of Random Determinants*. Springer Netherlands, 1990.
- [29] T. Tao, V. Vu, and M. Krishnapur, “Random matrices: Universality of ESDs and the circular law,” *The Annals of Probability*, vol. 38, pp. 2023 – 2065, Sep. 2010.
- [30] T. Tao, *Topics in Random Matrix Theory*. Graduate studies in mathematics, American Mathematical Society, 2012.
- [31] F. L. Metz, I. Neri, and T. Rogers, “Spectral theory of sparse non-hermitian random matrices,” *Journal of Physics A: Mathematical and Theoretical*, vol. 52, p. 434003, Oct. 2019.
- [32] S. N. Evangelou and E. N. Economou, “Spectral density singularities, level statistics, and localization in a sparse random matrix ensemble,” *Physical Review Letters*, vol. 68, pp. 361–364, Jan. 1992.
- [33] R. B. Griffiths, “Nonanalytic behavior above the critical point in a random ising ferromagnet,” *Physical Review Letters*, vol. 23, pp. 17–19, Jul. 1969.
- [34] S. Bornholdt and H. Schuster, *Handbook of Graphs and Networks: From the Genome to the Internet*. Wiley, 2006.
- [35] M. Newman, *Networks: An Introduction*. OUP Oxford, 2010.
- [36] G. J. Rodgers and A. J. Bray, “Density of states of a sparse random matrix,” *Physical Review B*, vol. 37, pp. 3557–3562, Mar. 1988.
- [37] G. J. Rodgers and C. D. Dominicis, “Density of states of sparse random matrices,” *Journal of Physics A: Mathematical and General*, vol. 23, pp. 1567–1573, May. 1990.
- [38] Y. V. Fyodorov and A. D. Mirlin, “On the density of states of sparse random matrices,” *Journal of Physics A: Mathematical and General*, vol. 24, pp. 2219–2223, May. 1991.
- [39] A. D. Mirlin and Y. V. Fyodorov, “Universality of level correlation function of sparse random matrices,” *Journal of Physics A: Mathematical and General*, vol. 24, pp. 2273–2286, May. 1991.
- [40] A. J. Bray and G. J. Rodgers, “Diffusion in a sparsely connected space: A model for glassy relaxation,” *Physical Review B*, vol. 38, pp. 11461–11470, Dec. 1988.

- [41] G. Biroli and R. Monasson, “A single defect approximation for localized states on random lattices,” *Journal of Physics A: Mathematical and General*, vol. 32, pp. L255–L261, Jan. 1999.
- [42] G. Semerjian and L. F. Cugliandolo, “Sparse random matrices: the eigenvalue spectrum revisited,” *Journal of Physics A: Mathematical and General*, vol. 35, pp. 4837–4851, May 2002.
- [43] T. Nagao and T. Tanaka, “Spectral density of sparse sample covariance matrices,” *Journal of Physics A: Mathematical and Theoretical*, vol. 40, pp. 4973–4987, Apr. 2007.
- [44] T. Rogers and I. Pérez Castillo, “Cavity approach to the spectral density of non-hermitian sparse matrices,” *Physical Review E*, vol. 79, p. 012101, Jan. 2009.
- [45] I. Pérez Castillo and F. L. Metz, “Theory for the conditioned spectral density of noninvariant random matrices,” *Physical Review E*, vol. 98, p. 020102, Aug. 2018.
- [46] F. Schwabl and W. Brewer, *Statistical Mechanics*. Advanced Texts in Physics, Springer Berlin Heidelberg, 2006.
- [47] B. McCoy, *Advanced Statistical Mechanics*. Advanced Statistical Methods, OUP Oxford, 2010.
- [48] P. Deift, “Universality for mathematical and physical systems,” *arXiv e-prints*, pp. math-ph/0603038, Mar. 2006.
- [49] S. Ross, *A First Course in Probability*. Pearson India Education Services Pvt. Limited, 2014.
- [50] B. Arnold, N. Balakrishnan, and H. Nagaraja, *A First Course in Order Statistics*. Classics in Applied Mathematics, Society for Industrial and Applied Mathematics, 2008.
- [51] L. de Haan and A. Ferreira, *Extreme Value Theory*. Springer New York, 2006.
- [52] S. N. Majumdar, A. Pal, and G. Schehr, “Extreme value statistics of correlated random variables: A pedagogical review,” *Physics Reports*, vol. 840, pp. 1–32, Jan. 2020.
- [53] B. Gnedenko, “Sur la distribution limite du terme maximum d’une serie aleatoire,” *The Annals of Mathematics*, vol. 44, p. 423, Jul. 1943.
- [54] R. A. Fisher and L. H. C. Tippett, “Limiting forms of the frequency distribution of the largest or smallest member of a sample,” *Mathematical Proceedings of the Cambridge Philosophical Society*, vol. 24, pp. 180–190, Apr. 1928.
- [55] E. Gumbel, *Statistics of Extremes*. Dover books on mathematics, Dover Publications, 2004.
- [56] J.-P. Bouchaud and M. Mézard, “Universality classes for extreme-value statistics,” *Journal of Physics A: Mathematical and General*, vol. 30, pp. 7997–8015, Dec. 1997.
- [57] D. S. Dean and S. N. Majumdar, “Extreme value statistics of eigenvalues of Gaussian random matrices,” *Physical Review E*, vol. 77, p. 041108, Apr. 2008.
- [58] Y. V. Fyodorov and J.-P. Bouchaud, “Freezing and extreme-value statistics in a random energy model with logarithmically correlated potential,” *Journal of Physics A: Mathematical and Theoretical*, vol. 41, p. 372001, Aug. 2008.
- [59] B. C. Arnold, N. Balakrishnan, and H. N. Nagaraja, *A First Course in Order Statistics*. Society for Industrial and Applied Mathematics, Jan. 2008.
- [60] F. Haake, S. Gnutzmann, and M. Kuś, *Quantum Signatures of Chaos*. Springer Series in Synergetics, Springer International Publishing, 2019.
- [61] S. N. Majumdar and G. Schehr, “Large deviations,” *arXiv e-prints*, p. arXiv:1711.07571, Nov. 2017.
- [62] R. Kissell and J. Poserina, “Chapter 4 - advanced math and statistics,” in *Optimal Sports Math, Statistics, and Fantasy* (R. Kissell and J. Poserina, eds.), pp. 103–135, Academic Press, 2017.

- [63] K. Fokianos, “Chapter 12 - count time series models,” in *Time Series Analysis: Methods and Applications* (T. Subba Rao, S. Subba Rao, and C. Rao, eds.), vol. 30 of *Handbook of Statistics*, pp. 315–347, Elsevier, 2012.
- [64] A. Cameron and P. Trivedi, *Regression Analysis of Count Data*. Econometric Society Monographs, Cambridge University Press, 1998.
- [65] L. Hodges, “Chapter 2 - common univariate distributions,” in *Statistical Methods for Physical Science* (J. L. Stanford and S. B. Vardeman, eds.), vol. 28 of *Methods in Experimental Physics*, pp. 35–61, Academic Press, 1994.
- [66] R. Riffenburgh, “Chapter 6 - finding probabilities,” in *Statistics in Medicine (Third Edition)* (R. Riffenburgh, ed.), pp. 117–136, San Diego: Academic Press, third edition ed., 2012.
- [67] J. I. Hoffman, “Chapter 18 - the poisson distribution,” in *Biostatistics for Medical and Biomedical Practitioners* (J. I. Hoffman, ed.), pp. 259–278, Academic Press, 2015.
- [68] F. H. Stephenson, “Chapter 3 - cell growth,” in *Calculations for Molecular Biology and Biotechnology (Third Edition)* (F. H. Stephenson, ed.), pp. 43–79, Boston: Academic Press, third edition ed., 2016.
- [69] H. Cramér and H. Touchette, “On a new limit theorem in probability theory (Translation of ‘Sur un nouveau théorème-limite de la théorie des probabilités’),” *arXiv e-prints*, p. arXiv:1802.05988, Feb. 2018.
- [70] M. D. Donsker and S. R. S. Varadhan, “Asymptotic evaluation of certain Markov process expectations for large time, I,” *Communications on Pure and Applied Mathematics*, vol. 28, pp. 1–47, Jan. 1975.
- [71] M. D. Donsker and S. R. S. Varadhan, “Asymptotic evaluation of certain Markov process expectations for large time, II,” *Communications on Pure and Applied Mathematics*, vol. 28, pp. 279–301, Mar. 1975.
- [72] M. D. Donsker and S. R. S. Varadhan, “Asymptotic evaluation of certain Markov process expectations for large time—III,” *Communications on Pure and Applied Mathematics*, vol. 29, pp. 389–461, Jul. 1976.
- [73] M. D. Donsker and S. R. S. Varadhan, “Asymptotic evaluation of certain Markov process expectations for large time. IV,” *Communications on Pure and Applied Mathematics*, vol. 36, pp. 183–212, Mar. 1983.
- [74] M. I. Freidlin and A. D. Wentzell, *Random Perturbations of Dynamical Systems*. Springer Berlin Heidelberg, 2012.
- [75] S. R. S. Varadhan, *Large Deviations and Applications*. Society for Industrial and Applied Mathematics, Jan. 1984.
- [76] F. den Hollander, *Large Deviations*. American Mathematical Society, Jun. 2008.
- [77] A. Dembo and O. Zeitouni, *Large Deviations Techniques and Applications*. Stochastic Modelling and Applied Probability, Springer Berlin Heidelberg, 2009.
- [78] H. Touchette, “The large deviation approach to statistical mechanics,” *Physics Reports*, vol. 478, pp. 1–69, Jul. 2009.
- [79] A. Vulpiani, F. Cecconi, M. Cencini, A. Puglisi, and D. Vergni, eds., *Large Deviations in Physics*. Springer Berlin Heidelberg, 2014.
- [80] R. S. Ellis, “The theory of large deviations: from Boltzmann’s 1877 calculation to equilibrium macrostates in 2d turbulence,” *Physica D: Nonlinear Phenomena*, vol. 133, pp. 106–136, Sep. 1999.
- [81] P. Vivo, “Large deviations of the maximum of independent and identically distributed random variables,” *European Journal of Physics*, vol. 36, p. 055037, Aug. 2015.
- [82] J. Gärtner, “On large deviations from the invariant measure,” *Theory of Probability & Its Applications*, vol. 22, no. 1, pp. 24–39, 1977.
- [83] R. S. Ellis, “Large Deviations for a General Class of Random Vectors,” *The Annals of Probability*, vol. 12, pp. 1 – 12, Feb. 1984.

- [84] H. Touchette, “Legendre-fenchel transforms in a nutshell,” <http://www.maths.qmul.ac.uk/~ht/archive/lfth2.pdf>, 2005.
- [85] G. Hardy, K. M. R. Collection, J. Littlewood, G. Pólya, G. Pólya, and D. Littlewood, *Inequalities*. Cambridge Mathematical Library, Cambridge University Press, 1952.
- [86] J. Van Tiel, *Convex Analysis: An Introductory Text*. Wiley, 1984.
- [87] R. Rockafellar, *Convex Analysis: (PMS-28)*. Princeton Landmarks in Mathematics and Physics, Princeton University Press, 2015.
- [88] R. S. Ellis, “An overview of the theory of large deviations and applications to statistical mechanics,” *Scandinavian Actuarial Journal*, vol. 1995, no. 1, pp. 97–142, 1995.
- [89] A. Barabási and M. Pósfai, *Network Science*. Cambridge University Press, 2016.
- [90] R. Wilson, *Introduction to Graph Theory*. Longman, 1996.
- [91] B. Bollobas, *Graph Theory: An Introductory Course*. Graduate Texts in Mathematics, Springer New York, 2012.
- [92] B. Bollobas, *Modern Graph Theory*. Graduate Texts in Mathematics, Springer New York, 2013.
- [93] R. Solomonoff and A. Rapoport, “Connectivity of random nets,” *The Bulletin of Mathematical Biophysics*, vol. 13, pp. 107–117, Jun. 1951.
- [94] P. Erdős and A. Rényi, “On random graph,” *Publicationes Mathematicae*, vol. 6, pp. 290–297, 1959.
- [95] P. Erdős and A. Rényi, “On the evolution of random graphs,” *Publications of the Mathematical Institute of the Hungarian Academy of Sciences*, vol. 5, no. 1, pp. 17–60, 1960.
- [96] M. Mezard and A. Montanari, *Information, Physics, and Computation*. USA: Oxford University Press, Inc., 2009.
- [97] M. Sonderegger, “Applications of graph theory to an english rhyming corpus,” *Computer Speech & Language*, vol. 25, pp. 655 – 678, Jul. 2011.
- [98] O. Mason and M. Verwoerd, “Graph theory and networks in biology,” *IET Systems Biology*, vol. 1, pp. 89–119, Mar. 2007.
- [99] J. Scott, “Social network analysis,” *Sociology*, vol. 22, pp. 109–127, Feb. 1988.
- [100] A. Blum, J. Hopcroft, and R. Kannan, *Foundations of Data Science*. Cambridge University Press, 2020.
- [101] A. Barrat, M. Barthélemy, and A. Vespignani, *Dynamical Processes on Complex Networks*. Cambridge University Press, 2012.
- [102] C. Li, N. Tang, and J. Wang, “Directed graphs of dna sequences and their numerical characterization,” *Journal of Theoretical Biology*, vol. 241, pp. 173–177, Jul. 2006.
- [103] V. N. S. Kavya, K. Tayal, R. Srinivasan, and N. Sivadasan, “Sequence alignment on directed graphs,” *Journal of Computational Biology*, vol. 26, pp. 53–67, Jan. 2019.
- [104] W. Huber, V. J. Carey, L. Long, S. Falcon, and R. Gentleman, “Graphs in molecular biology,” *BMC Bioinformatics*, vol. 8, Sep. 2007.
- [105] D. Cvetkovic, D. Cvetković, M. Doob, and H. Sachs, *Spectra of Graphs: Theory and Application*. Pure and applied mathematics : a series of monographs and textbooks, Academic Press, 1980.
- [106] A. Brouwer and W. Haemers, *Spectra of Graphs*. Universitext, Springer New York, 2011.
- [107] B. Bollobás, “Degree sequences of random graphs,” *Discrete Mathematics*, vol. 33, no. 1, pp. 1–19, 1981.
- [108] B. Gnedenko, *Theory of Probability*. CRC Press, 2018.

- [109] S. N. Evangelou, “Quantum percolation and the anderson transition in dilute systems,” *Physical Rev B*, vol. 27, pp. 1397–1400, Jan. 1983.
- [110] M. Bauer and O. Golinelli, “Random incidence matrices: Moments of the spectral density,” *Journal of Statistical Physics*, vol. 103, pp. 301–337, Apr. 2001.
- [111] A. D. Mirlin, “Statistics of energy levels and eigenfunctions in disordered systems,” *Physics Reports*, vol. 326, pp. 259 – 382, Mar. 2000.
- [112] O. Golinelli, “Statistics of delta peaks in the spectral density of large random trees,” *arXiv e-prints*, pp. cond-mat/0301437, Jan. 2003.
- [113] F. L. Metz and I. Pérez Castillo, “Condensation of degrees emerging through a first-order phase transition in classical random graphs,” *Physical Review E*, vol. 100, p. 012305, Jul. 2019.
- [114] P. F. Committee, *The Logic of Personal Knowledge: Essays Presented to Michael Polanyi on His Seventieth Birthday, 11th March, 1961*. Routledge Library Editions: Epistemology, Routledge, 2016.
- [115] P. Deift and D. Gioev, *Random Matrix Theory: Invariant Ensembles and Universality*. Courant Lecture Notes, American Mathematical Soc., 2009.
- [116] C. Porter, *Statistical Theories of Spectra: Fluctuations; a Collection of Reprints and Original Papers, with an Introductory Review*. Perspectives in Physics, Academic Press, 1965.
- [117] L. P. Gor’kov and G. M. Éliashberg, “Minute metallic particles in an electromagnetic field,” *Zh. Eksp. Theor. Fiz.* 48 (1965) 1407 [*Soviet Physics-JETP* 21 (1965) 940], vol. 21, pp. 940–947, Nov. 1965.
- [118] K. Efetov, “Supersymmetry and theory of disordered metals,” *Advances in Physics*, vol. 32, pp. 53–127, Jan. 1983.
- [119] T. A. Brody, J. Flores, J. B. French, P. A. Mello, A. Pandey, and S. S. M. Wong, “Random-matrix physics: spectrum and strength fluctuations,” *Reviews of Modern Physics*, vol. 53, pp. 385–479, Jul. 1981.
- [120] D. Wales, *Energy Landscapes: Applications to Clusters, Biomolecules and Glasses*. Cambridge Molecular Science, Cambridge University Press, 2004.
- [121] J. Kurchan and L. Laloux, “Phase space geometry and slow dynamics,” *Journal of Physics A: Mathematical and General*, vol. 29, pp. 1929–1948, May 1996.
- [122] T. S. Grigera, A. Cavagna, I. Giardina, and G. Parisi, “Geometric approach to the dynamic glass transition,” *Physical Review Letters*, vol. 88, Jan. 2002.
- [123] A. Cavagna, J. P. Garrahan, and I. Giardina, “Index distribution of random matrices with an application to disordered systems,” *Physical Review B*, vol. 61, pp. 3960–3970, Feb. 2000.
- [124] G. Biroli, J.-P. Bouchaud, and M. Potters, “Extreme value problems in random matrix theory and other disordered systems,” *Journal of Statistical Mechanics: Theory and Experiment*, vol. 2007, pp. P07019–P07019, Jul. 2007.
- [125] W. Bietenholz, S. Shcheredin, and K. Jansen, “Spectral properties of the overlap dirac operator in QCD,” *Journal of High Energy Physics*, vol. 2003, pp. 01–015, Jul. 2003.
- [126] P. J. Forrester, N. C. Snaith, and J. J. M. Verbaarschot, “Developments in random matrix theory,” *Journal of Physics A: Mathematical and General*, vol. 36, p. R1, Mar. 2003.
- [127] L. Erdős, S. Péché, J. A. Ramírez, B. Schlein, and H.-T. Yau, “Bulk universality for Wigner matrices,” *Communications on Pure and Applied Mathematics*, vol. 63, pp. 895–925, Feb. 2010.
- [128] L. Erdős, J. Ramírez, B. Schlein, T. Tao, van Vu, and H.-T. Yau, “Bulk universality for Wigner hermitian matrices with subexponential decay,” *Mathematical Research Letters*, vol. 17, pp. 667–674, Jan. 2010.
- [129] L. Erdős, “Universality of Wigner random matrices: a survey of recent results,” *Russian Mathematical Surveys*, vol. 66, pp. 507–626, Jun. 2011.

- [130] T. Tao and V. Vu, “Random matrices: Universality of local eigenvalue statistics,” *Acta Mathematica*, vol. 206, no. 1, pp. 127 – 204, 2011.
- [131] T. Tao and V. Vu, “Random matrices: Universality of local spectral statistics of non-Hermitian matrices,” *The Annals of Probability*, vol. 43, pp. 782 – 874, Mar. 2015.
- [132] M. A. Stephanov, J. J. M. Verbaarschot, and T. Wettig, “Random Matrices,” *arXiv e-prints*, pp. hep-ph/0509286, Sep. 2005.
- [133] F. J. Dyson, “The threefold way. algebraic structure of symmetry groups and ensembles in quantum mechanics,” *Journal of Mathematical Physics*, vol. 3, pp. 1199–1215, Nov. 1962.
- [134] F. J. Dyson, “Statistical theory of the energy levels of complex systems. I,” *Journal of Mathematical Physics*, vol. 3, pp. 140–156, Jan.-Feb. 1962.
- [135] F. J. Dyson, “Statistical theory of the energy levels of complex systems. II,” *Journal of Mathematical Physics*, vol. 3, pp. 157–165, Jan.-Feb. 1962.
- [136] F. J. Dyson, “Statistical theory of the energy levels of complex systems. III,” *Journal of Mathematical Physics*, vol. 3, pp. 166–175, Jan.-Feb. 1962.
- [137] F. J. Dyson and M. L. Mehta, “Statistical theory of the energy levels of complex systems. IV,” *Journal of Mathematical Physics*, vol. 4, pp. 701–712, May 1963.
- [138] R. Allez, J.-P. Bouchaud, S. N. Majumdar, and P. Vivo, “Invariant β -wishart ensembles, crossover densities and asymptotic corrections to the marčenko–pastur law,” *Journal of Physics A: Mathematical and Theoretical*, vol. 46, p. 015001, Dec. 2012.
- [139] N. Lehmann and H.-J. Sommers, “Eigenvalue statistics of random real matrices,” *Physical Review Letters*, vol. 67, pp. 941–944, Aug. 1991.
- [140] A. Edelman, “The probability that a random real gaussian matrix has real eigenvalues, related distributions, and the circular law,” *Journal of Multivariate Analysis*, vol. 60, pp. 203–232, Feb. 1997.
- [141] H. J. Sommers, A. Crisanti, H. Sompolinsky, and Y. Stein, “Spectrum of large random asymmetric matrices,” *Physical Review Letters*, vol. 60, pp. 1895–1898, May 1988.
- [142] C. Bordenave and D. Chafaï, “Around the circular law,” *Probability Surveys*, vol. 9, pp. 1 – 89, Jan. 2012.
- [143] M. Mezard, G. Parisi, and M. Virasoro, *Spin Glass Theory And Beyond: An Introduction To The Replica Method And Its Applications*. World Scientific Lecture Notes In Physics, World Scientific Publishing Company, 1987.
- [144] E. Ising, “Beitrag zur theorie des ferromagnetismus,” *Zeitschrift für Physik*, vol. 31, pp. 253–258, Feb. 1925.
- [145] D. Stein and C. Newman, *Spin Glasses and Complexity*. Primers in Complex Systems, Princeton University Press, 2013.
- [146] R. Solé, *Phase Transitions*. Primers in Complex Systems, Princeton University Press, 2011.
- [147] S. Roy and S. M. Bhattacharjee, “Is small-world network disordered?,” *Physics Letters A*, vol. 352, pp. 13–16, Mar. 2006.
- [148] E. J. Torres-Herrera, I. Vallejo-Fabila, A. J. Martínez-Mendoza, and L. F. Santos, “Self-averaging in many-body quantum systems out of equilibrium: Time dependence of distributions,” *Physical Review E*, vol. 102, p. 062126, Dec. 2020.
- [149] J. L. van Hemmen and R. G. Palmer, “The replica method and a solvable spin glass model,” *Journal of Physics A: Mathematical and General*, vol. 12, pp. 563–580, Apr. 1979.
- [150] M. Potters and J. Bouchaud, *A First Course in Random Matrix Theory: for Physicists, Engineers and Data Scientists*. Cambridge University Press, 2020.

- [151] S. F. Edwards and R. C. Jones, “The eigenvalue spectrum of a large symmetric random matrix,” *Journal of Physics A: Mathematical and General*, vol. 9, pp. 1595–1603, Oct. 1976.
- [152] P. Vivo, “Index of a matrix, complex logarithms, and multidimensional fresnel integrals,” *Journal of Physics A: Mathematical and Theoretical*, vol. 54, p. 025002, Dec. 2020.
- [153] E. Kanzieper, “Replica Approach in Random Matrix Theory,” *arXiv e-prints*, p. arXiv:0909.3198, Sep. 2009.
- [154] E. Kanzieper, “Random matrices and the replica method,” *Nuclear Physics B*, vol. 596, pp. 548–566, Mar. 2001.
- [155] M. Reed and B. Simon, *I: Functional Analysis. Methods of Modern Mathematical Physics*, Elsevier Science, 1981.
- [156] R. Bartle, *The Elements of Integration and Lebesgue Measure*. Wiley Classics Library, Wiley, 2014.
- [157] J. Julve, R. Cepedello, and F. J. de Urries, “The complex Dirac Delta, Plemelj formula, and integral representations,” *arXiv e-prints*, p. arXiv:1603.05530, Mar. 2016.
- [158] J. Feinberg and A. Zee, “Non-hermitian random matrix theory: Method of hermitian reduction,” *Nuclear Physics B*, vol. 504, pp. 579–608, Jul. 1997.
- [159] S. Pilati and P. Pieri, “Simulating disordered quantum ising chains via dense and sparse restricted boltzmann machines,” *Physical Review E*, vol. 101, p. 063308, Jun. 2020.
- [160] L. Viana and A. J. Bray, “Phase diagrams for dilute spin glasses,” *Journal of Physics C: Solid State Physics*, vol. 18, pp. 3037–3051, May. 1985.
- [161] I. Kanter and H. Sompolinsky, “Mean-field theory of spin-glasses with finite coordination number,” *Physical Review Letters*, vol. 58, pp. 164–167, Jan. 1987.
- [162] M. Mézard and G. Parisi, “Mean-field theory of randomly frustrated systems with finite connectivity,” *Europhysics Letters (EPL)*, vol. 3, pp. 1067–1074, May. 1987.
- [163] Mézard, M. and Parisi, G., “Replicas and optimization,” *Journal de Physique Lettres*, vol. 46, pp. 771–778, Sep. 1985.
- [164] J. R. Banavar, D. Sherrington, and N. Sourlas, “Graph bipartitioning and statistical mechanics,” *Journal of Physics A: Mathematical and General*, vol. 20, pp. L1–L8, Jan. 1987.
- [165] D. Sherrington and K. Y. M. Wong, “Graph bipartitioning and the bethe spin glass,” *Journal of Physics A: Mathematical and General*, vol. 20, pp. L785–L791, Aug. 1987.
- [166] F. Haake, S. Gnutzmann, and M. Kuś, *Quantum Signatures of Chaos*. Springer Series in Synergetics, Springer International Publishing, 2019.
- [167] O. Khorunzhiy, W. Kirsch, and P. Müller, “Lifshitz tails for spectra of Erdős–Rényi random graphs,” *The Annals of Applied Probability*, vol. 16, pp. 295 – 309, Feb. 2006.
- [168] J. Friedman, “A proof of Alon’s second eigenvalue conjecture and related problems,” *arXiv e-prints*, p. cs/0405020, May. 2004.
- [169] C. Bordenave, “A new proof of Friedman’s second eigenvalue Theorem and its extension to random lifts,” *arXiv e-prints*, p. arXiv:1502.04482, Feb. 2015.
- [170] R. Albert and A.-L. Barabási, “Statistical mechanics of complex networks,” *Reviews of Modern Physics*, vol. 74, pp. 47–97, Jan. 2002.
- [171] S. N. Dorogovtsev, A. V. Goltsev, J. F. F. Mendes, and A. N. Samukhin, “Spectra of complex networks,” *Physical Review E*, vol. 68, p. 046109, Oct. 2003.
- [172] R. Kühn, J. van Mourik, M. Weigt, and A. Zippelius, “Finitely coordinated models for low-temperature phases of amorphous systems,” *Journal of Physics A: Mathematical and Theoretical*, vol. 40, pp. 9227–9252, Jul. 2007.

- [173] T. Rogers, I. Pérez Castillo, R. Kühn, and K. Takeda, “Cavity approach to the spectral density of sparse symmetric random matrices,” *Physical Review E*, vol. 78, p. 031116, Sep. 2008.
- [174] R. Kühn, “Spectra of sparse random matrices,” *Journal of Physics A: Mathematical and Theoretical*, vol. 41, p. 295002, Jun. 2008.
- [175] V. A. Marčenko and L. A. Pastur, “Distribution of eigenvalues for some sets of random matrices,” *Mathematics of the USSR-Sbornik*, vol. 1, p. 457, Apr. 1967.
- [176] J. Feinberg and A. Zee, “Non-gaussian non-hermitian random matrix theory: Phase transition and addition formalism,” *Nuclear Physics B*, vol. 501, pp. 643–669, Jun. 1997.
- [177] R. Marino, S. N. Majumdar, G. Schehr, and P. Vivo, “Phase transitions and edge scaling of number variance in gaussian random matrices,” *Physical Review Letters*, vol. 112, p. 254101, Jun. 2014.
- [178] I. Pérez Castillo, “Spectral order statistics of gaussian random matrices: Large deviations for trapped fermions and associated phase transitions,” *Physical Review E*, vol. 90, p. 040102, Oct. 2014.
- [179] R. Marino, S. N. Majumdar, G. Schehr, and P. Vivo, “Number statistics for β -ensembles of random matrices: Applications to trapped fermions at zero temperature,” *Physical Review E*, vol. 94, p. 032115, Sep. 2016.
- [180] B. Lacroix-A-Chez-Toine, J. A. M. Garzón, C. S. H. Calva, I. Pérez Castillo, A. Kundu, S. N. Majumdar, and G. Schehr, “Intermediate deviation regime for the full eigenvalue statistics in the complex ginibre ensemble,” *Physical Review E*, vol. 100, p. 012137, Jul. 2019.
- [181] B. Lacroix-A-Chez-Toine, S. N. Majumdar, and G. Schehr, “Rotating trapped fermions in two dimensions and the complex ginibre ensemble: Exact results for the entanglement entropy and number variance,” *Physical Review A*, vol. 99, p. 021602, Feb. 2019.
- [182] F. L. Metz and I. P. Castillo, “Level compressibility for the anderson model on regular random graphs and the eigenvalue statistics in the extended phase,” *Physical Review B*, vol. 96, p. 064202, Aug. 2017.
- [183] K. S. Tikhonov and A. D. Mirlin, “Statistics of eigenstates near the localization transition on random regular graphs,” *Physical Review B*, vol. 99, p. 024202, Jan. 2019.
- [184] Y. V. Fyodorov and B. A. Khoruzhenko, “Nonlinear analogue of the May-Wigner instability transition,” *Proceedings of the National Academy of Sciences*, vol. 113, pp. 6827–6832, Jun. 2016.
- [185] R. E. McMurtrie, “Determinants of stability of large randomly connected systems,” *Journal of Theoretical Biology*, vol. 50, pp. 1–11, Mar. 1975.
- [186] S. Allesina and S. Tang, “Stability criteria for complex ecosystems,” *Nature*, vol. 483, pp. 205–208, Feb. 2012.
- [187] S. N. Majumdar, C. Nadal, A. Scardicchio, and P. Vivo, “Index distribution of Gaussian random matrices,” *Physical Review Letters*, vol. 103, p. 220603, Nov. 2009.
- [188] S. N. Armstrong, S. Serfaty, and O. Zeitouni, “Remarks on a constrained optimization problem for the Ginibre ensemble,” *arXiv e-prints*, p. arXiv:1304.1964, Apr. 2013.
- [189] R. Allez, J. Touboul, and G. Wainrib, “Index distribution of the ginibre ensemble,” *Journal of Physics A: Mathematical and Theoretical*, vol. 47, p. 042001, Jan. 2014.
- [190] M. Krishnapur and B. Virág, “The Ginibre Ensemble and Gaussian Analytic Functions,” *International Mathematics Research Notices*, vol. 2014, pp. 1441–1464, Nov. 2012.
- [191] S. Ghosh and A. Nishry, “Gaussian complex zeros on the hole event: The emergence of a forbidden region,” *Communications on Pure and Applied Mathematics*, vol. 72, pp. 3–62, Nov. 2019.
- [192] S. Ghosh and M. Krishnapur, “Rigidity Hierarchy in Random Point Fields: Random Polynomials and Determinantal Processes,” *Communications in Mathematical Physics*, vol. 388, pp. 1205–1234, Dec. 2021.
- [193] K. Rajan and L. F. Abbott, “Eigenvalue spectra of random matrices for neural networks,” *Physical Review Letters*, vol. 97, p. 188104, Nov. 2006.

- [194] H. Sompolinsky, A. Crisanti, and H. J. Sommers, “Chaos in random neural networks,” *Physical Review Letters*, vol. 61, pp. 259–262, Jul. 1988.
- [195] F. Schuessler, A. Dubreuil, F. Mastrogiuseppe, S. Ostojic, and O. Barak, “Dynamics of random recurrent networks with correlated low-rank structure,” *Physical Review Research*, vol. 2, p. 013111, Feb. 2020.
- [196] G. Wainrib and J. Touboul, “Topological and dynamical complexity of random neural networks,” *Physical Review Letters*, vol. 110, p. 118101, Mar. 2013.
- [197] G. Hermann and J. Touboul, “Heterogeneous connections induce oscillations in large-scale networks,” *Physical Review Letters*, vol. 109, p. 018702, Jul. 2012.
- [198] J. Als-Nielsen and R. J. Birgeneau, “Mean field theory, the ginzburg criterion, and marginal dimensionality of phase transitions,” *American Journal of Physics*, vol. 45, pp. 554–560, Jun. 1977.
- [199] D. J. Amit, “The ginzburg criterion-rationalized,” *Journal of Physics C: Solid State Physics*, vol. 7, p. 3369, Sep. 1974.
- [200] N. Hatano and D. R. Nelson, “Localization transitions in non-hermitian quantum mechanics,” *Phys. Rev. Lett.*, vol. 77, pp. 570–573, Jul. 1996.
- [201] A. F. Tzortzakakis, K. G. Makris, and E. N. Economou, “Non-hermitian disorder in two-dimensional optical lattices,” *Physical Review B*, vol. 101, p. 014202, Jan. 2020.
- [202] Y. Huang and B. I. Shklovskii, “Spectral rigidity of non-hermitian symmetric random matrices near the anderson transition,” *Physical Review B*, vol. 102, p. 064212, Aug. 2020.
- [203] R. B. Griffiths, “A proof that the free energy of a spin system is extensive,” *Journal of Mathematical Physics*, vol. 5, pp. 1215–1222, Sep. 1964.
- [204] J. L. López and P. J. Pagola, “An explicit formula for the coefficients of the saddle point method,” *Constructive Approximation*, vol. 33, pp. 145–162, Feb. 2010.
- [205] C. Rainone, *Metastable Glassy States Under External Perturbations: Monitoring the Effects of Compression and Shear-strain*. Springer Theses, Springer International Publishing, 2017.
- [206] D. Wales, *Energy Landscapes: Applications to Clusters, Biomolecules and Glasses*. Cambridge Molecular Science, Cambridge University Press, 2003.
- [207] M. Jesi, *Spin Glasses: Criticality and Energy Landscapes*. Springer Theses, Springer International Publishing, 2016.
- [208] F. L. Metz and I. Pérez Castillo, “Large deviation function for the number of eigenvalues of sparse random graphs inside an interval,” *Physical Review Letters*, vol. 117, p. 104101, Sep. 2016.
- [209] S. Ross, *Introductory Statistics*. Elsevier Science, 2010.
- [210] F. Slanina, “Localization of eigenvectors in random graphs,” *The European Physical Journal B*, vol. 85, Oct. 2012.
- [211] G. H. Zhang and D. R. Nelson, “Eigenvalue repulsion and eigenvector localization in sparse non-hermitian random matrices,” *Physical Review E*, vol. 100, p. 052315, Nov. 2019.
- [212] S. Allesina, J. Grilli, G. Barabás, S. Tang, J. Aljadeff, and A. Maritan, “Predicting the stability of large structured food webs,” *Nature Communications*, vol. 6, Jul. 2015.
- [213] R. M. May, “Will a large complex system be stable?,” *Nature*, vol. 238, pp. 413–414, Aug. 1972.
- [214] F. L. Metz and I. Pérez Castillo, “Level compressibility for the Anderson model on regular random graphs and the eigenvalue statistics in the extended phase,” *Physical Review B*, vol. 96, p. 064202, Aug. 2017.
- [215] Y. Zhao and R. M. Strat, “Measuring order in disordered systems and disorder in ordered systems: Random matrix theory for isotropic and nematic liquid crystals and its perspective on pseudo-nematic domains,” *The Journal of Chemical Physics*, vol. 148, p. 204501, May 2018.

- [216] S. N. Majumdar, C. Nadal, A. Scardicchio, and P. Vivo, “How many eigenvalues of a gaussian random matrix are positive?,” *Physical Review E*, vol. 83, p. 041105, Apr. 2011.
- [217] A. Cavagna, I. Giardinà, and G. Parisi, “Analytic computation of the instantaneous normal modes spectrum in low-density liquids,” *Physical Review Letters*, vol. 83, pp. 108–111, Jul. 1999.
- [218] M. Yamada and A. Vilenkin, “Hessian eigenvalue distribution in a random gaussian landscape,” *Journal of High Energy Physics*, vol. 2018, Mar. 2018.
- [219] A. Kobakhidze and L. Mersini-Houghton, “Birth of the universe from the landscape of string theory,” *The European Physical Journal C*, vol. 49, pp. 869–873, Nov. 2006.
- [220] R. Holman and L. Mersini-Houghton, “Why the universe started from a low entropy state,” *Physical Review D*, vol. 74, p. 123510, Dec. 2006.
- [221] J. Pennington and Y. Bahri, “Geometry of neural network loss surfaces via random matrix theory,” in *Proceedings of the 34th International Conference on Machine Learning* (D. Precup and Y. W. Teh, eds.), vol. 70 of *Proceedings of Machine Learning Research*, pp. 2798–2806, PMLR, 06–11 Aug. 2017.
- [222] R. Marino, S. N. Majumdar, G. Schehr, and P. Vivo, “Index distribution of Cauchy random matrices,” *Journal of Physics A: Mathematical and Theoretical*, vol. 47, p. 055001, Jan. 2014.
- [223] I. Pérez Castillo, “Large deviations of the shifted index number in the gaussian ensemble,” *Journal of Statistical Mechanics: Theory and Experiment*, vol. 2016, p. 063207, Jun. 2016.
- [224] S. N. Majumdar and P. Vivo, “Number of relevant directions in principal component analysis and Wishart random matrices,” *Physical Review Letters*, vol. 108, p. 200601, May 2012.
- [225] C. Bordenave and D. Chafaï, “Around the circular law,” *Probability Surveys*, vol. 9, no. none, pp. 1 – 89, 2012.
- [226] F. L. Metz, I. Neri, and D. Bollé, “Localization transition in symmetric random matrices,” *Physical Review E*, vol. 82, p. 031135, Sep. 2010.
- [227] F. L. Metz, “Replica-symmetric approach to the typical eigenvalue fluctuations of gaussian random matrices,” *Journal of Physics A: Mathematical and Theoretical*, vol. 50, p. 495002, Nov. 2017.
- [228] A. Zangwill, *Modern Electrodynamics*. Modern Electrodynamics, Cambridge University Press, 2013.
- [229] J. Zinn-Justin, *Quantum Field Theory and Critical Phenomena*. International series of monographs on physics, Oxford University Press, 2021.
- [230] M. Olvera-Cravioto, “Convergence of the Population Dynamics algorithm in the Wasserstein metric,” *arXiv e-prints*, p. arXiv:1705.09747, May 2017.
- [231] U. Roesler, *The Weighted Branching Process*, pp. 219–236. Cham: Springer International Publishing, 2016.
- [232] M. Newman and G. Barkema, *Monte Carlo Methods in Statistical Physics*. Clarendon Press, 1999.
- [233] D. P. Kroese, T. Brereton, T. Taimre, and Z. I. Botev, “Why the monte carlo method is so important today,” *WIREs Computational Statistics*, vol. 6, pp. 386–392, Nov.-Dec. 2014.
- [234] C. Graham and D. Talay, *Stochastic Simulation and Monte Carlo Methods: Mathematical Foundations of Stochastic Simulation*. Stochastic Modelling and Applied Probability, Springer Berlin Heidelberg, 2013.
- [235] A. Blum, J. Hopcroft, and R. Kannan, *Foundations of Data Science*. Cambridge University Press, 2020.
- [236] A. Johansen, “Monte carlo methods,” in *International Encyclopedia of Education (Third Edition)* (P. Peterson, E. Baker, and B. McGaw, eds.), pp. 296–303, Oxford: Elsevier, third edition ed., 2010.
- [237] K. Binder and D. Heermann, *Monte Carlo Simulation in Statistical Physics: An Introduction*. Graduate Texts in Physics, Springer Berlin Heidelberg, 2010.
- [238] B. Ripley, *Stochastic Simulation*. Wiley Series in Probability and Statistics, Wiley, 2009.

-
- [239] D. Starnes, D. Yates, and D. Moore, *The Practice of Statistics*. W. H. Freeman, 2010.
- [240] P. Jones and P. Smith, *Stochastic Processes: An Introduction, Third Edition*. Chapman & Hall/CRC Texts in Statistical Science, CRC Press, 2017.
- [241] A. Basu, *Introduction to Stochastic Processes*. Alpha Science International, 2003.
- [242] J. Doob, *Stochastic Processes*. Probability and Statistics Series, Wiley, 1953.
- [243] N. Metropolis, A. W. Rosenbluth, M. N. Rosenbluth, A. H. Teller, and E. Teller, "Equation of state calculations by fast computing machines," *The Journal of Chemical Physics*, vol. 21, pp. 1087–1092, Jun. 1953.
- [244] W. K. Hastings, "Monte Carlo sampling methods using Markov chains and their applications," *Biometrika*, vol. 57, pp. 97–109, Apr. 1970.
- [245] C. P. Robert, "The Metropolis-Hastings algorithm," *arXiv e-prints*, p. arXiv:1504.01896, Apr. 2015.